Chapter 6

Outdoor Experimental Characterisation of an Asymmetric Compound Parabolic Photovoltaic Concentrator

6.1 Introduction

An asymmetric parabolic photovoltaic concentrator system was designed and constructed suitable for indoor and outdoor experimental characterisation. The predicted optical performance is detailed in chapter 3 and a thermofluid analysis undertaken and presented in chapter 4. The optical analysis shows that the air filled ACPPVC-50 accepts solar radiation incident over a wide angular range with an optical efficiency of up to 85.15% and collection efficiency of 100%. The isotherms throughout the system; at the aperture, reflector, solar cell and the aluminium back plate and the air flow were predicted for different solar radiation intensities. Indoor experimental characterisation was performed using a solar simulator and measured performance presented in chapter 5. Based on the measured performance in the indoor experimental characterisation, the reflector support was modified as described in chapter 3 for the outdoor experimental characterisation. This chapter details the experimental characterisation of two ACPPVC-50 systems. The electrical and thermal measurements for a number of ‘PV’ strings connected in series of the first ACPPVC-50 system, PV panel with concentrator and without concentrator of the first ACPPVC-50, and both PV panels with and without concentrators at real time are presented.

6.2 The ACPPVC-50 Systems Developed for Outdoor Experimental Characterisation

The design and construction procedures for the two systems used for outdoor experimental characterisation were detailed in chapter 3. Both APPVC-50 systems are shown in figure 6.2.1. Although the geometrical and physical characteristics of both systems were intended to be the same, during system construction one of the solar cells short circuited with the rear aluminium plate and was replaced as shown in figure 6.2.1(a). The replaced solar cell did not affect the electrical output when it was tested under normal conditions i.e. the short circuit current and open circuit voltage were the same as for the other strings in the system.

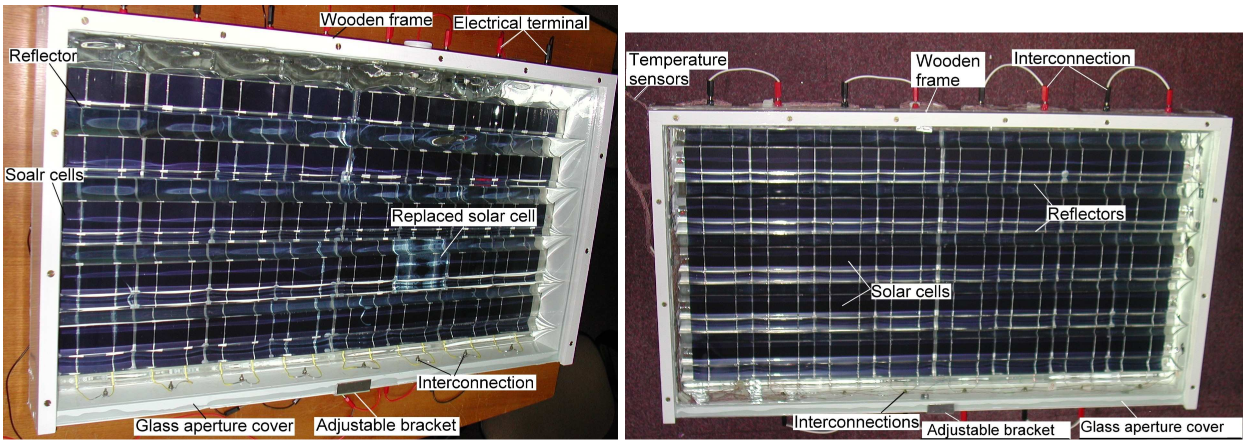

(a) System 1 (b) System 2

Figure 6.2.1 Fabricated ACPPVC-50 systems for outdoor experimental characterisation: (a) System 1 clearly indicating the location of the replaced solar cell (b) System 2.

6.3 Experimental Set-up for Outdoor Experimental Characterisation

Measurements of current and voltage under forward bias condition for photovoltaic cells were taken incorporating the loading circuit as detailed in chapter 5. For the outdoor experimental characterisation of the ACPPVC-50 systems the data acquisition system KI2700 was replaced by a high speed data acquisition system KI2750 (maximum speed of 2500 rds s^{-1}) and the source meter KI2400 was replaced by KI2430. All remaining instrumentation was as before. The accuracy and specification of KI2750 and KI2430 are detailed in Appendix B. The circuit diagram for all measurements is shown in figure 6.3.1.

Figure 6.3.2 details the electrical connections of the source meter and data acquisition system used for measuring the current and voltage developed by the PV panels when under illumination i.e. forward bias conditions. A switching relay card is required when two or more PV systems are tested at the same time, the solar radiation, temperature and wind velocity sensors were connected directly to the data acquisition card. An internal cold junction compensated data acquisition card (Anon, 2001m) was used for all temperature measurements in this experiment. The solar radiation sensor was connected to a voltage channel which was set with the correct calibration factor used for the instrument. The thermocouple locations at which the solar cell temperature and reflector substrate temperature were measured are shown in figure 6.3.3. Figure 6.3.4 and figure 6.3.5 illustrates the thermocouple locations used to measure the temperature of the aluminium back plate for both systems.

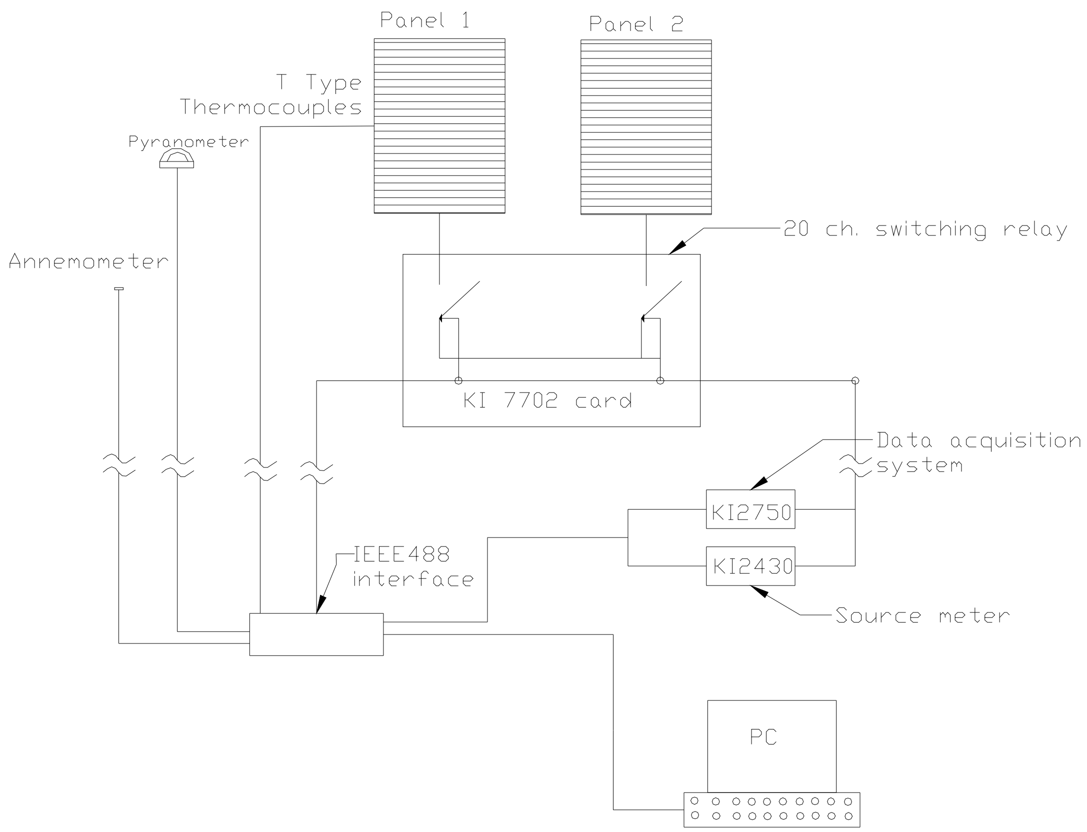

Figure 6.3.1 Block diagram of equipment for testing of PV systems.

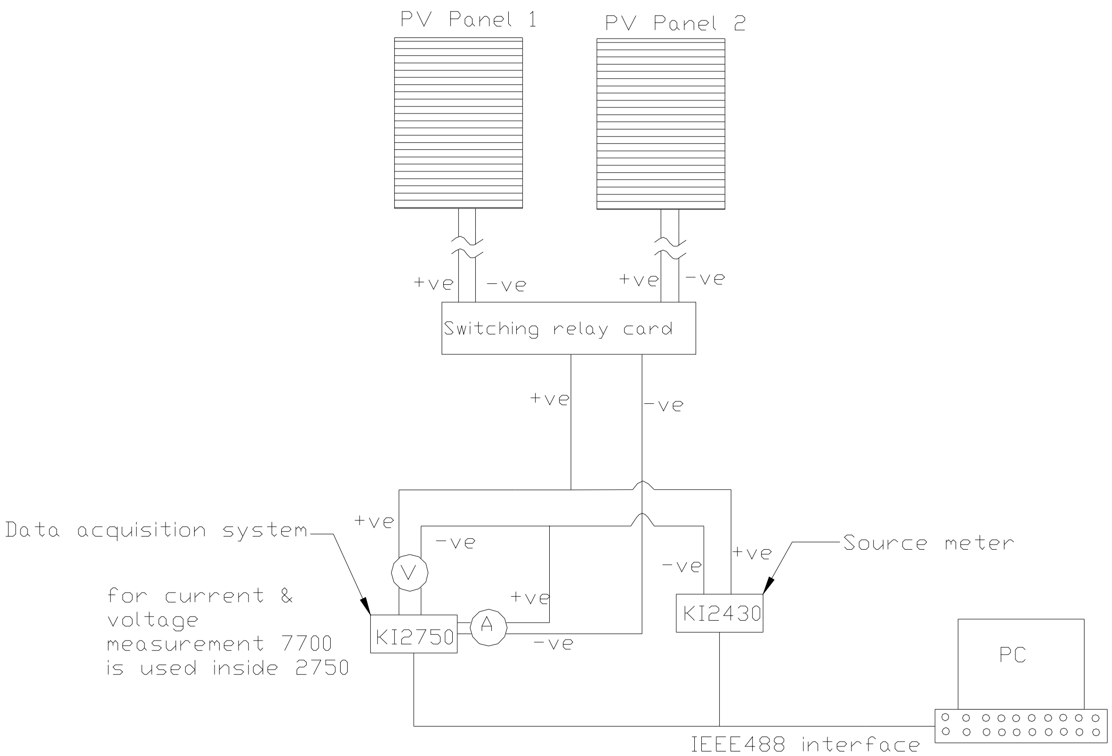

Figure 6.3.2 Electrical circuit connections used for measuring current and voltage generated by the photovoltaic systems through a 40-channel switching card.

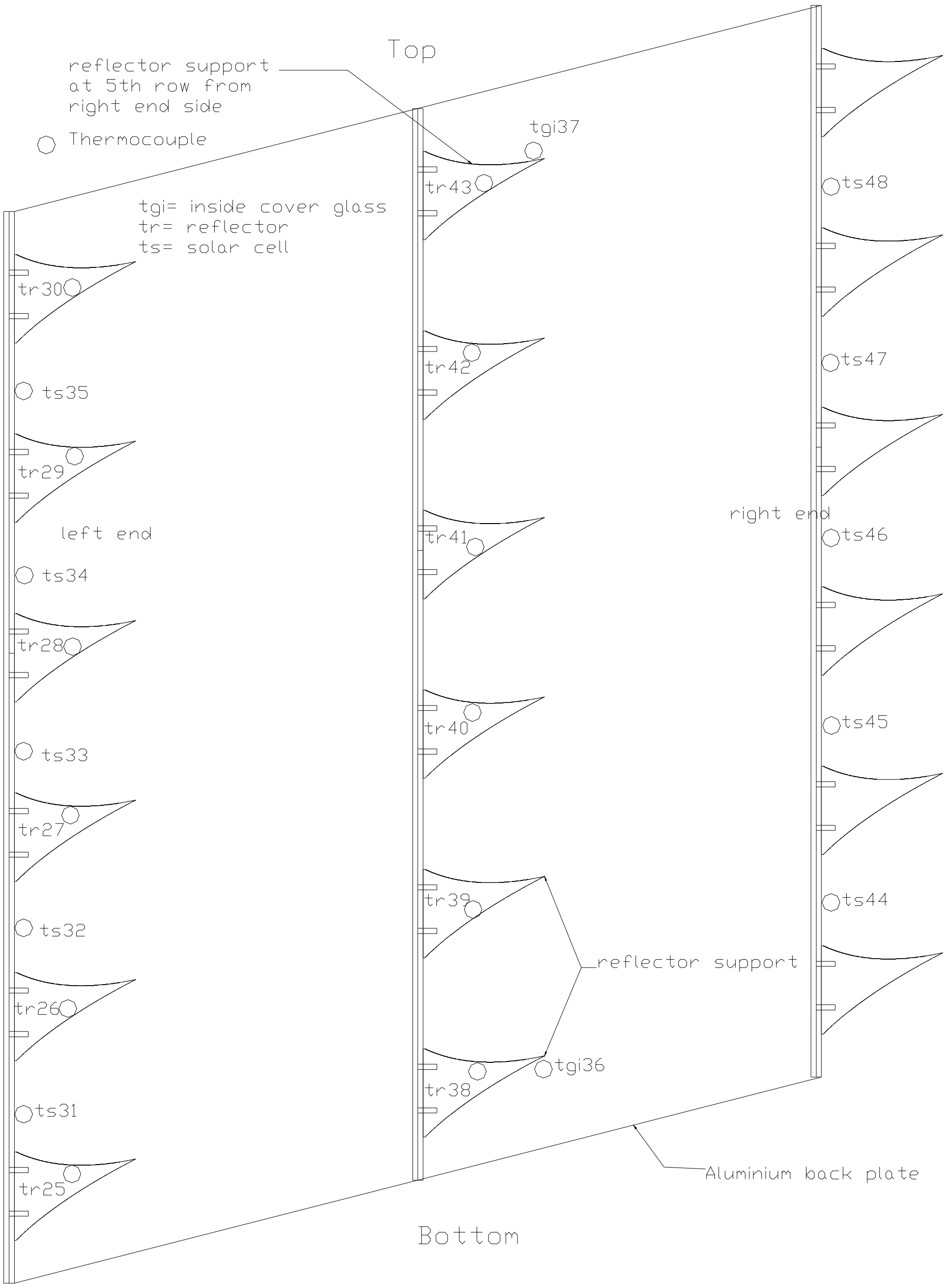

Figure 6.3.3 Thermocouple connections at the reflector back plate and at either side of solar cell edge to measure reflector and solar cell temperature respectively.

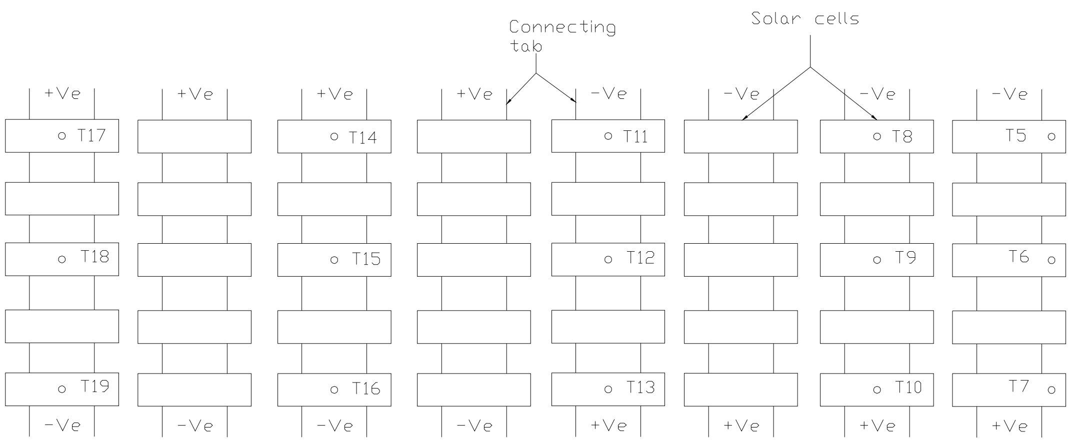

Figure 6.3.4 Thermocouple locations at which the aluminium back plate temperature was measured for System 1.

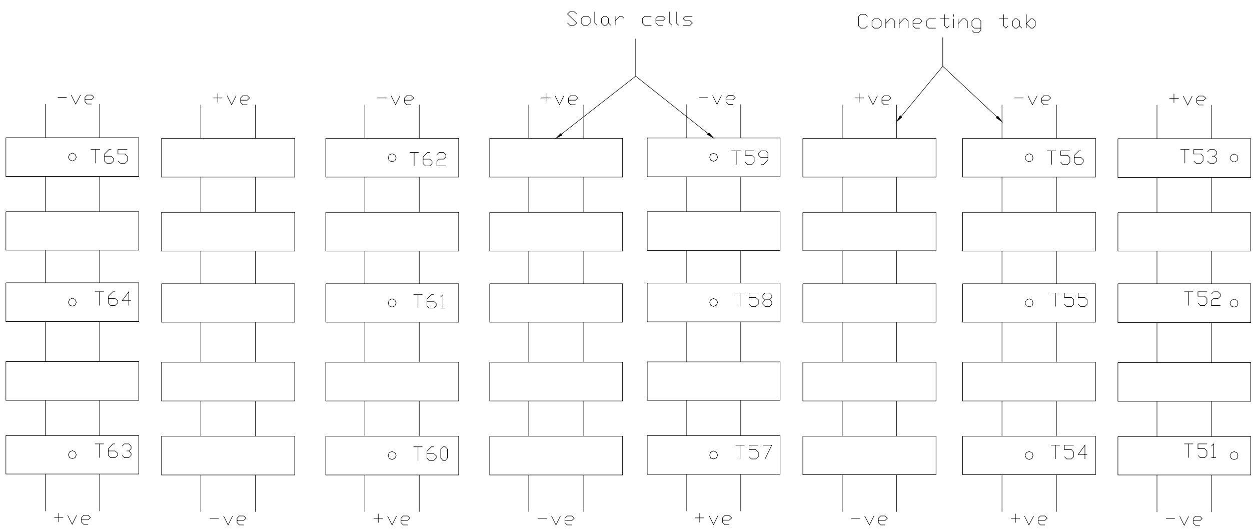

Figure 6.3.5 Thermocouple locations at which the rear aluminium back plate temperature was measured for System 2.

6.4 Experimental Measurements and Data Analysis for the Two Fabricated ACPPVC-50 Systems

The experiments were performed at the Centre for Sustainable Technologies (CST), at the University of Ulster, Jordanstown, NI, UK, at 56ºN and 5º6' W. The systems were mounted at 18º, 30º and 0º inclination angles to the vertical as illustrated in figure 6.4.1 to 6.4.3.

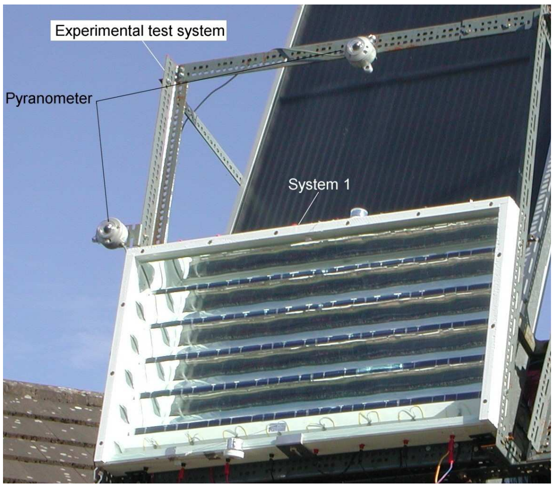

Figure 6.4.1 System 1 mounted at an angle 18º from the vertical.

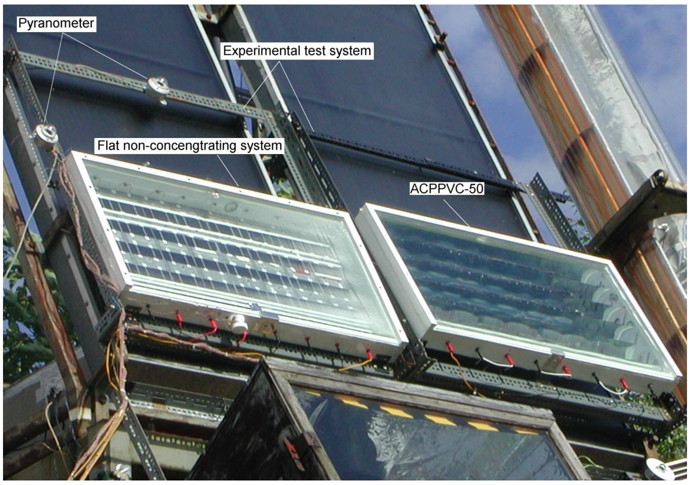

Figure 6.4.2 A non-concentrating and an ACPPVC-50 mounted at an inclination angle of 30º to the vertical.

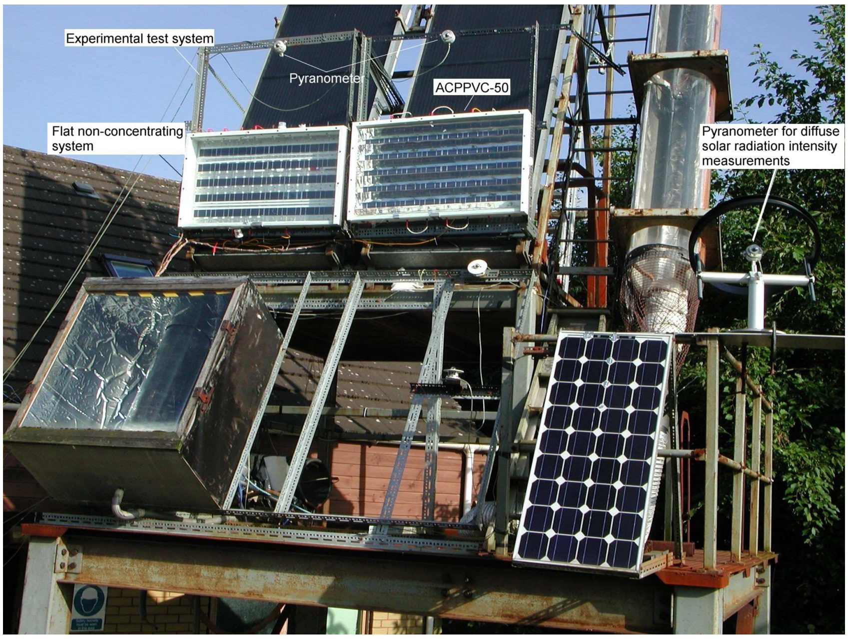

Figure 6.4.3 A non-concentrating and an ACPPVC-50 mounted vertically.

6.4.1 Electrical and Thermal Performance Analysis of System 1

The electrical output, solar radiation and temperatures from System 1 were monitored for a period of over 24 days. When measuring a single system, the data acquisition terminal was connected directly to the device output. Programmes were written in "Test Point" (Anon, 2001j) to control the monitoring and storage of all electrical and thermal measurements. Electrical parameters measured were the output current from the PV panel, the output voltage, the short circuit current and the open circuit voltage. The ambient temperature, the cover glass temperature and the aluminium back plate temperature were measured. A "Linear Sweep" mode was used to obtain each set of I-V curves. Each sweep took 10 seconds to measure current, voltage, solar radiation, temperature and wind speed. A delay of 30 seconds was implemented between successive sweeps to reset and cool the source meter (Anon, 2001n). The system was mounted at an angle of 18º to the vertical. The variation of solar radiation, ambient temperature, aperture cover temperature and average aluminium back plate temperature are shown in figure 6.4.1.1 for the 21st August 2002. A time delay can be seen between the peak temperature and the peak solar radiation on that day. This is due to the thermal inertia of the aperture cover and aluminium back plate.

The I-V curves measured at different times of the day (differing solar incidence angle and intensity) are shown in figure 6.4.1.2 (a) and figure 6.4.1.2 (b) shows the change of short circuit current due to change of the solar incidence angle. On this day a period prolonged sunshine prior to and after solar noon leads to a low value of the short circuit current. This is due to the shading created by the wooden frame as shown in figures 6.4.1.3 and 6.4.1.4. Figure 6.4.1.5 illustrates the variation in power generated by the PV panel with the voltage developed by it. The maximum power point shifts towards the left as shown by the voltage-power curve at 13:00 and 14:00 although for the latter curve the solar radiation was 100 Wm^{-2} higher compared to the first one.

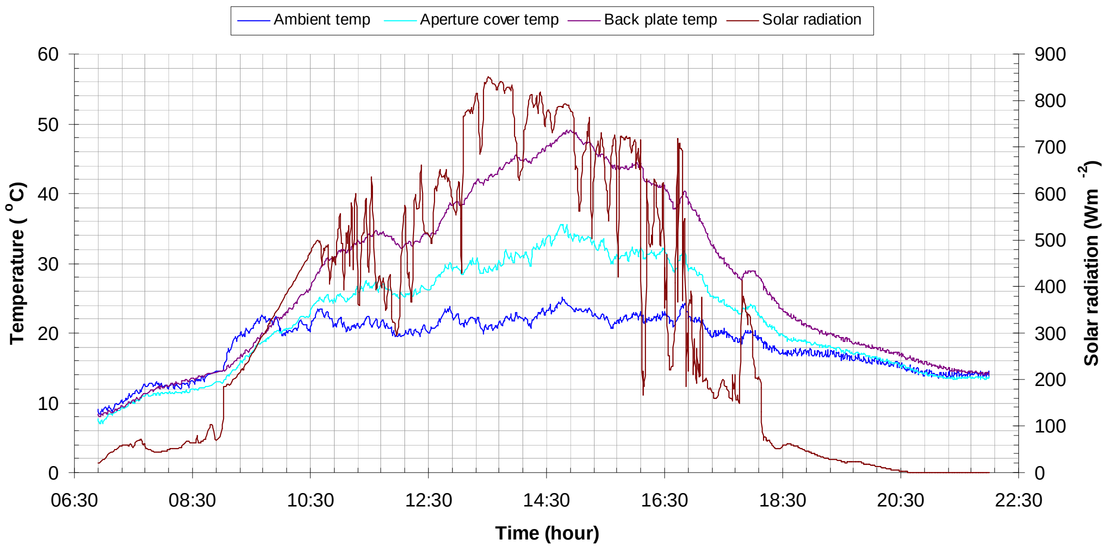

Figure 6.4.1.1 Measured solar radiation and temperatures for the ACPPVC-50 on the 21st August 2002.

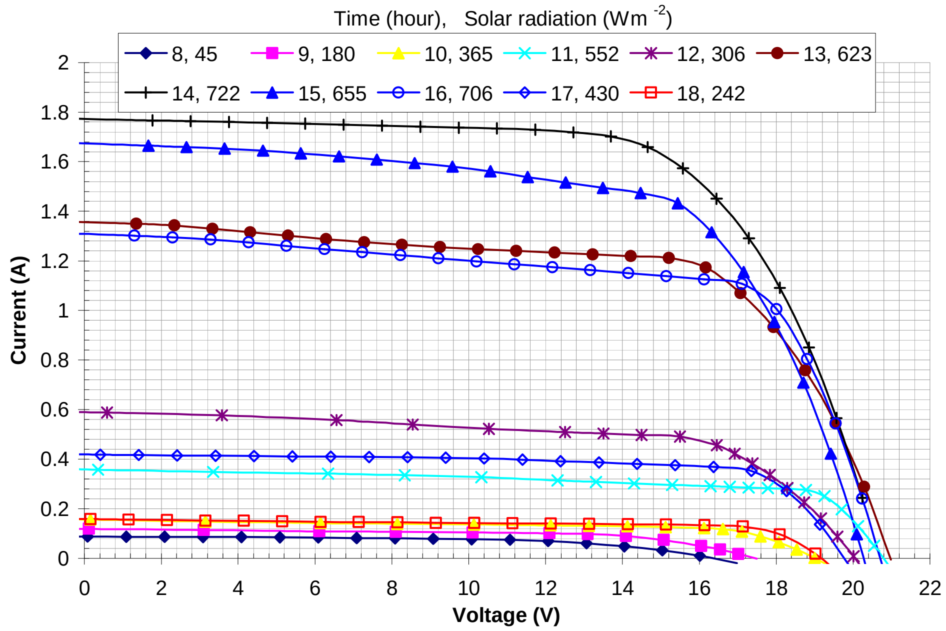

(a)

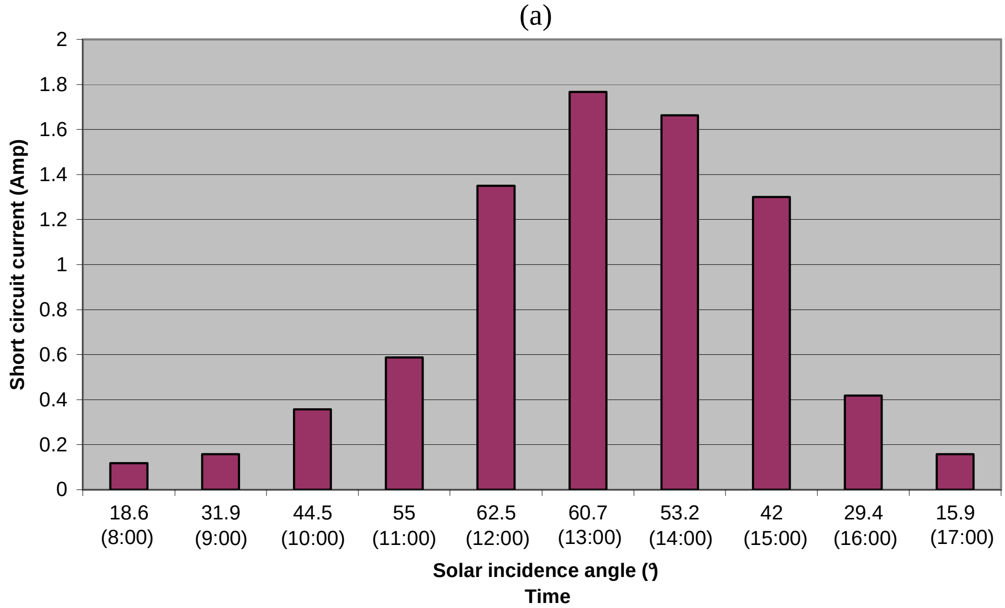

(b)

Figure 6.4.1.2 (a) I-V curves at different times for different incident solar radiation intensities, (b) variation of short circuit current with solar incidence angle and time.

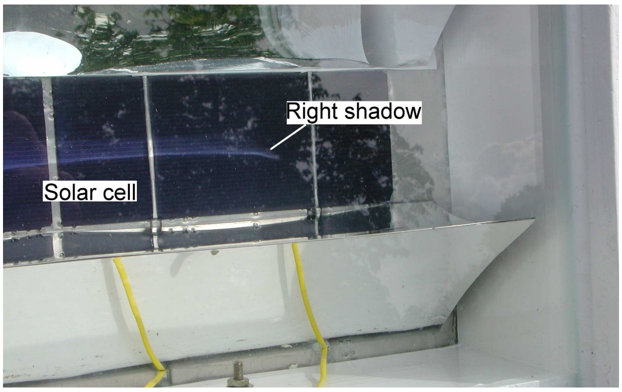

Figure 6.4.1.3 Shadow created on the right-end solar cell by the wooden frame at 11:54:32 on 21st August 2002.

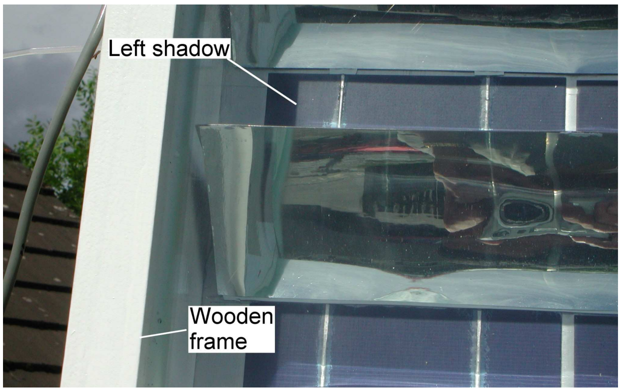

Figure 6.4.1.4 Shadow created on the left-end solar cell by the wooden frame at 14:55:39 on 21st August 2002.

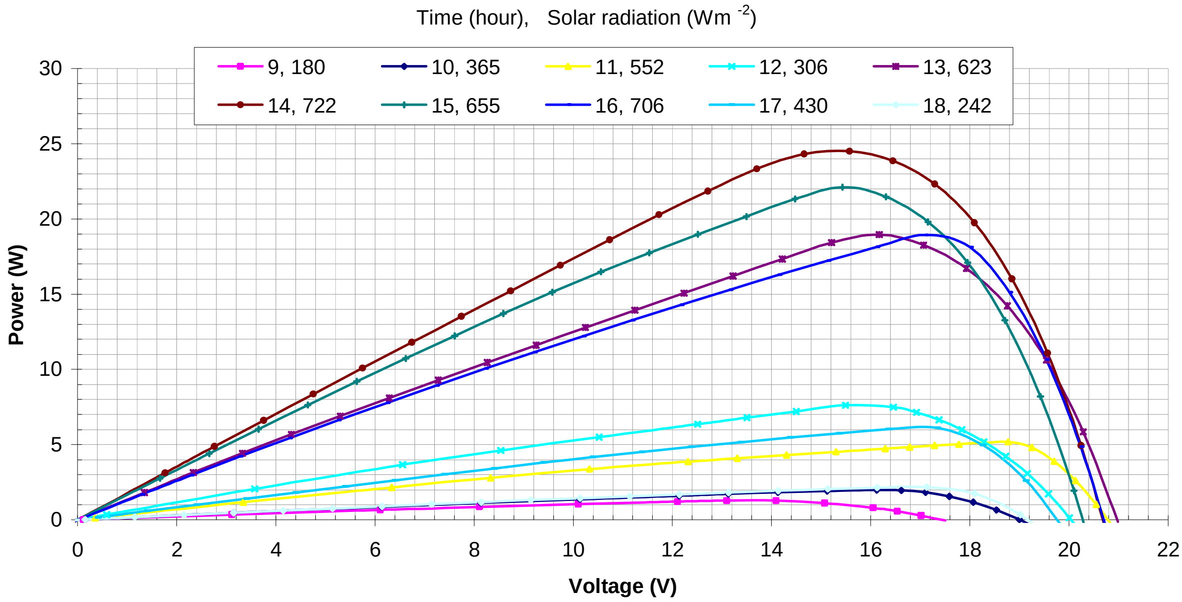

Figure 6.4.1.5 Instantaneous power output with voltage developed by System 1 at different times for different incident solar radiation intensities.

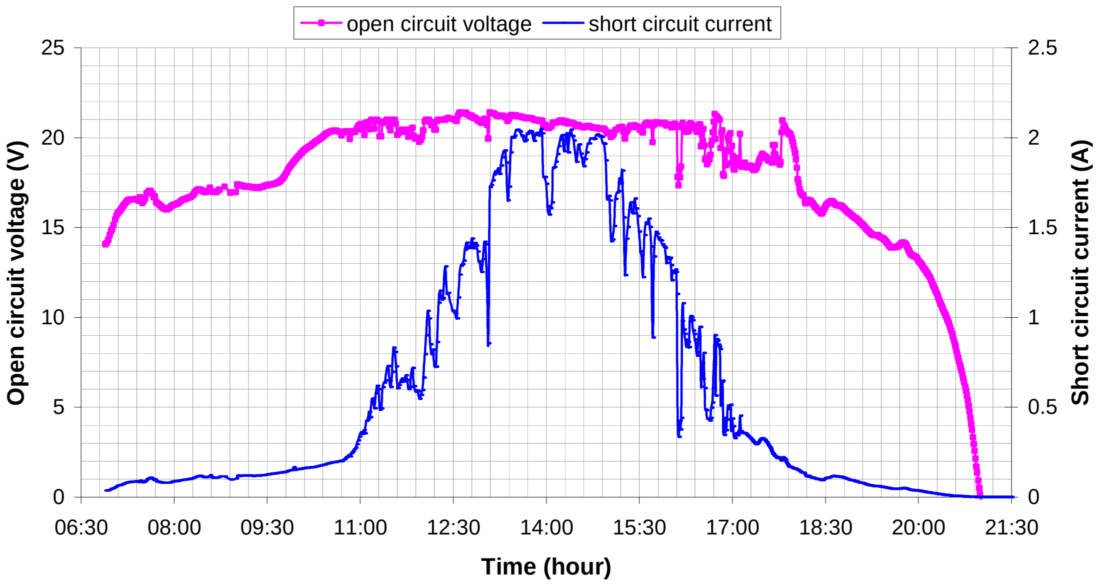

Figure 6.4.1.6 Change in open circuit voltage and short circuit current with time for System 1.

The variation in short circuit current and open circuit voltage with time is shown in figure 6.4.1.6. The open circuit voltage increases exponentially with incident solar radiation intensity until it achieves its maximum value. For a wide range of solar radiation intensities (between 11:00 to 17:00) the open circuit voltage remained nearly constant. The open circuit voltage decreased around mid day, due to the increase in PV temperature. The open circuit voltage decreased after 20:00 since solar radiation decreased significantly. This sudden drop in the open circuit voltage is caused by a shadow cast by the wooden frame on the left solar cell string as illustrated in figures 6.4.1.4 and 6.4.1.7.

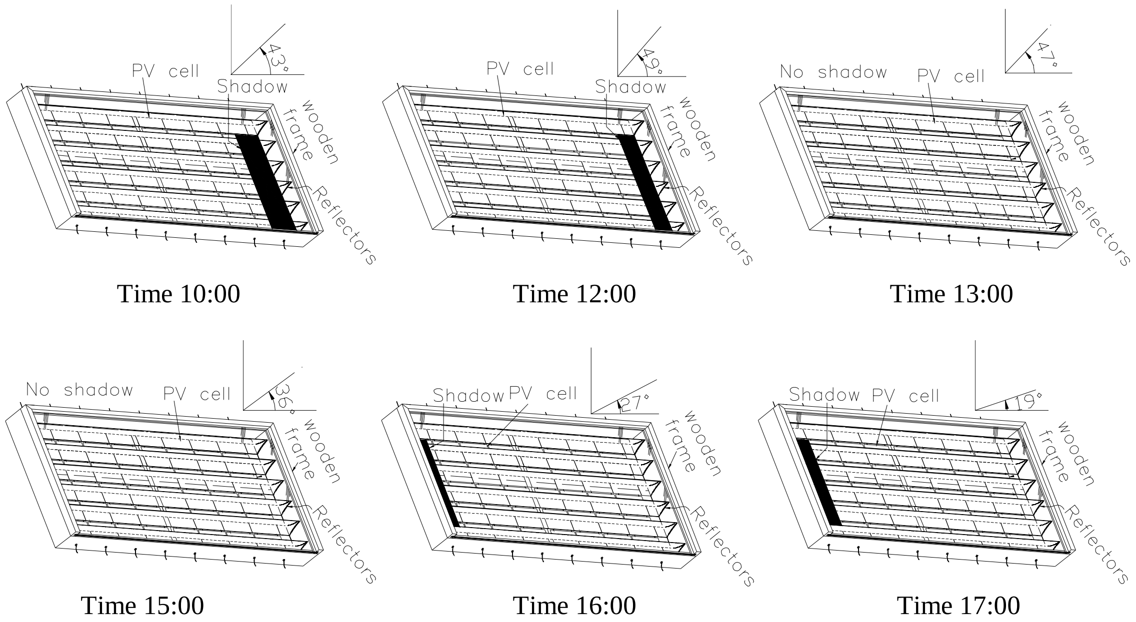

Figure 6.4.1.7 Shadow cast by the wooden frame onto the solar cells at different times of the day.

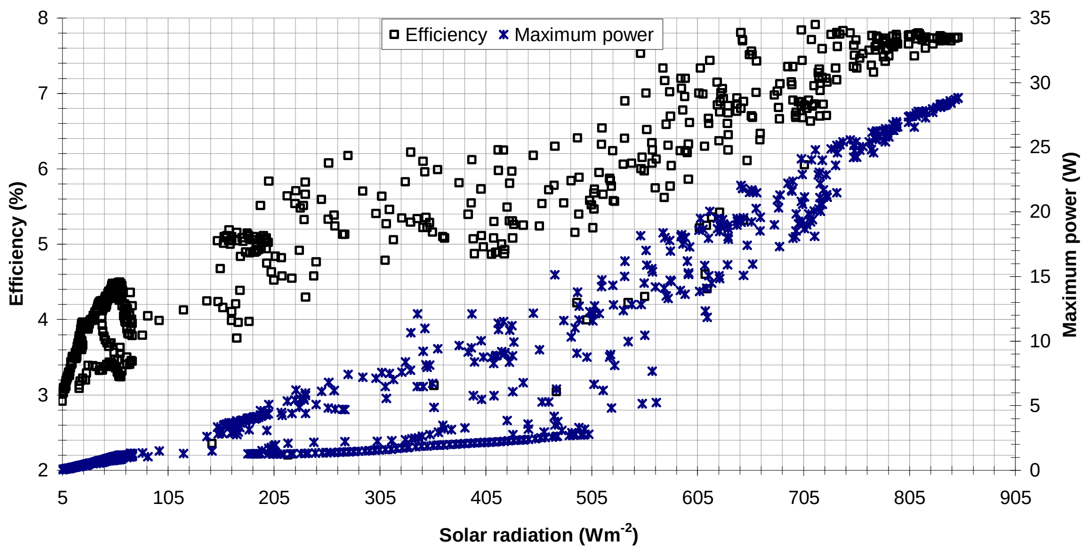

Figure 6.4.1.8 Maximum power output and efficiency of System 1 with incident solar radiation intensity.

The efficiency and maximum power generated by the system with incident solar radiation intensity are shown in figure 6.4.1.8. It can be observed from figure 6.4.1.8. that despite intervals of cloud at low levels of incident solar radiations up to 500 Wm^{-2}, the maximum power output and efficiency were low. This was because of shadows cast on the PV at either side of the system by the wooden frame. A maximum efficiency of 7.8% was achieved at 800 Wm^{-2} solar incident radiation when the maximum power generated by the system was 26 W.

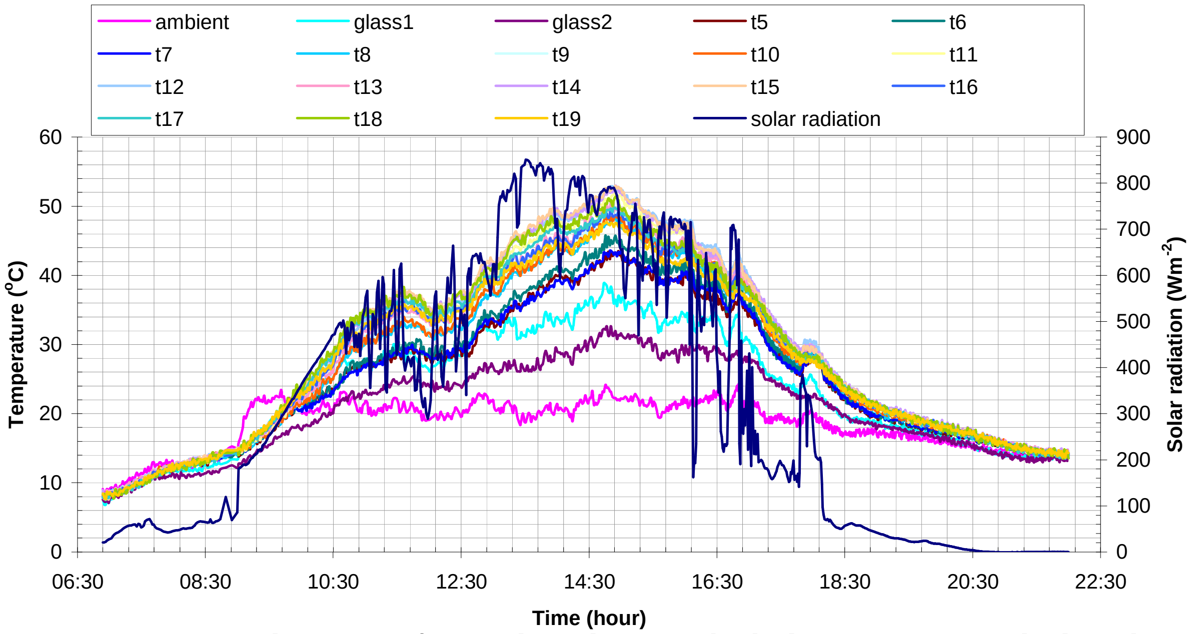

Figure 6.4.1.9 Diurnal variation of cover glass, aluminium back plate temperature and solar radiation.

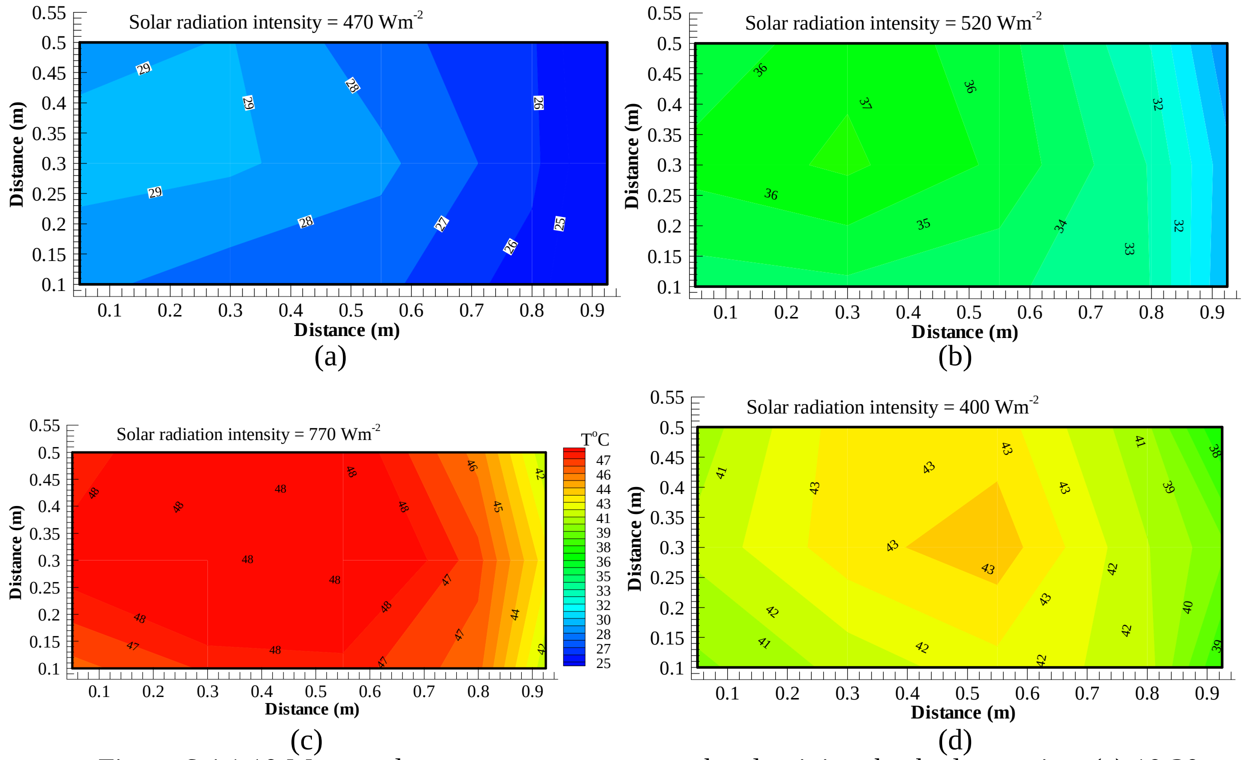

Figure 6.4.1.10 Measured temperature contours at the aluminium back plate at time (a) 10:30 (b) 12:30 (c) 14:30 (d) 16:30 on the 21st of August 2002.

The temperature distribution at the aluminium back plate is shown in figure 6.4.1.9. The highest back plate temperature of 50ºC was at thermocouple position 't12' near to the centre of the back plate (see figure 6.3.4). The maximum temperatures recorded by the thermocouples positioned at the top and bottom of the cover glass were 38ºC and 30ºC respectively. The average ambient temperature was 20ºC. Figure

6.4.1.10 shows the measured temperature contours of the aluminium back plate at different times and with different solar radiation intensities. The peak temperature shifts from left to right as seen from figure 6.4.1.10(a) and figure 6.4.1.10(d). This is due to the following reasons:

- Shading effect as illustrated in figure 6.4.1.7.
- Effective heat loss from the edge reduced due to the second system mounted close to the first system as shown in figure 6.4.3.

The variation in the rear aluminium back plate temperature at thermocouple positions ‘t5’ and ‘t17’ are shown in figure 6.4.1.11.

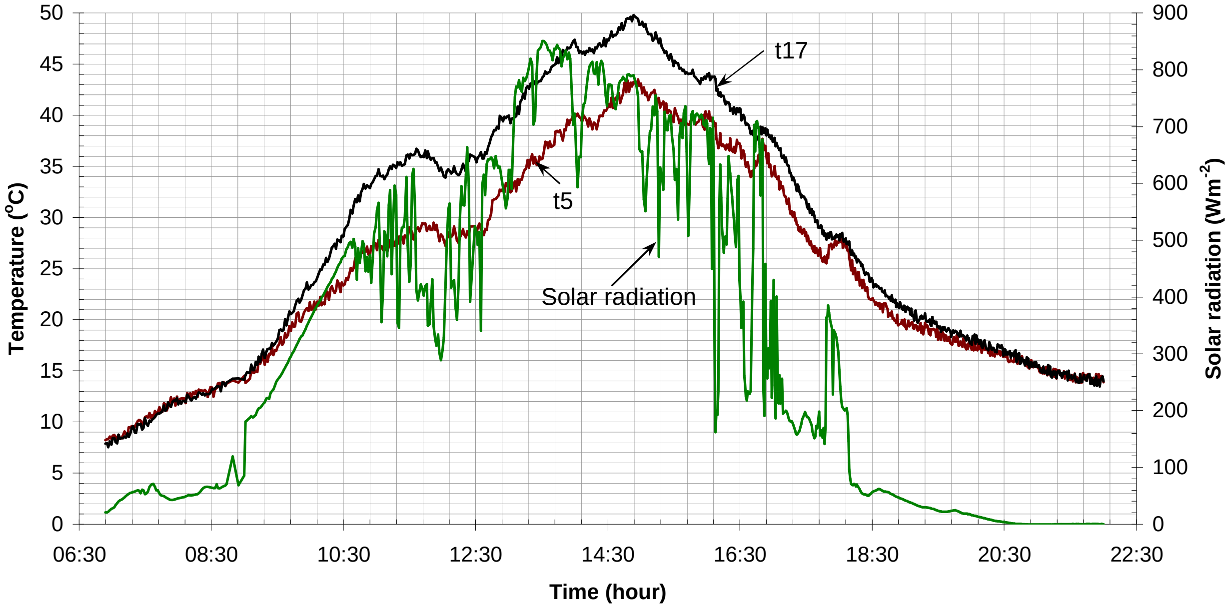

Figure 6.4.1.11 Diurnal variation of solar radiation and back plate temperature at thermocouple positions ‘t5’ and ‘t17’.

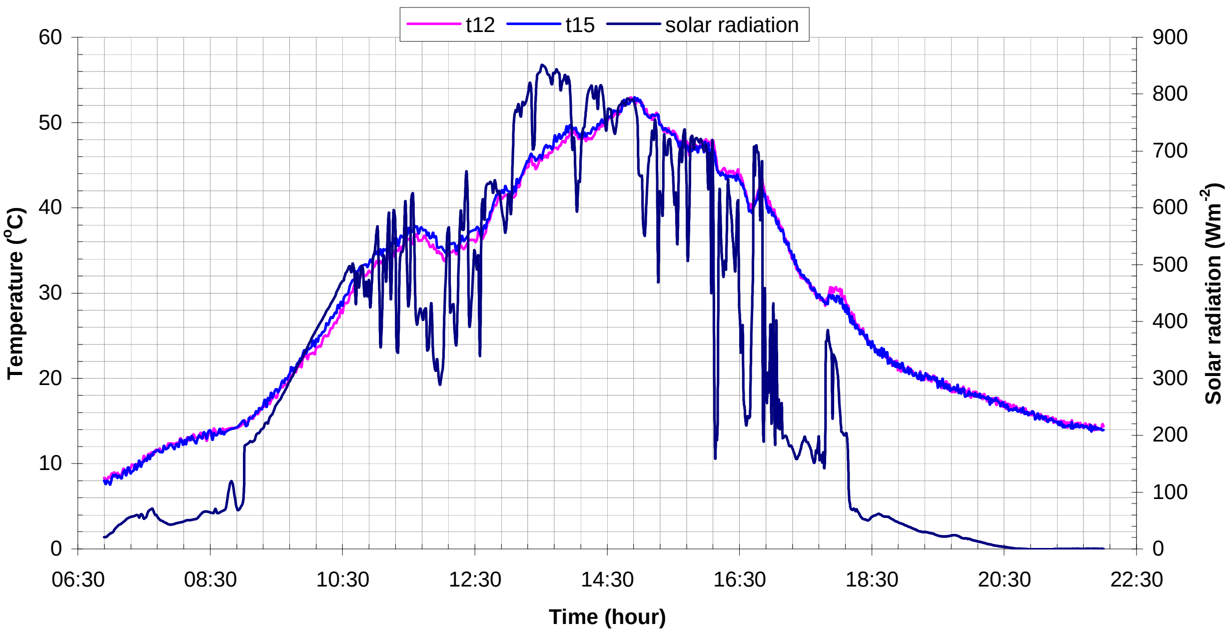

Figure 6.4.1.12 Diurnal variation of solar radiation and aluminium back plate temperature at thermocouple positions 12 and 15 as shown in figure 6.3.4.

The temperature in the central region of the aluminium back plate becomes nearly uniform as shown in figure 6.4.1.12 at thermocouple positions ‘t12’ and ‘t15’. A temperature difference of 3ºC can be seen in the central vertical direction of the aluminium back plate at thermocouple positions of ‘t11’, ‘t12’ and ‘t13’ as shown in figure 6.4.1.13. Figure 6.4.1.14 illustrates the variation of back plate temperatures along the central line in the horizontal direction. At lower intensities of solar radiation i.e. in the morning and the evening all temperatures are similar. The measured temperature contours at the aluminium back plate in figure 6.4.1.15 shows that each side of the back plate does not exhibit the same edge heat loss. A peak temperature difference of 7ºC can be seen between the top and bottom of the aperture cover glass as shown in figure 6.4.1.16. The average rear aluminium plate temperature was 48ºC, 25ºC above the ambient temperature as shown in figure 6.4.1.17.

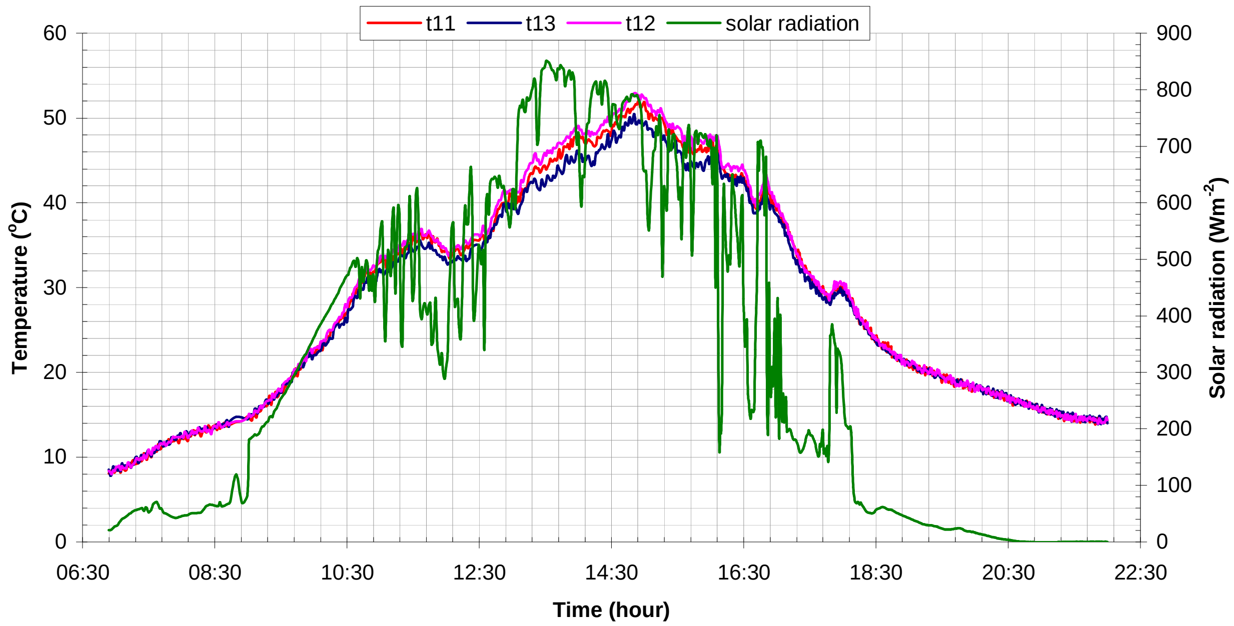

Figure 6.4.1.13 Diurnal variation of solar radiation and the aluminium back plate temperature at thermocouple locations t11, t12 and t13 as shown in figure 6.3.4.

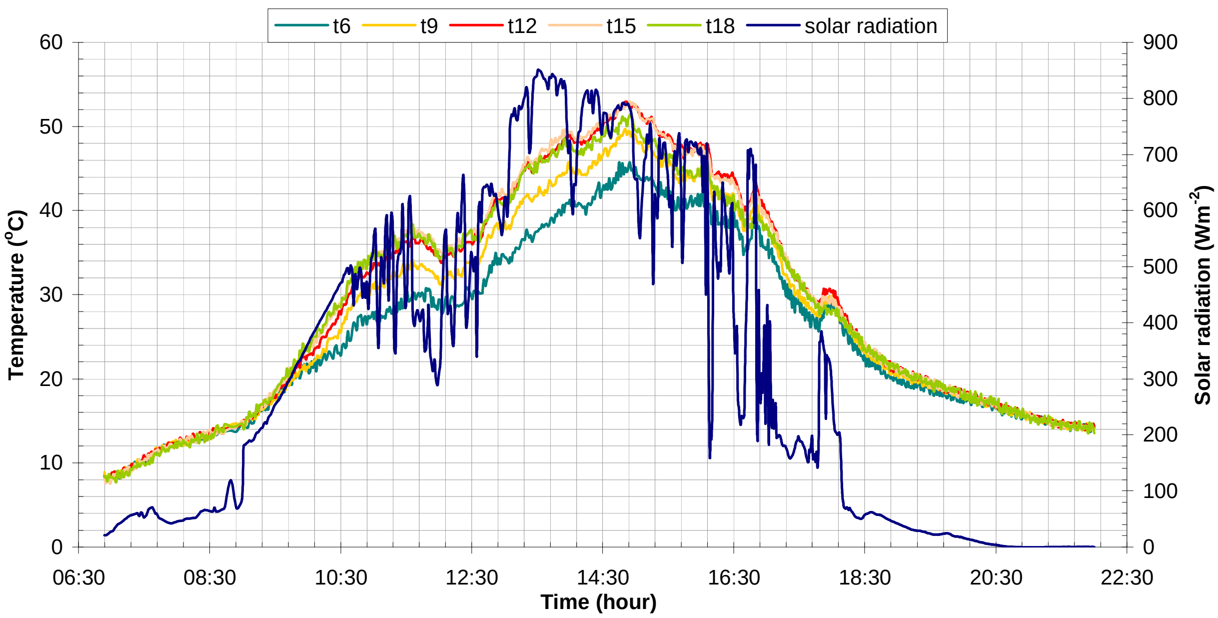

Figure 6.4.1.14 Diurnal variation of solar radiation and temperature of the aluminium back plate at thermocouple locations t6, t9, t12, t15 and t18 as shown in figure 6.3.4.

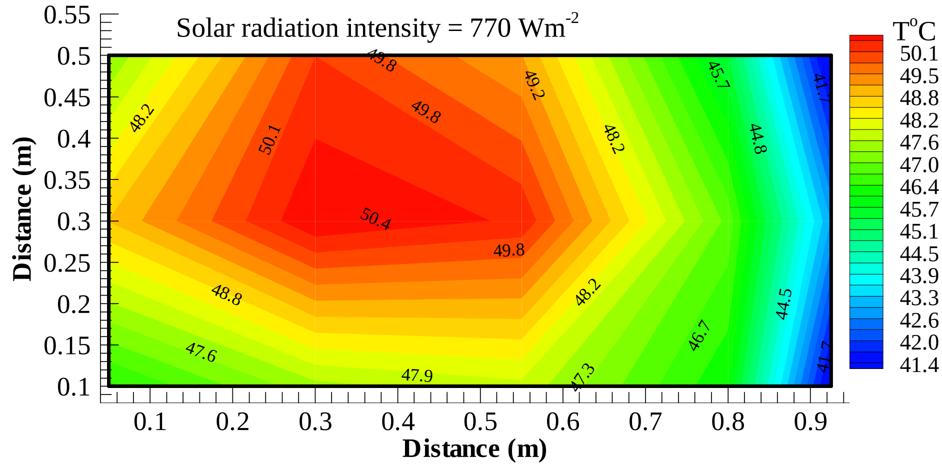

Figure 6.4.1.15 Measured temperature contours of the aluminium back plate at time 14:50 on the 21st of August 2002.

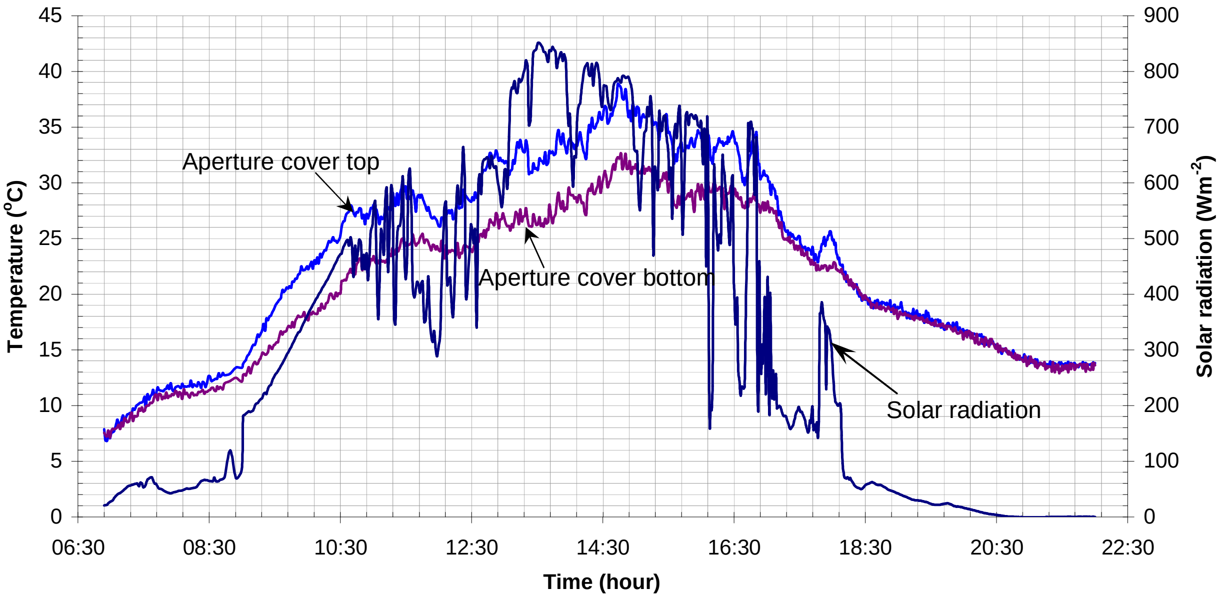

Figure 6.4.1.16 Diurnal variation of solar radiation, top and bottom aperture cover glass temperature for System 1.

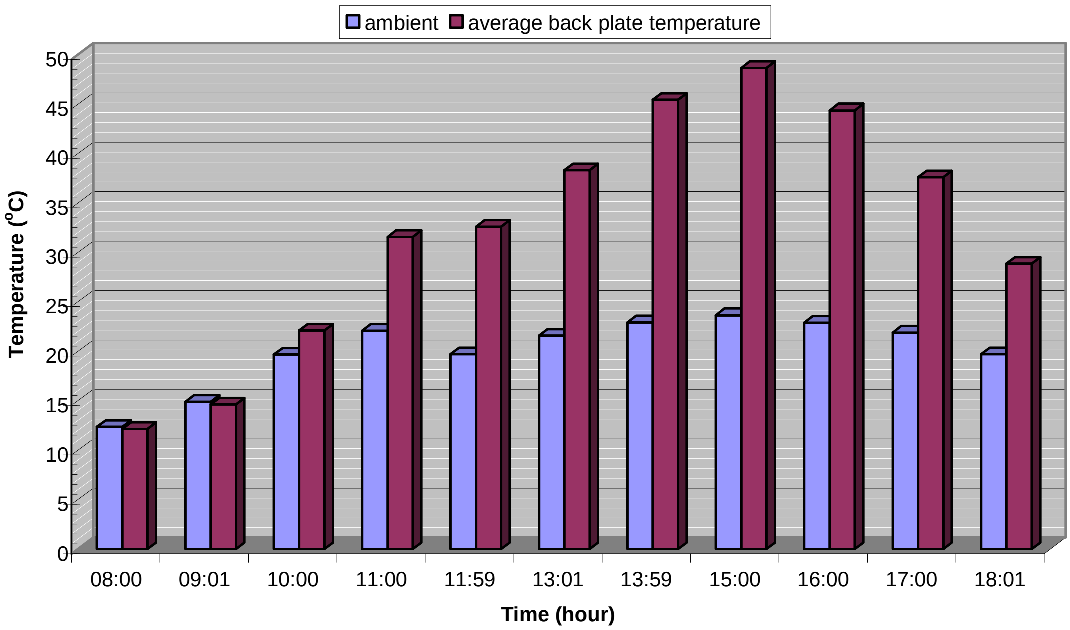

Figure 6.4.1.17 Variation of average back plate temperature and ambient temperature with time for System 1. All eight PV strings were connected in series.

6.4.2 Electrical and Thermal Performance Analysis of System 1 with Seven PV Strings Connected in Series

The outdoor experimental characterisation was undertaken for nine days with seven PV strings connected in series. For this period not a single day was continuously clear and sunny. The PV string containing the replacement PV cell was disconnected for these measurements. The variation of incident solar radiation with time is shown in figure 6.4.2.1. The methodology of measurement remained unchanged from previous experiments.

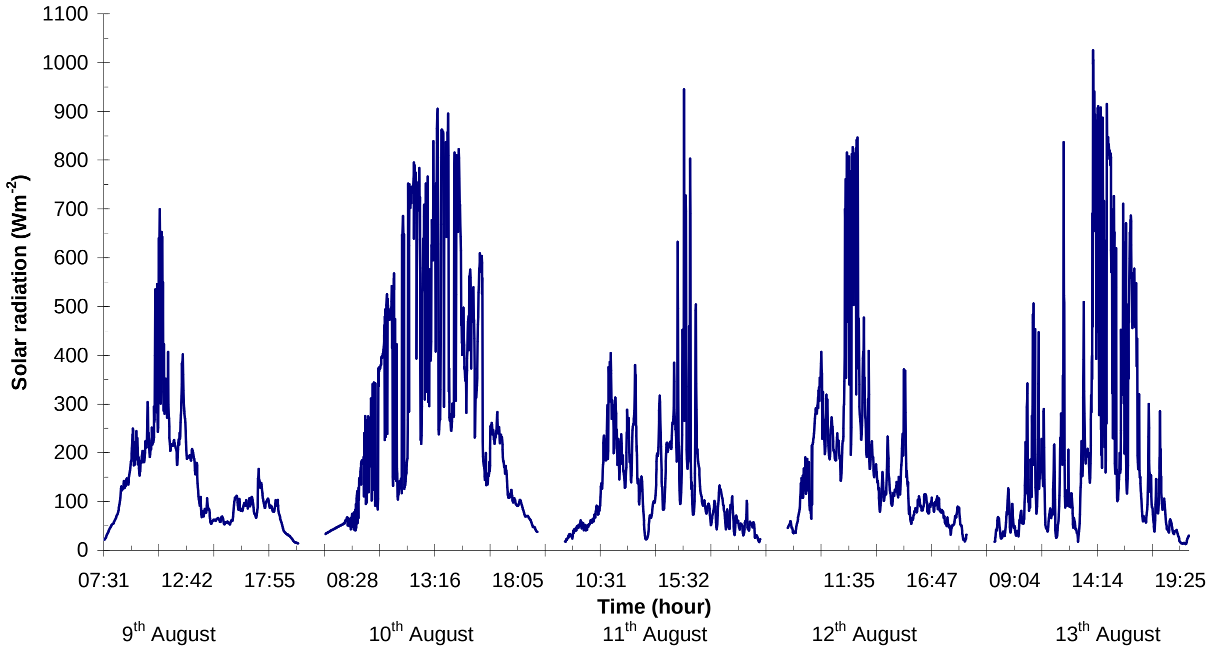

(a)

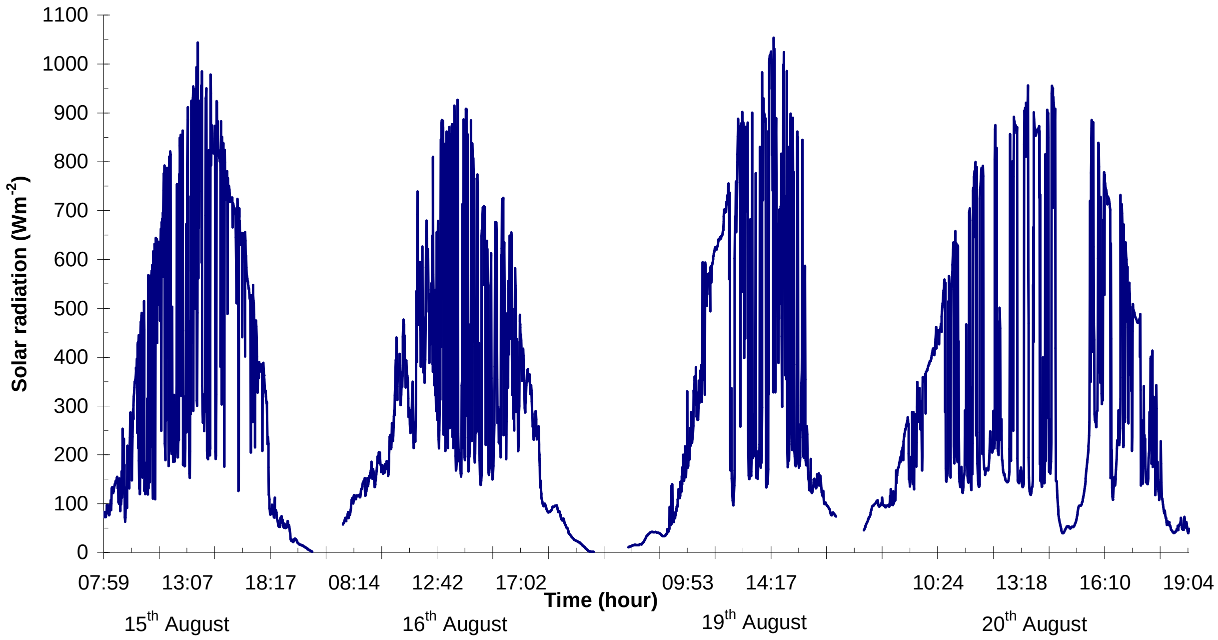

(b)

Figure 6.4.2.1 The change of solar radiation with time for nine days (a) 9th to 13th August (b) 15th to 20th August. The solar radiation was measured at 55 second intervals.

Variations in the maximum power generated by the system with incident solar radiation for these experiments with seven PV strings connected in series are illustrated in figure 6.4.2.2. The maximum power generated by this system was 20 Watts when the intensity of incident solar radiation was 800 Wm^{-2}. Due to the shading on either side of the system, the maximum power point dropped by up to $1/3^{rd}$ of its peak value. At higher intensities of solar radiation, close to either side of solar noon, the maximum power obtained from the system reached a corresponding maximum value. The solar radiation intensity was measured on the plane of the experimental apparatus. The corresponding hourly variation of maximum power generated by System 1 is shown in figure 6.4.2.3.

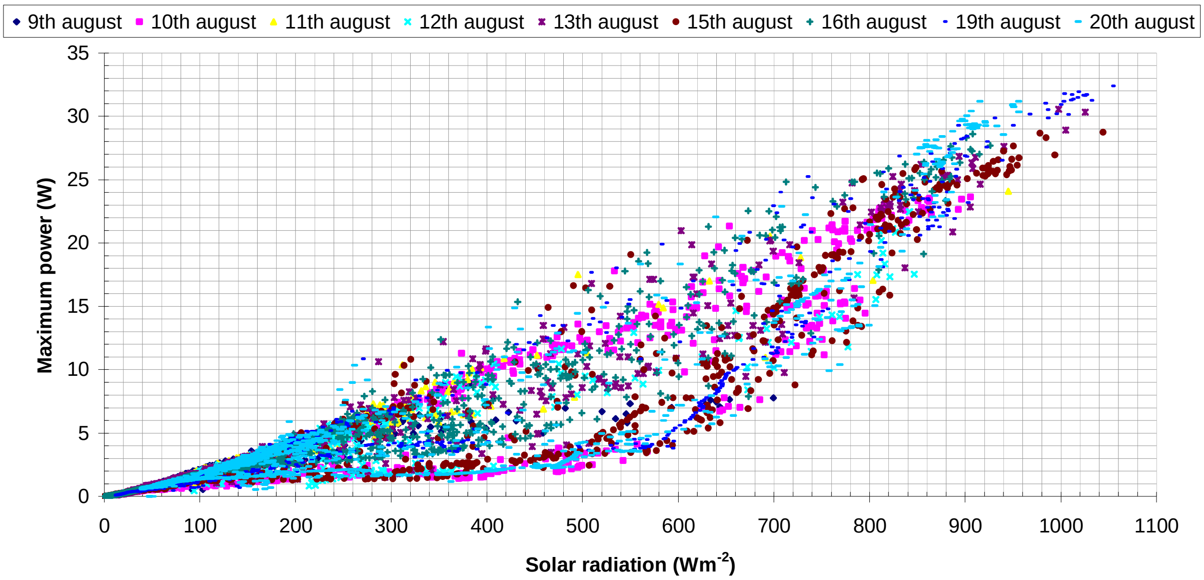

Figure 6.4.2.2 Variation of maximum power generated by System 1 with incident solar radiation intensity.

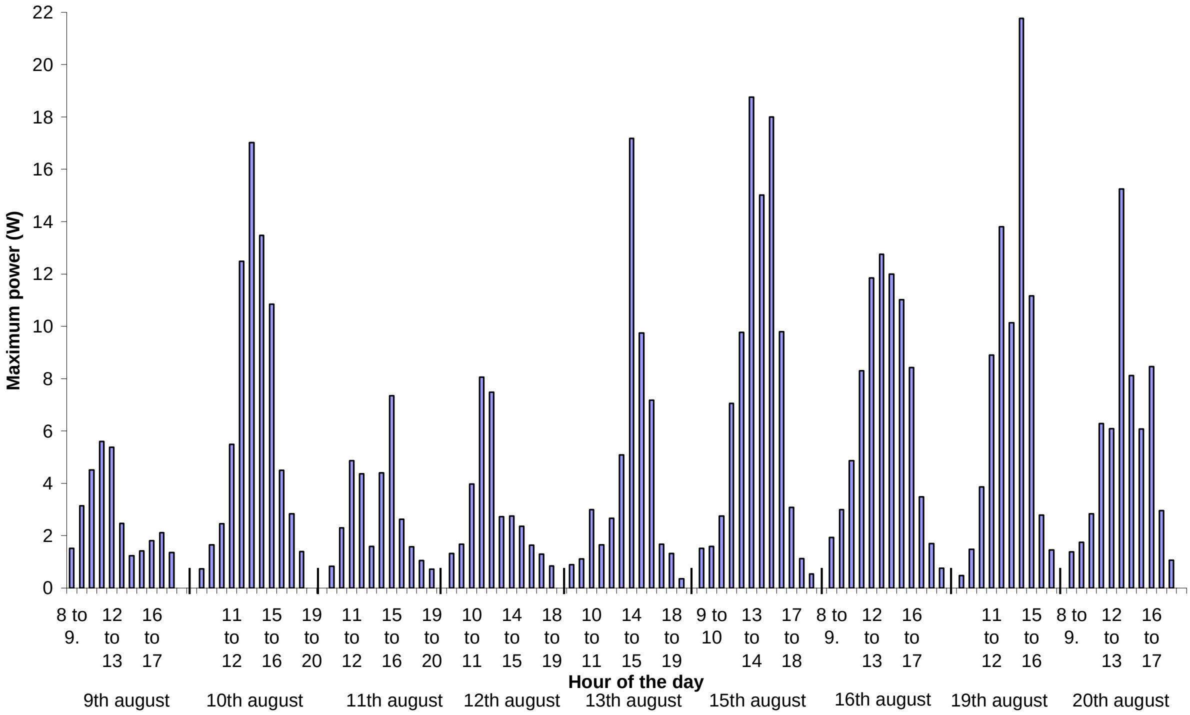

Figure 6.4.2.3 Hourly variation of maximum power of System 1 for nine days in August 2002.

6.4.3 Electrical and Thermal Performance Analysis of System 1 with Six PV Strings Connected in Series

Measurements were conducted for ten days with six PV strings connected in series, both left and right side PV strings were electrically disconnected from the others. The variation of solar radiation, ambient temperature, glass cover temperature and average rear aluminium back plate temperature with time are shown in figure 6.4.3.1. The highest solar radiation observed was 900 Wm^{-2} apart from a few sharp peaks that occurred before noon due to cloud. The peak cover glass temperature and average back plate temperatures did not respond at the same rate and time due to the thermal inertia of the metal plate and cover glass.

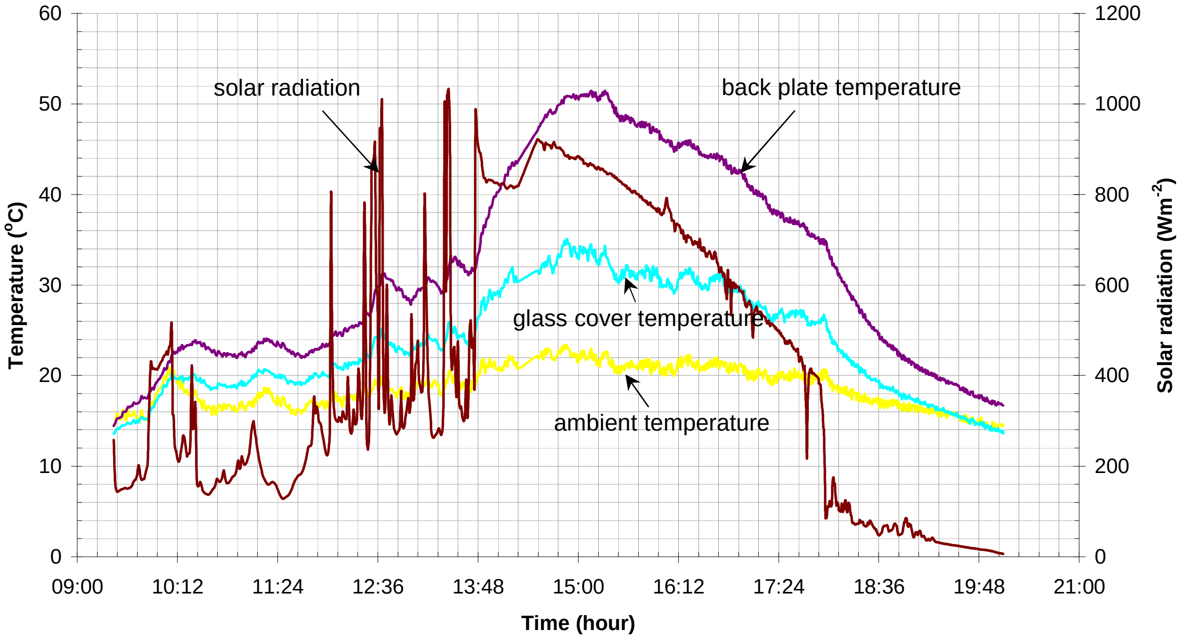

Figure 6.4.3.1 Variation of solar radiation, ambient temperature, cover glass temperature and aluminium back plate temperature with time for System 1 with six PV strings connected in series.

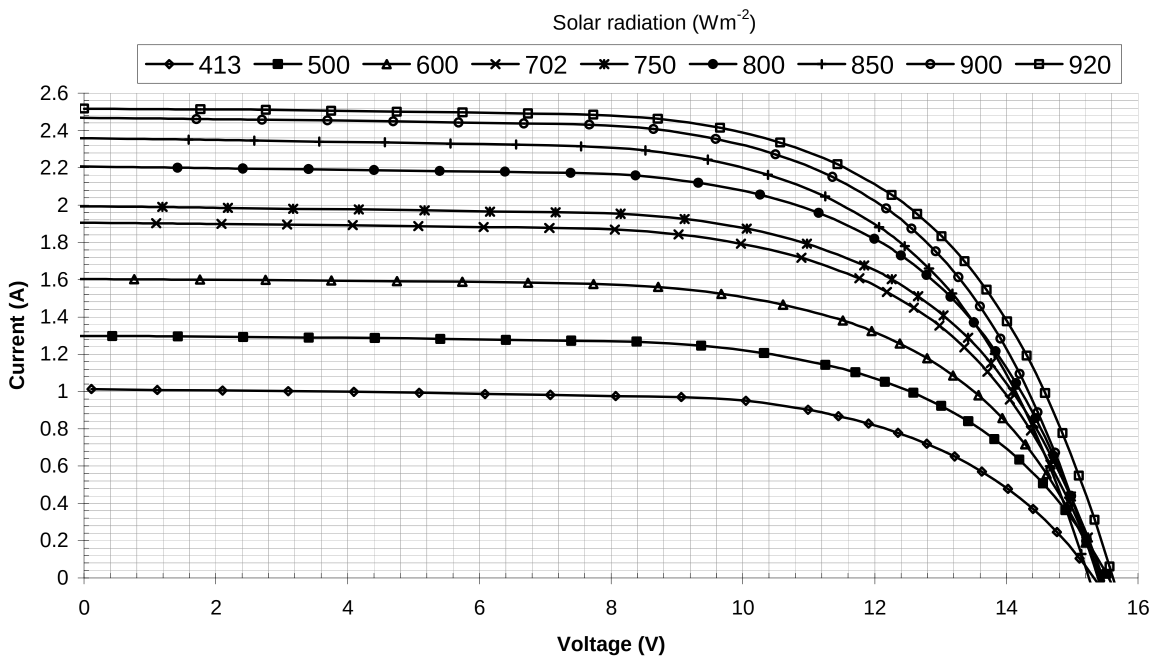

Figure 6.4.3.2 The I-V curves for different incident solar radiation intensities for System 1 with six PV strings were connected in series.

The I-V curves for different incident solar radiation intensities are shown in figure 6.4.3.2 and the corresponding voltage vs. power curves are shown in figure 6.4.3.3. At greater solar radiation intensities the maximum power point shifts towards the lower voltage due to increased PV cell operating temperature.

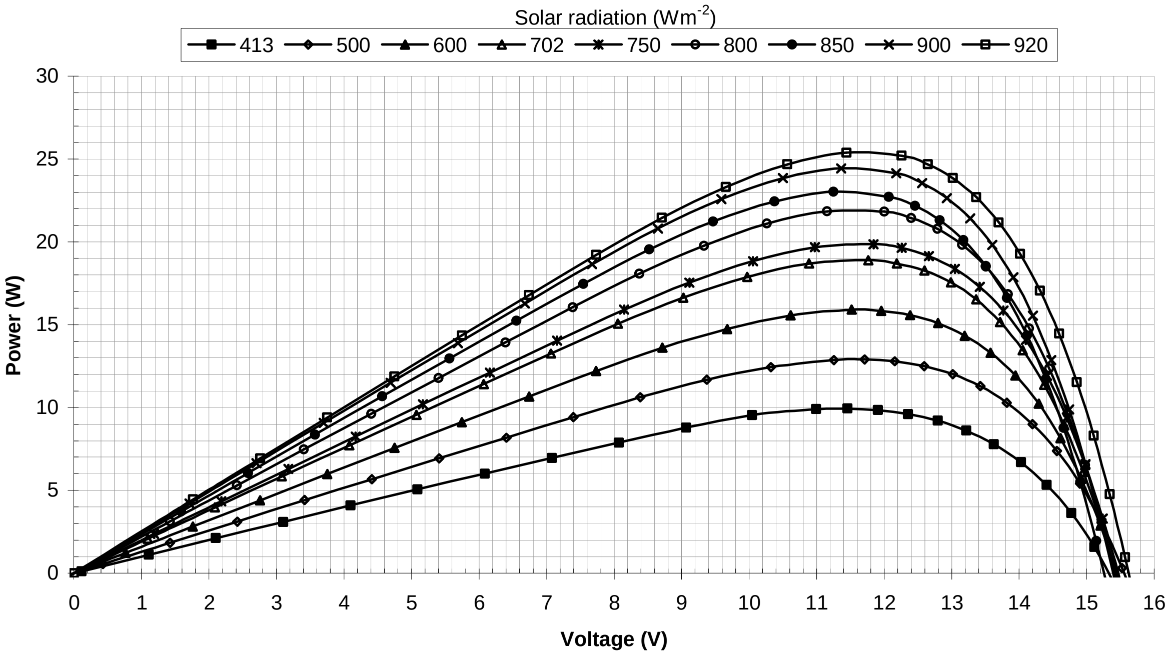

Figure 6.4.3.3 Output voltage vs. power generated for System 1 with six PV strings connected in series.

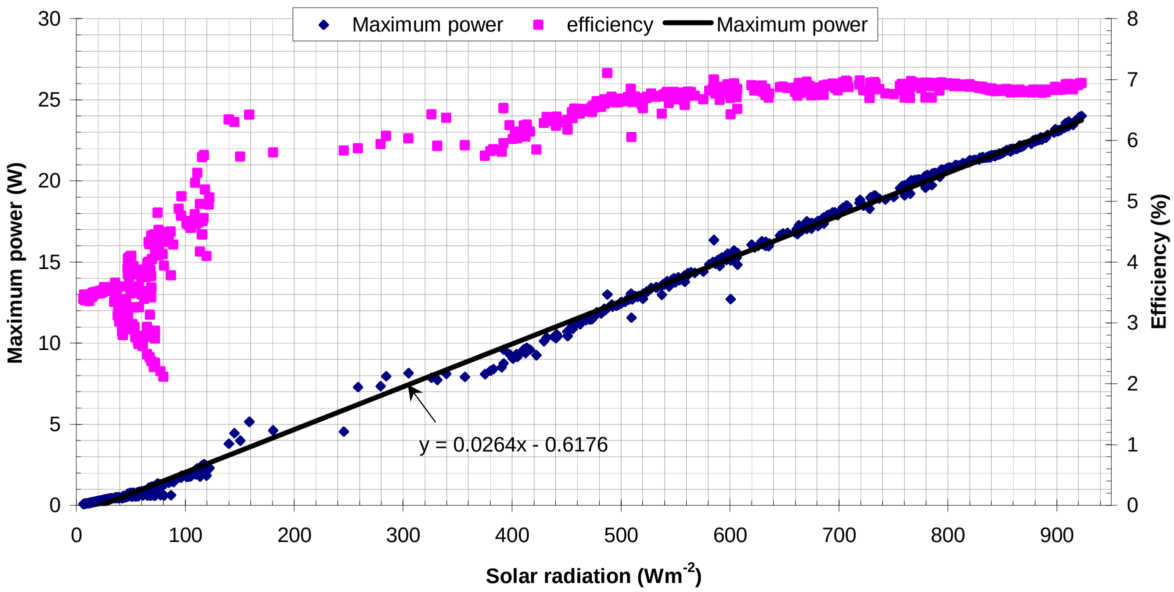

Figure 6.4.3.4 Variation of efficiency and maximum power generated with incident solar radiation by System 1 when six PV strings were connected in series.

The variation of efficiency and maximum power generated by System 1 with incident solar radiation is presented in figure 6.4.3.4. The maximum power varies linearly with incident solar radiation as expected from consideration of the PV electrical characteristics, however at lower solar radiation intensities the efficiency increased with incident solar radiation exponentially until it reached its highest value. The fill factor for the system with six PV strings connected in series for different incident solar radiation intensities is illustrated in figure 6.4.3.5. The highest fill factor of 62% was achieved for a large range of solar radiation intensities. A low fill factor implies significant electrical power losses from the system. The variation of temperature with time for the cover glass, ambient and the aluminium back plate at different thermocouple locations are illustrated in figure 6.4.3.6. The highest temperature was measured by the thermocouple at location ‘t12’ in the middle of the aluminium back plate. Heat is transferred from the back plate to the cool air flowing over it, reducing its temperature significantly. Figure 6.4.3.7 indicates that the central region of the back plate achieved the highest temperature measured compared to the sides of the back plate, due to unequal edge heat loss from the metal back plate.

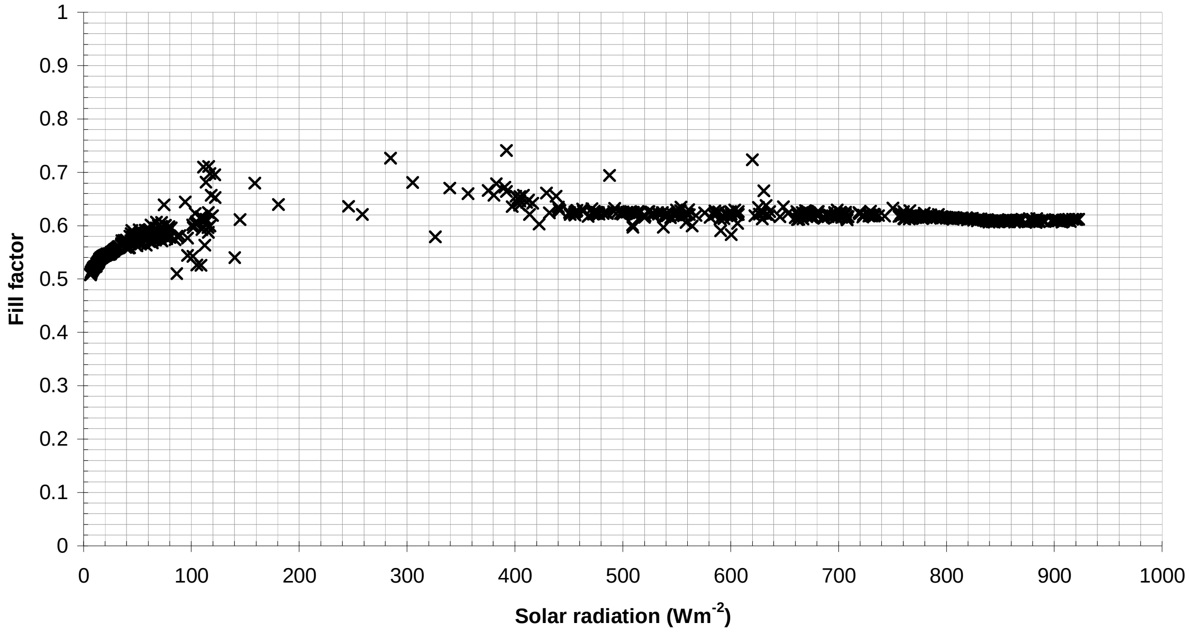

Figure 6.4.3.5 Variation in fill factor with incident solar radiation for System 1 with six PV strings connected in series.

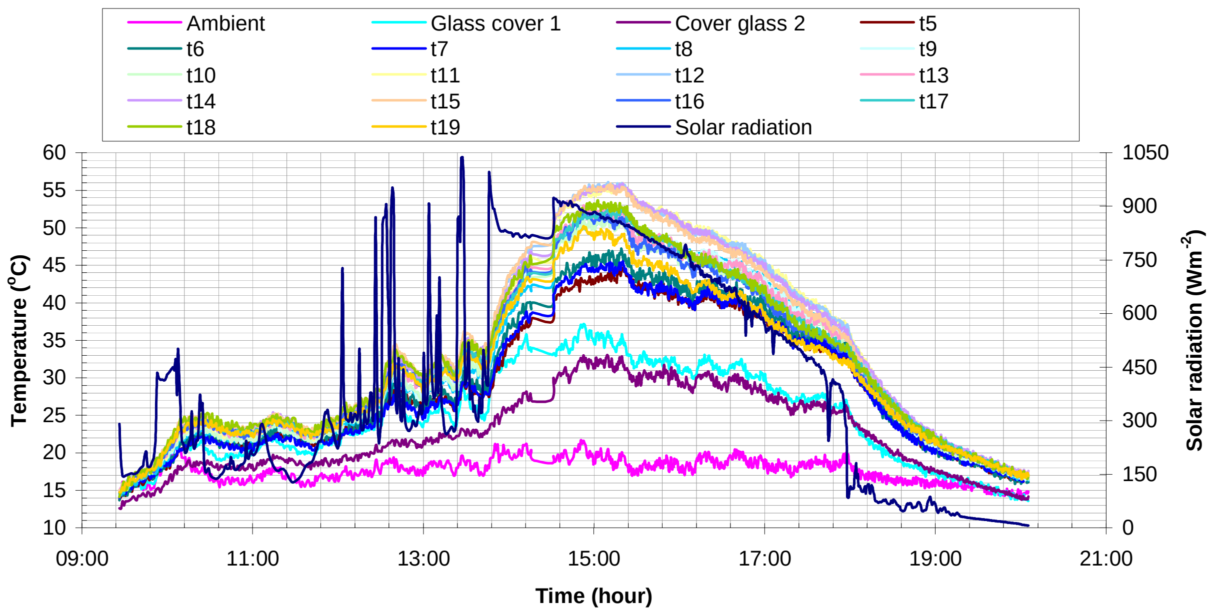

Figure 6.4.3.6 Variation in temperatures and incident solar radiation with time for System 1 with six PV strings connected in series.

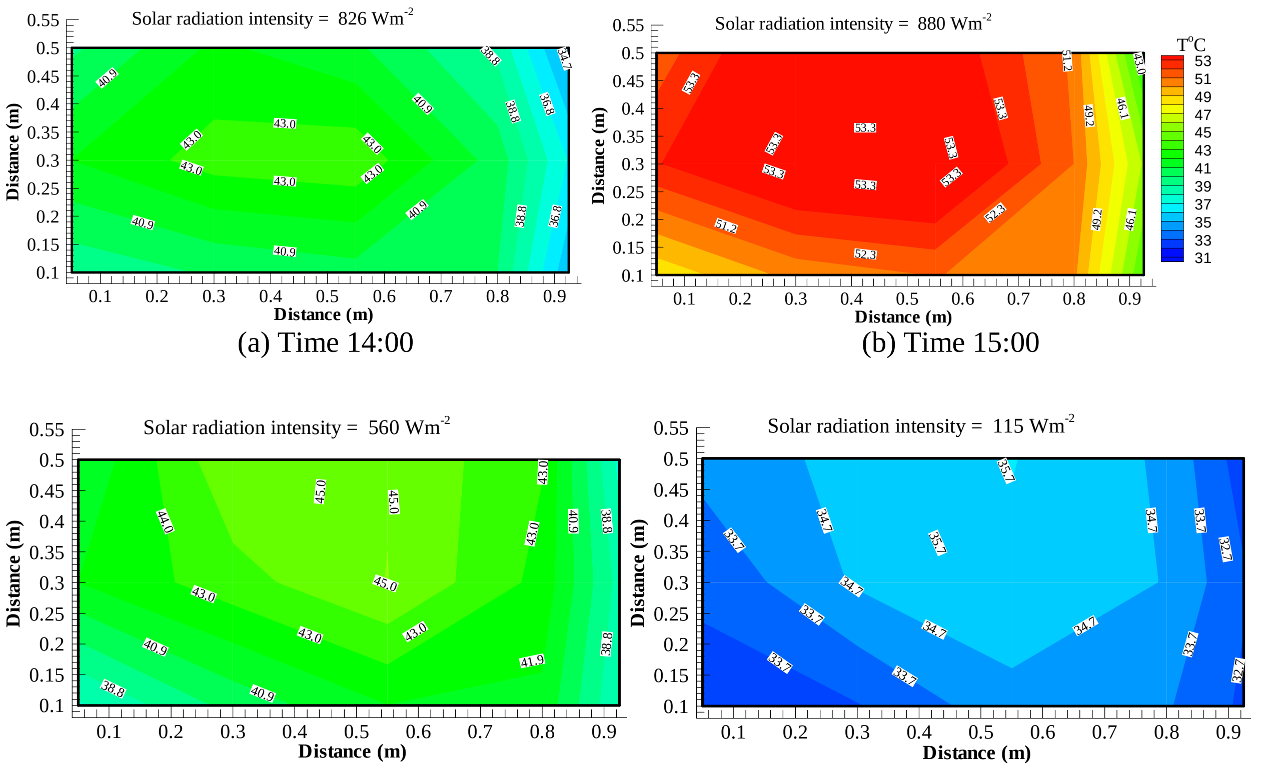

Figure 6.4.3.7 Measured temperature contours of the aluminium back plate at time (a) 14:00 (b) 15:00 (c) 16:00 (d) 18:00, on the 30th of August 2002.

6.4.4 Electrical and Thermal Performance Analysis of System 1 With Six PV Strings Connected in Series Without Concentrator Present

The reflector system was removed from System 1 to provide base data with which to compare the electrical output of the concentrator system. All the solar cell connections remained the same. The experimental investigation was conducted on the 2nd of September 2002 for six PV strings connected in series. The measurements were taken at 30 second intervals for solar radiation, wind speed, output current and voltage generated by the PV panel, glass cover temperature, ambient temperature, and aluminium back plate temperature. The variation of incident solar radiation and wind speed with time are shown in figure 6.4.4.1. The highest solar radiation recorded was 950 Wm^{-2} on the plane of the experimental test system. Lower values of solar radiation after solar noon are the result of cloud cover. The average wind speed was 1.42 ms^{-1}, which increased the convective heat transfer from the aperture cover glass and the aluminium back plate decreasing PV operating temperatures.

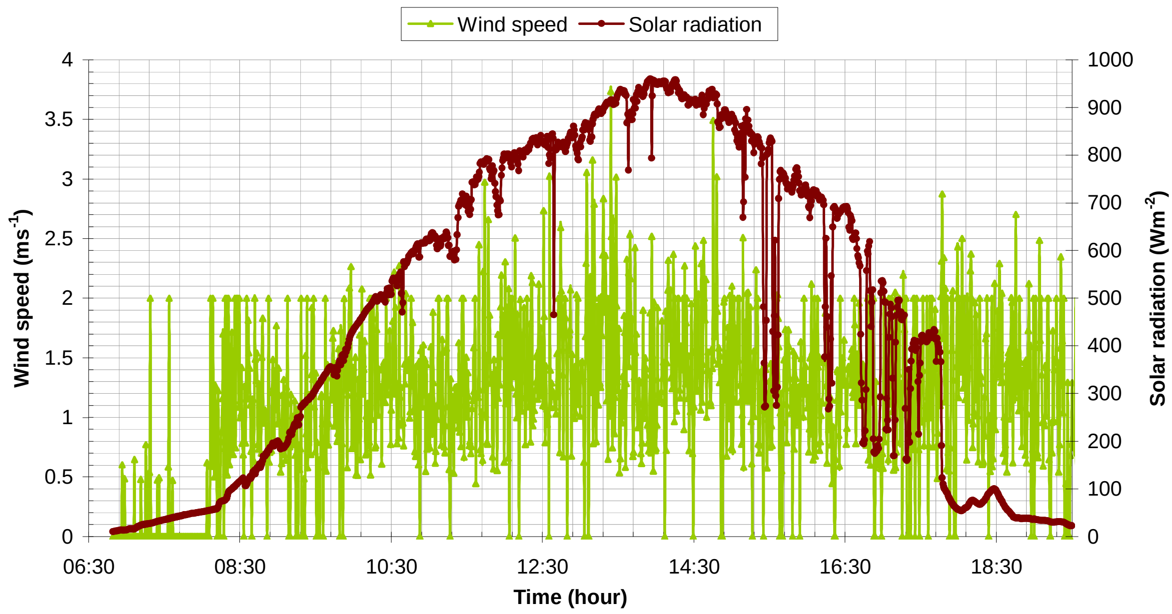

Figure 6.4.4.1 Variation of solar radiation and wind speed with time on the 2nd of September 2002.

Figure 6.4.4.2 shows the I-V curve for the system with no concentrators with six PV strings connected in series for different solar radiation intensities. Data from the non-fluctuating part of the solar radiation curve was used to plot I-V curves. One full measurement procedure for current and voltage data took 5 seconds, for which solar radiation fluctuated less than 1% (which did not effect PV output significantly). The short circuit current increases linearly with incident solar radiation intensity and the open circuit voltage remains constant as would be expected from basic solar cell characteristics. The maximum short circuit current generated by the system was 1.6 A at a solar radiation intensity of 900 Wm^{-2}, for the same PV system with concentrators the short circuit current was 2.5 A for the same incident solar radiation intensity of 900 Wm^{-2} (compare figure 6.4.3.2 and figure 6.4.4.2). The short circuit current increased by 1.56 times with the concentrator compared to the flat non-concentrating PV panel.

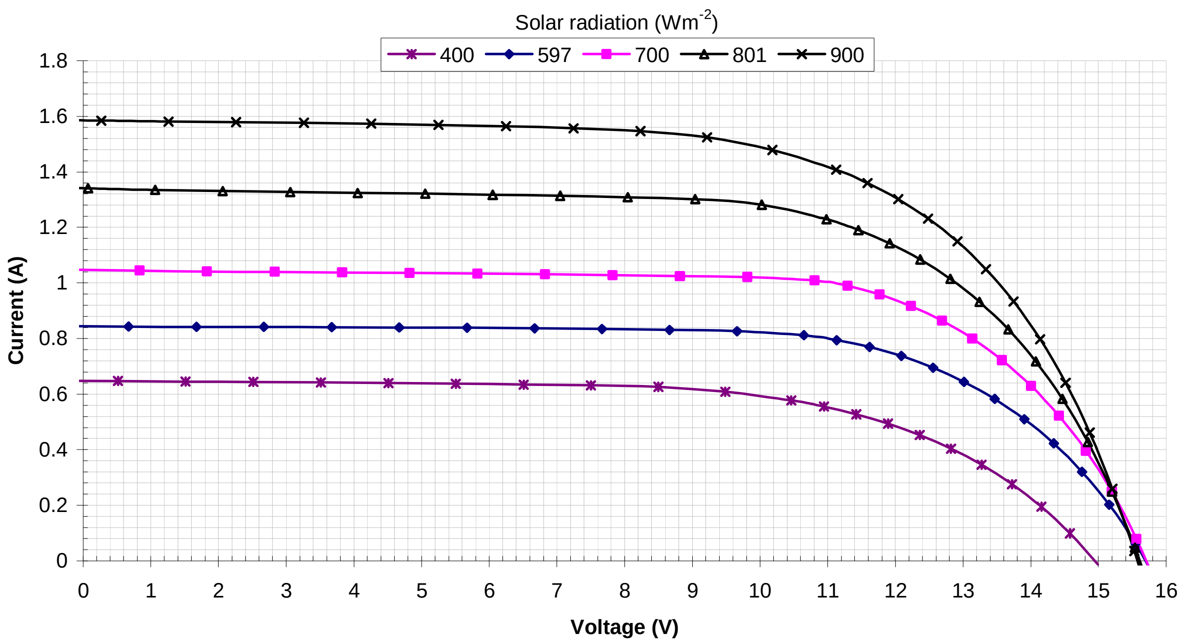

Figure 6.4.4.2 I-V curves at different solar radiation intensities for System 1 with six PV strings connected in series and the concentrator system removed.

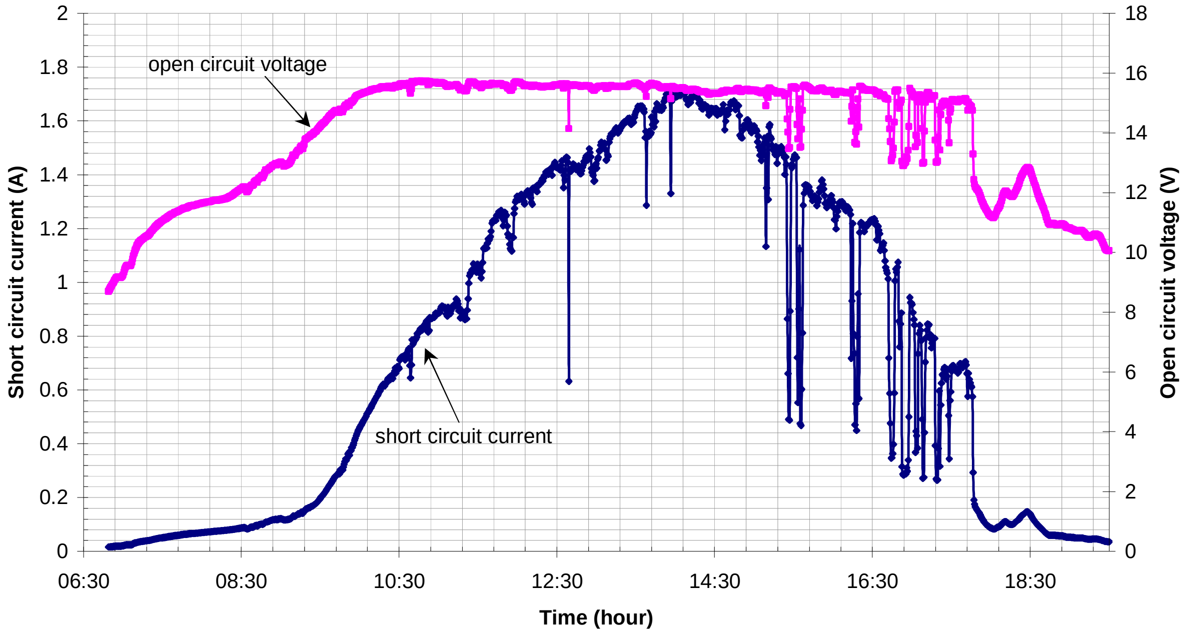

Figure 6.4.4.3 Variation of short circuit current and open circuit voltage with time for System 1 with six PV strings connected in series and concentrator system removed.

The diurnal variation of short circuit current and open circuit voltage is shown in figure 6.4.4.3. From 10:00 to 17:00 the open circuit voltage was nearly constant. This was because the open circuit voltage did not change at higher incident solar radiation intensity (the concurrent diurnal variation of insolation is shown in figure 6.4.4.1) but the short circuit current changed in a linear manner with incident solar radiation intensity. For a photovoltaic module only the solar cell area which is directly exposed to sunlight produces electricity. The wooden frame of this system created a shadow on some of the solar cells as shown in figure 6.4.1.7, decreasing the panel's power output and thus efficiency. Figure 6.4.4.4 shows the variation of maximum power generated by the panel and its efficiency with incident solar radiation intensity until 10:00. The "U" pattern of the efficiency curve can be explained by shading from the wooden frame. The maximum power point and efficiency however in general varies linearly with the incident solar radiation as shown in figure 6.4.4.5. The increase in efficiency at lower solar radiation intensities (<=500 Wm^{-2}) is due to the high voltage developed by the PV panel. The maximum efficiency achieved is 9.2% for incident solar radiation intensities of 700 Wm^{-2} to 980 Wm^{-2}. The maximum power generated by the PV system was 16.8 Watts at an incident solar radiation intensity of 970 Wm^{-2}.

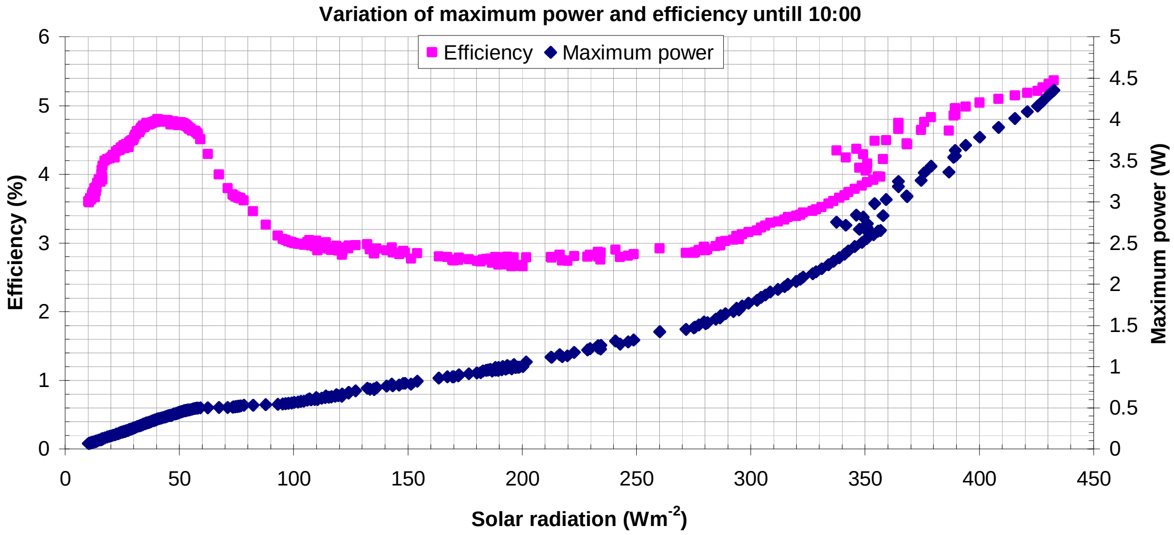

Figure 6.4.4.4 Variation of efficiency and maximum power output from System 1 with incident solar radiation, when six PV strings were connected in series and the concentrator system removed.

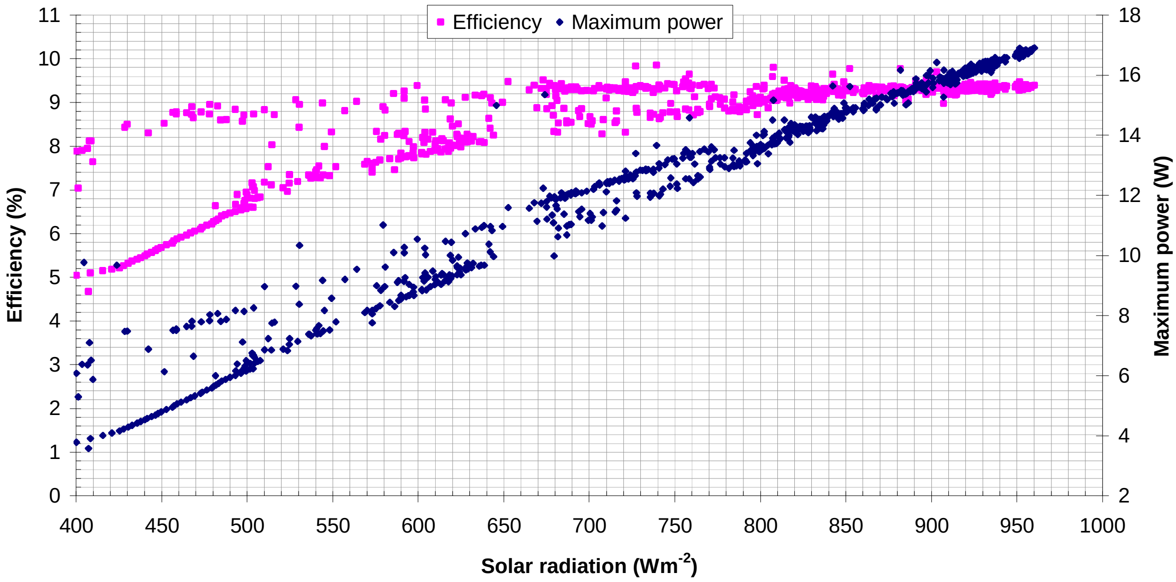

Figure 6.4.4.5 Variation of maximum power and efficiency with solar radiation intensity with six PV strings connected in series for System 1 and the concentrator system removed on the 2nd of September 2002.

Figure 6.4.4.6 illustrates the variation of ambient, cover glass and average back plate temperature with time. The peak cover glass temperature and the peak average back plate temperature do not occur simultaneously. A 40 minute delay can be seen for the peak average back plate temperature and the maximum solar radiation, illustrating the "thermal inertia" of the aluminium back plate. A peak temperature difference of 21ºC can be seen between the rear aluminium plate and the ambient temperature whereas the temperature difference between the aperture cover glass and the ambient is only 11ºC. The temperatures at the aluminium back plate are shown in figure 6.4.4.7, the maximum and minimum temperatures are shown in figure 6.4.4.8. A 4ºC temperature difference can be seen between the highest and lowest temperatures of the aluminium back plate at thermocouple positions 't8' and 't15' as shown in figure 6.3.4.

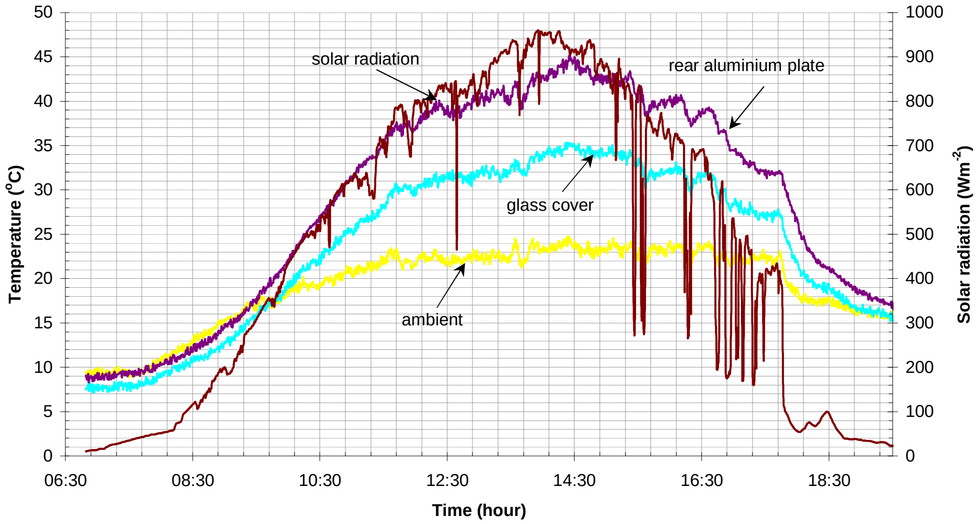

Figure 6.4.4.6 Variation of solar radiation, ambient temperature, cover glass temperature and average back plate temperature with time when six PV strings were connected in series and the concentrator system removed.

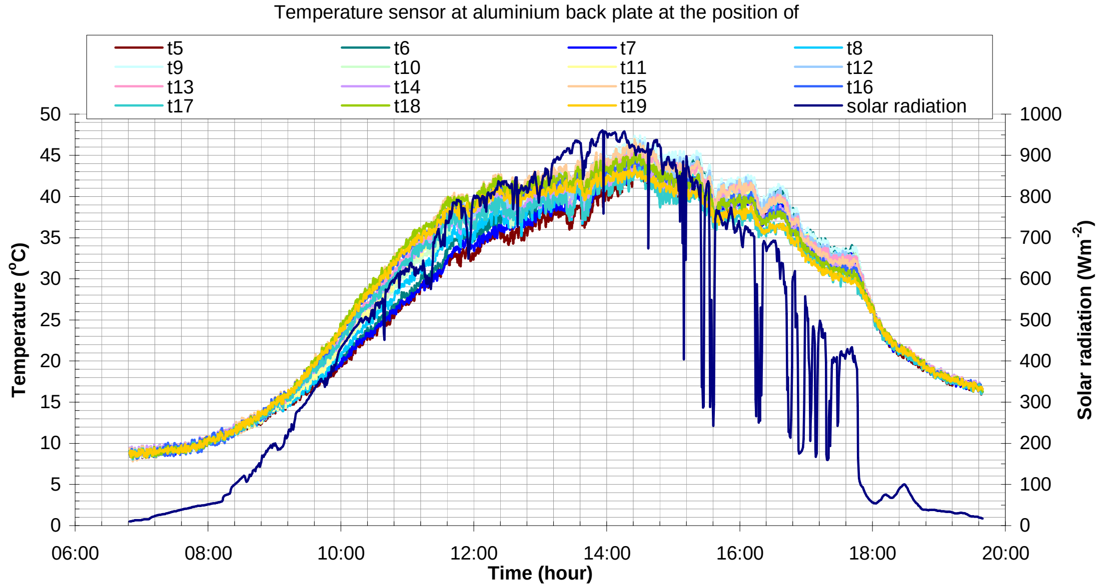

Figure 6.4.4.7 Diurnal variation of solar radiation and temperatures on the aluminium back plate for System 1 without concentrators when six PV strings were connected in series.

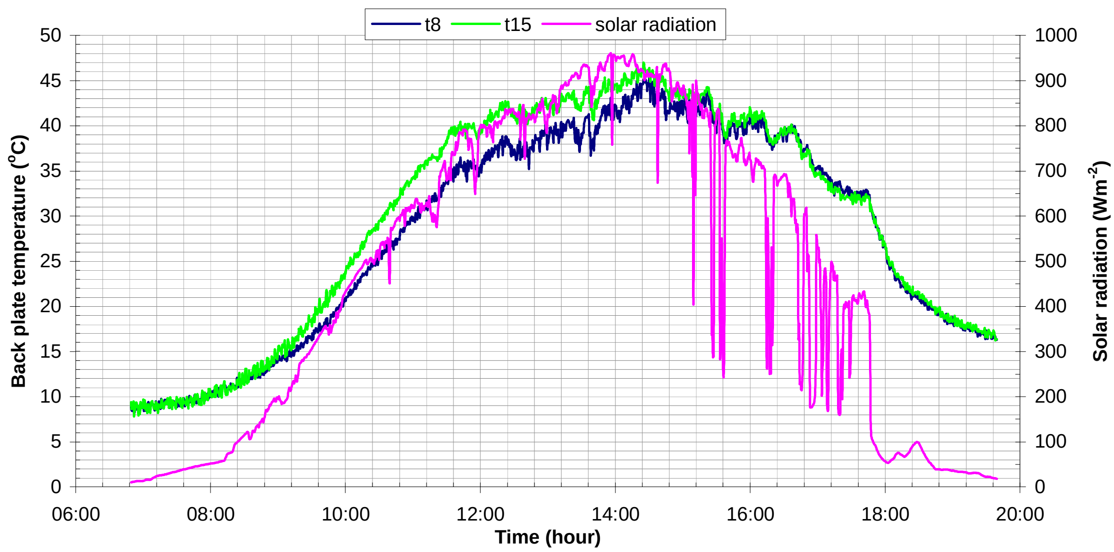

Figure 6.4.4.8 Diurnal variation of solar radiation, maximum and minimum back plate temperatures for System 1 without concentrators when six PV strings were connected in series. Thermocouples were located at the position of ‘t8’ and ‘t15’ as shown in figure 6.3.4.

6.4.5 Electrical and Thermal Performance Analysis of System 1 Without Concentrator For a Single PV String

The electrical and thermal performance of System 1 without concentrators was investigated for a single PV string with five solar cells connected in series. By measuring the open circuit voltage and short circuit current the electrical output of the 5th solar string (from the left side as shown in figure 6.3.4) was measured from 8:00 to 20:00 hour on the 6th of September 2002. The I-V curve and its corresponding voltage vs. power curve for different solar radiation intensities are shown in figures 6.4.5.1 and 6.4.5.2 respectively. The current increases linearly with incident solar radiation as can be seen from figure 6.4.5.1. The short circuit current remains almost constant at higher levels of solar radiation whereas the open circuit voltage is approximately one sixth of that for six PV strings connected in series (figures 6.4.5.1 and 6.4.4.2) as can be expected from solar cell characteristics. The maximum power point becomes approximately 15% lower when compared to six PV strings connected in series (figures 6.4.5.2 and 6.4.4.5). The maximum power point shifts towards the right side, i.e. the voltage corresponding to the maximum power point increases at higher incident solar radiation intensities.

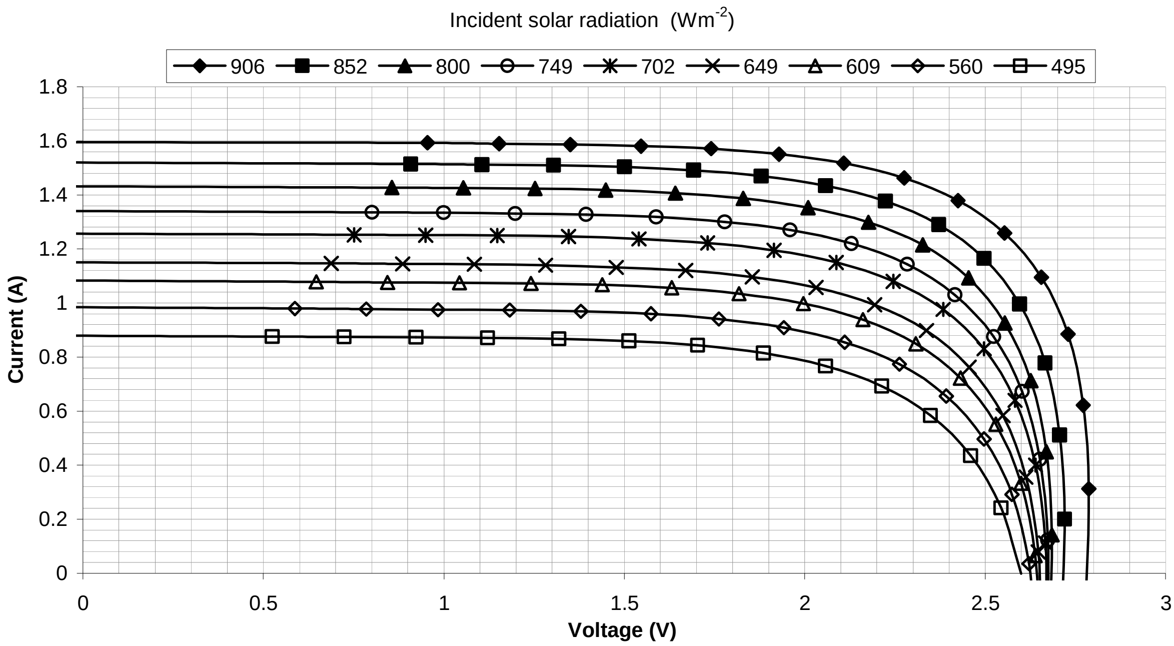

Figure 6.4.5.1 I-V curve for a single PV string without a concentrator for different solar radiation intensities. The string was the 5th from the left side as shown in figure 6.3.4.

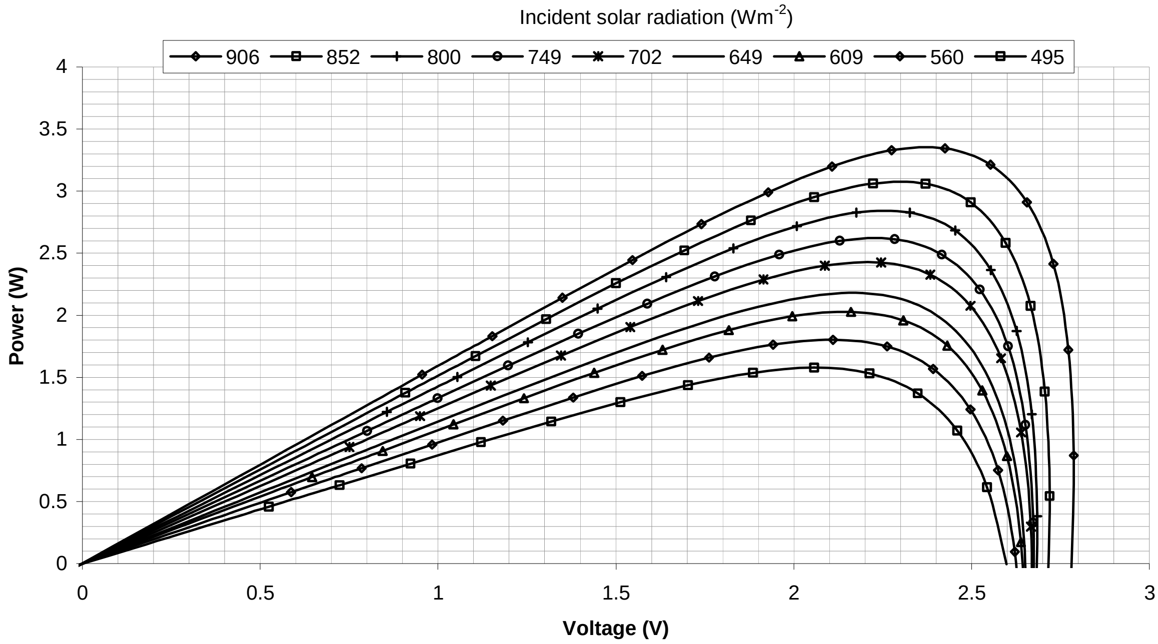

Figure 6.4.5.2 Power curve with voltage developed by a single string of five PV cells.

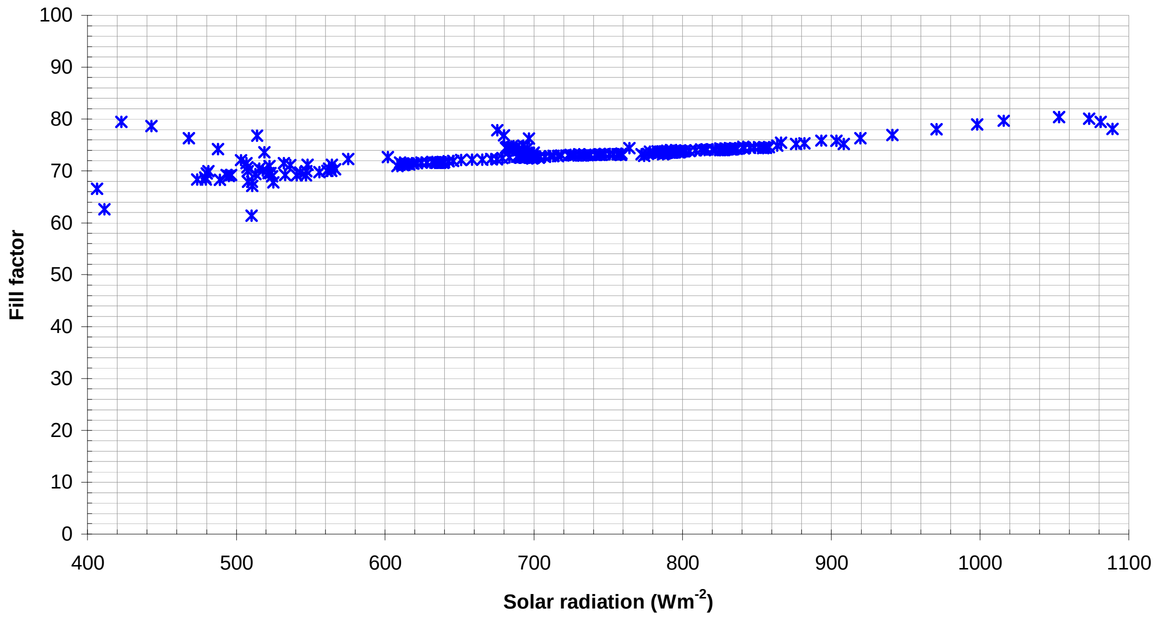

Figure 6.4.5.3 Variation of fill factor with incident solar radiation for System 1 without concentrator. A single PV string was considered for this measurement.

Figure 6.4.5.3 shows the variation of fill factor with incident solar radiation intensity for a single PV string of System 1 without a concentrator. The fill factor varies from 68% to 72% for a single string. The fill factor is relatively high compared to the PV system when two or more PV strings are connected in series. This is because of the resistive losses $\left(i^2 r\right)$ that occur between consecutive solar cell interconnections. Figure 6.4.5.4 shows the variation of open circuit voltage and short circuit current with incident solar radiation for the single PV string. As expected, the short circuit current is linearly proportional to the incident solar radiation whereas the open circuit voltage tends to a constant above an incident solar radiation intensity of 500 Wm^{-2}. Variation of efficiency and maximum power generated by the single PV string with incident solar radiation intensity are shown in figure 6.4.5.5. The highest efficiency achieved by this single PV string was 11.5% which is higher when compared to multiple PV strings connected in series. This is due to the higher $\left(i^2 r\right)$ losses for multiple PV strings connected in series.

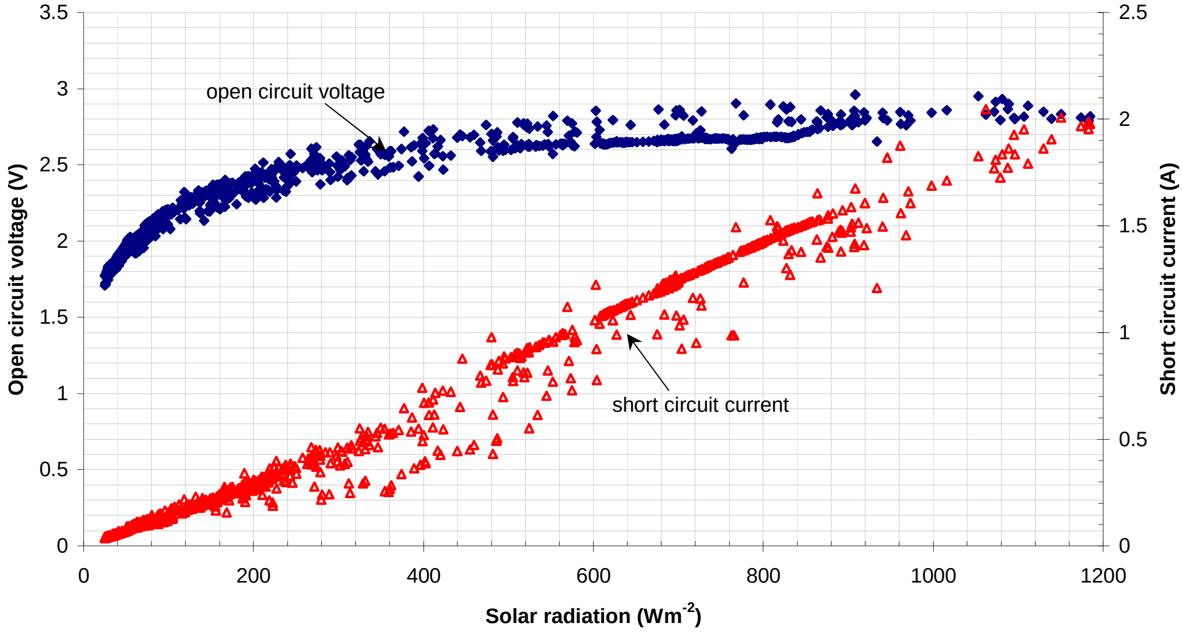

Figure 6.4.5.4 Variation of open circuit voltage and short circuit current with incident solar radiation for a single PV string of System 1 without concentrator.

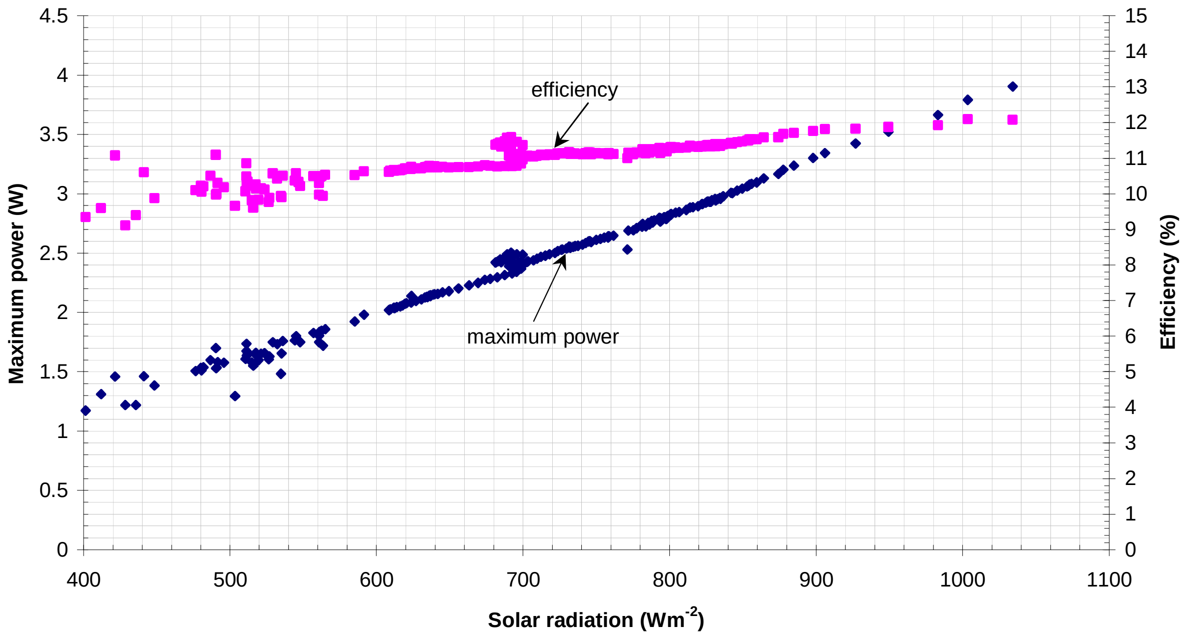

Figure 6.4.5.5 Effect of maximum output power and efficiency with incident solar radiation for a single PV string of System 1 without concentrator.

6.4.6 Electrical and Thermal Performance Analysis of a Flat Non-Concentrating PV Panel and an ACPPVC-50 Panel Mounted Vertically for Five PV Strings Connected in Series

An experimental investigation was undertaken for two systems with different numbers of PV strings connected in series. The first system was a flat non-concentrating system and the second system was the concentrator (ACPPVC-50) system. The systems characterised experimentally are shown in figure 6.4.6.1, the system on the left side is System 1 (fabricated first), characterised experimentally with and without concentrators described in the earlier sections of this chapter. This experimental investigation was conducted on the 20th of September 2002 with the measurements taken for twelve hours from 8:00 to 20:00 with 20 second intervals between consecutive sets of data points.

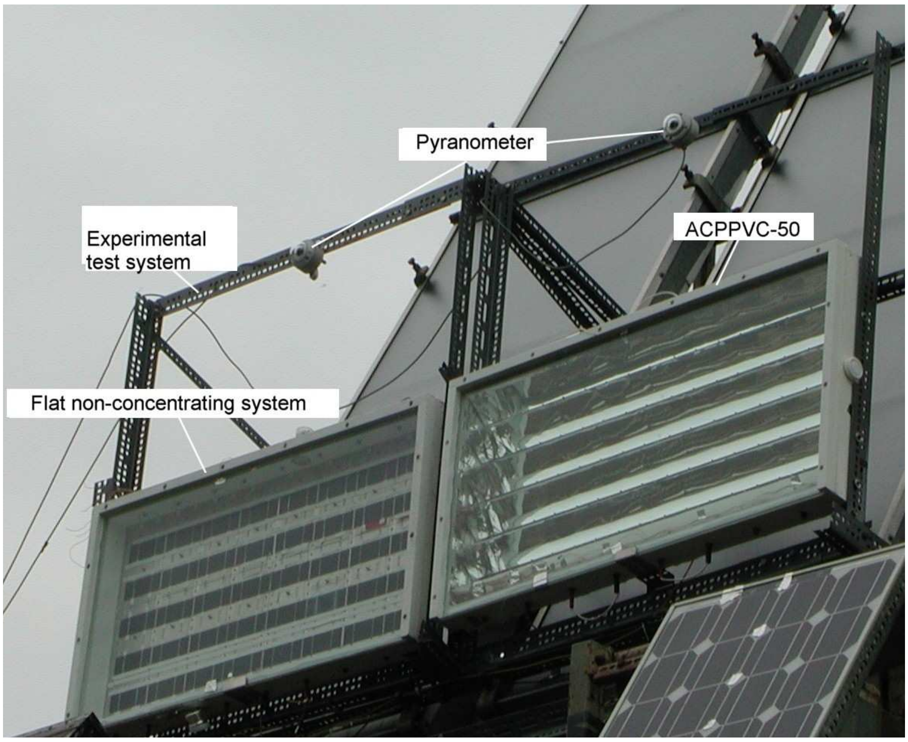

Figure 6.4.6.1 Flat non-concentrating and asymmetric compound parabolic photovoltaic concentrators under outdoor experimental characterisation at the University of Ulster. Both systems are identical with equal numbers of PV cells connected in series in each systems.

Figure 6.4.6.2 shows total and diffuse solar radiation measured on the plane of the experimental test systems. The maximum total radiation was 800 Wm^{-2} and the diffuse radiation was 240 Wm^{-2}. The variation of short circuit current and open circuit voltage with time for both flat non-concentrating system and the ACPPVC-50 are presented in figure 6.4.6.3. The open circuit voltage was 0.4 V higher for the ACPPVC-50 compared to the flat non-concentrating panel whereas the short circuit current for the ACPPVC-50 was approaching to the value of its theoretical concentration ratio of 2.0. This is due to the effective solar radiation at the PV surface for the ACPPVC-50 increased by its concentration ratio 2.0. The major problem with this experimental characterisation is the shadow cast by the top wooden frame since the PV systems are orientated vertically and therefore cast a shadow on the solar cells, effectively decreasing the output power of the system. The shadows created by the wooden frame for the flat non-concentrating PV system and the ACPPVC-50 system are shown in figure 6.4.6.4.

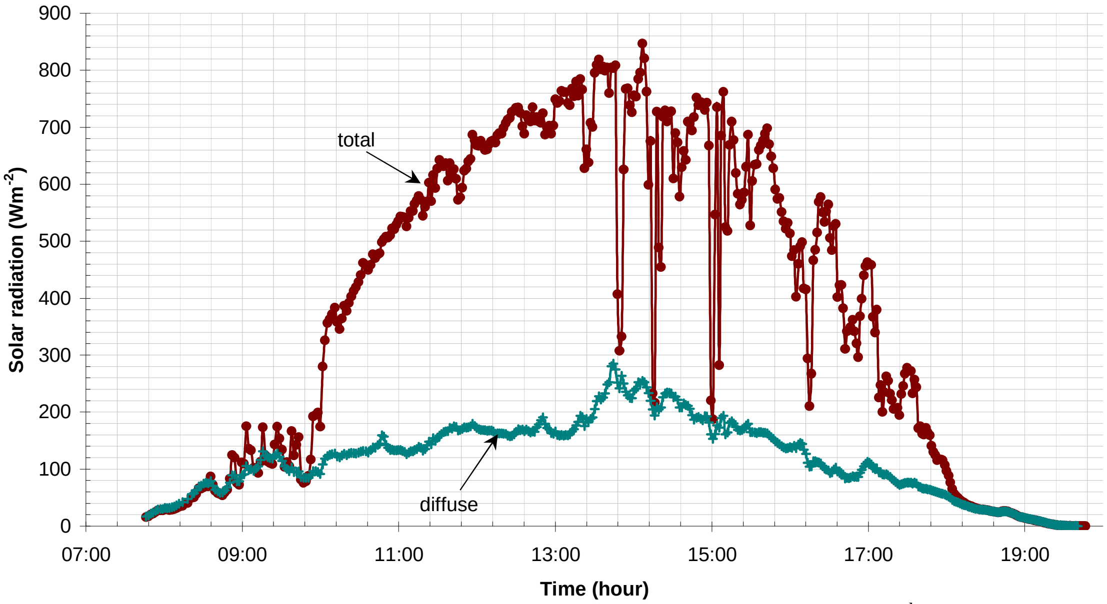

Figure 6.4.6.2 The variation of total and diffuse radiation with time on the 20th of September 2002.

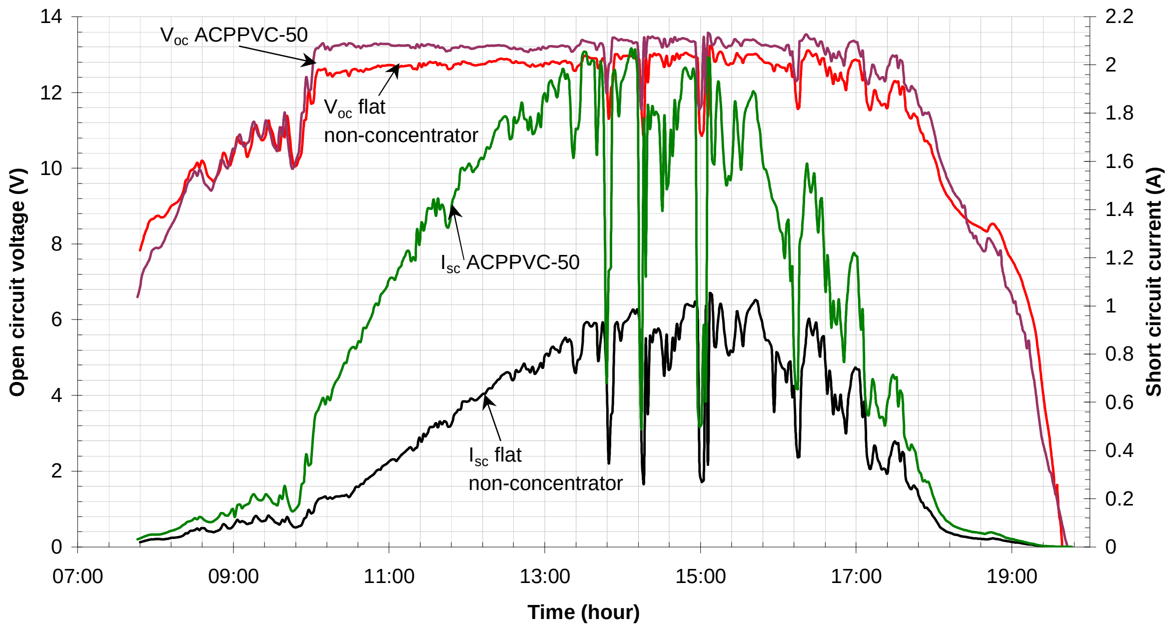

Figure 6.4.6.3 Short circuit current and open circuit voltage for the flat non-concentrating and the concentrating ACPPVC-50 with time on the 20th of September 2002.

(a) (b)

Figure 6.4.6.4 Shadow cast by the wooden frame on the top most solar cells for (a) the flat non-concentrating system and (b) the ACPPVC-50 at noon on the 20th of September 2002.

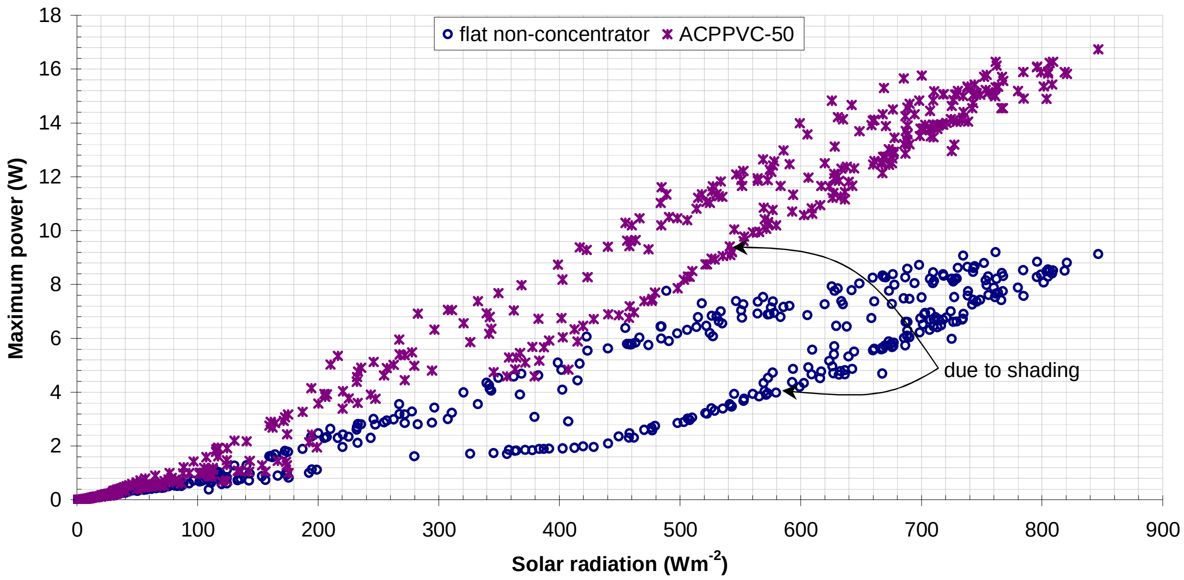

Figure 6.4.6.5 Variation of maximum power output for the flat non-concentrating and the concentrating ACPPVC-50 system with solar radiation intensity.

Figure 6.4.6.5 shows that the variation of maximum power generated by the flat non-concentrating PV panel and the ACPPVC-50 panel with incident solar radiation intensity. Each maximum power curve has two distinct lines between solar radiation intensities of 200 to 700 Wm^{-2}, this is due to the shadow from the supporting frame. Apart from an east-west shadow cast by the wooden frame, a third shadow fell on the PV solar cells as shown in figure 6.4.6.4 when the PV systems were mounted in the vertical plane. A portion of the top reflector in the ACPPVC-50 reflects incident solar radiation which becomes more effective compared to the flat non-concentrating PV panel, as a result a significant difference in the maximum power curve can be seen at lower incident radiation intensities. The upper line of the power curve at solar radiation intensities from 200 to 700 Wm^{-2} refers to the power obtained by the PV panels when there was no shadow cast on the PV cells. The consequences of this shading effect are lower efficiencies for the systems as shown in figure 6.4.6.6. The highest achieved efficiency for the flat non-concentrating PV panel was 8% whereas the efficiency for the ACPPVC-50 was 6.6% at incident solar radiation intensities from 400 to 500 Wm^{-2}. This is because at higher incident solar radiation intensities the solar cell temperature increases which decreases the open circuit voltage of the PV panel and thus the PV panel efficiency. Figure 6.4.6.7 shows the power ratio between the flat and concentrating PV panels. Although the concentrating PV panel has higher power losses $\left(i^2 r\right)$ resulting from a higher current compared to the flat panel, the maximum power ratio is 1.8 or more because of the partially shaded solar cells in the non-concentrating panel as shown in figure 6.4.6.4.

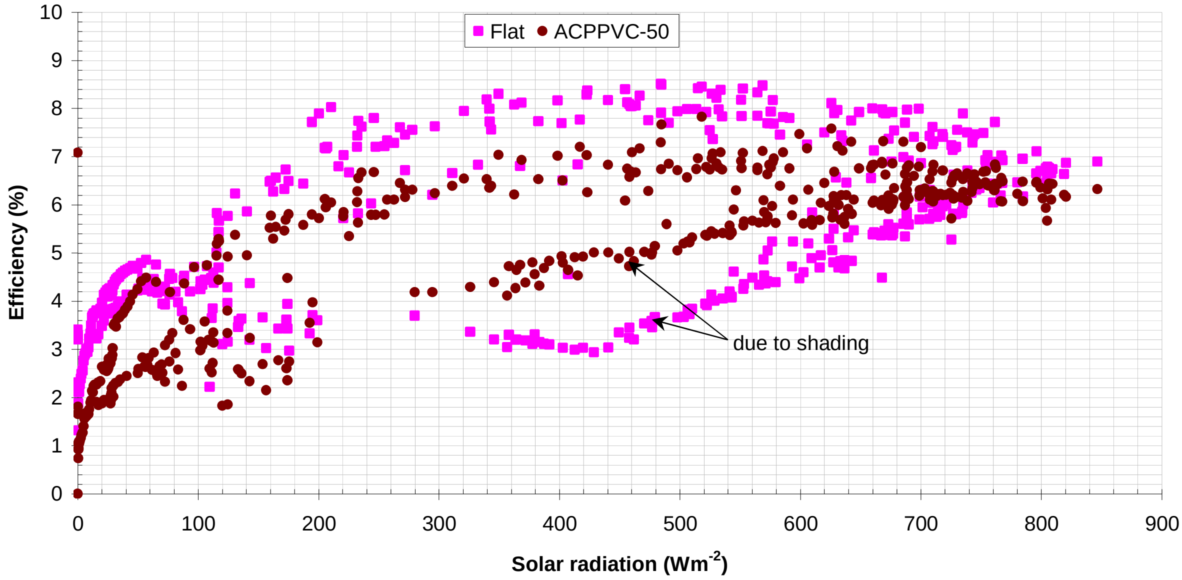

Figure 6.4.6.6 Effect of efficiency with incident solar radiation for the flat non-concentrating PV panel and the ACPPVC-50 system with six PV strings connected in series.

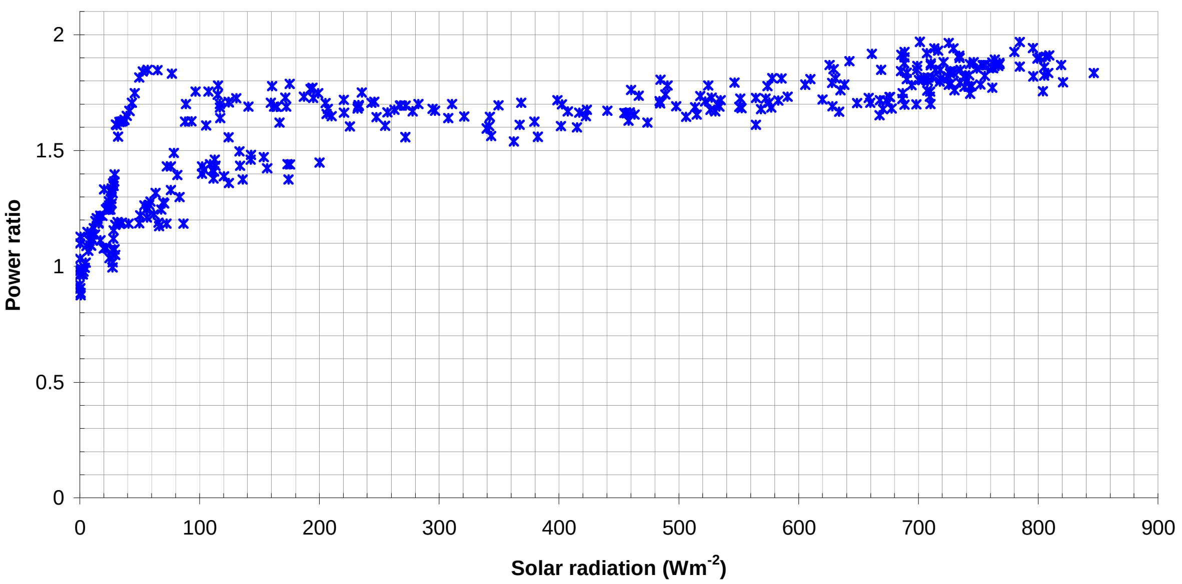

Figure 6.4.6.7 Maximum power point ratio of the flat non-concentrating PV panel and the ACPPVC-50 system with incident solar radiation for six PV strings connected in series.

The variation of reflector temperature and solar cell temperature are shown in figures 6.4.6.8 and 6.4.6.9 respectively. The solar cell temperature was measured by attaching a thermocouple at the edge of the solar cell, whereas the thermocouples were attached inside the reflector trough for reflector substrate temperature as shown in figure 6.3.3. The peak temperature difference between the reflector back plate and the solar cell was 3ºC. The maximum reflector back plate temperature was 48ºC, the maximum solar cell temperature was 46ºC for the concentrating PV panel. The peak temperature difference between the highest and lowest reflector back plate temperatures was 8ºC at thermocouple positions 'tr43' and 'tr38', the peak solar cell temperature difference between the highest and lowest solar cell temperatures was 13ºC at thermocouple positions 'ts48' and 'ts38'. Due to the temperature gradient along the solar cell, a power drop occurred which decreased the PV panel efficiency.

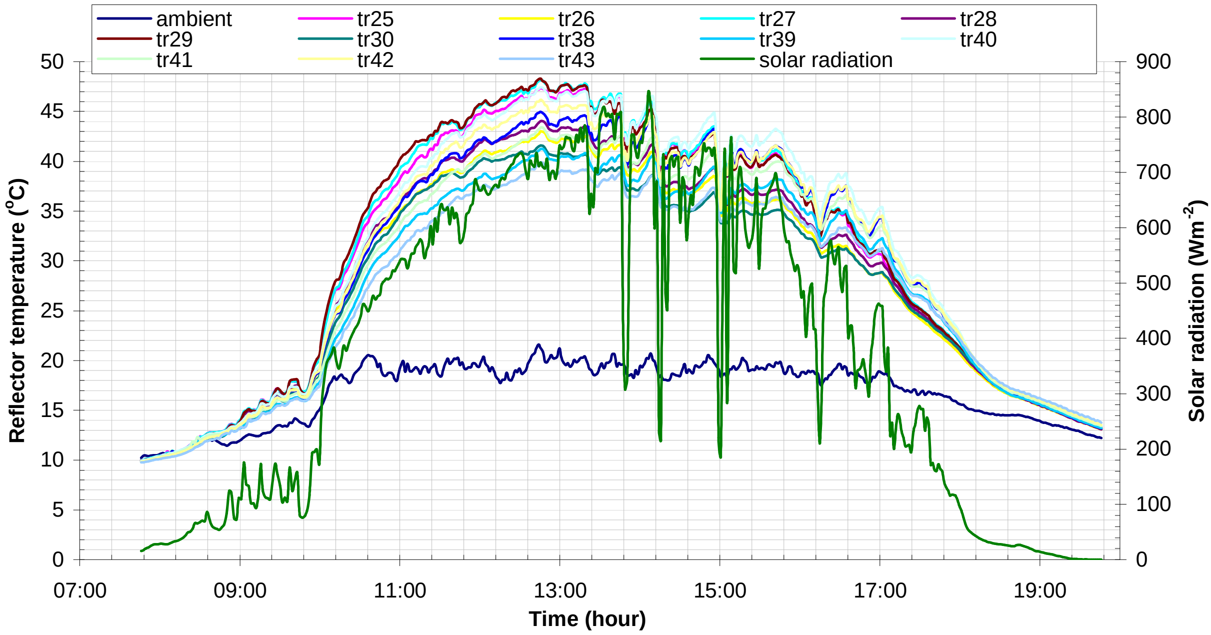

Figure 6.4.6.8 Diurnal variation of solar radiation and reflector substrate temperature for the ACPPVC-50. The thermocouples were connected inside the reflector troughs as shown in figure 6.3.3.

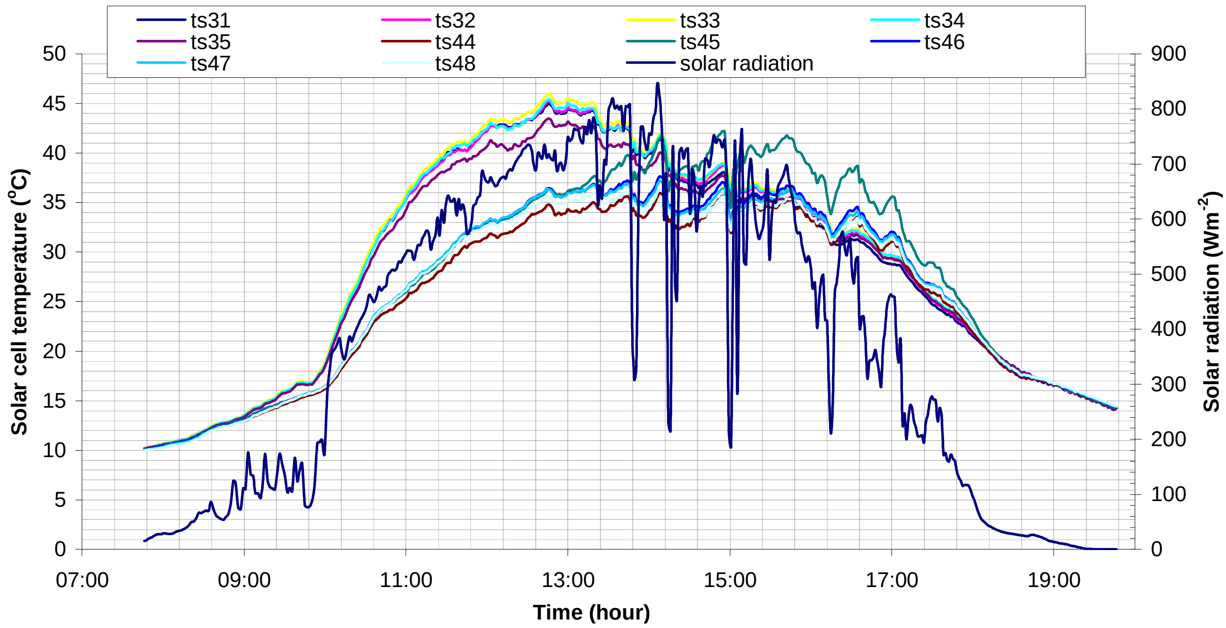

Figure 6.4.6.9 Diurnal variation of solar radiation and solar cell temperature for the ACPPVC-50. The thermocouples were connected at the edges of the solar cells as shown in figure 6.3.3.

The temperatures of the aluminium back plate for both the concentrating ACPPVC-50 and the flat non-concentrating system with time are shown in figures 6.4.6.10 and 6.4.6.11. Back plate temperatures varied in a similar way with time for both systems. Thermocouple locations are shown in figures 6.3.4 and 6.3.5. The highest back plate temperature of 44°C for the ACPPVC-50 occurred at thermocouple position 't62', for the flat non-concentrating PV system the highest temperature was 41°C. As expected for both systems the maximum temperatures occurred close to the central position. The thermal edge loss and the shading factor close to the edge solar cells resulted in lower temperatures compared to the central region of the aluminium back plate.

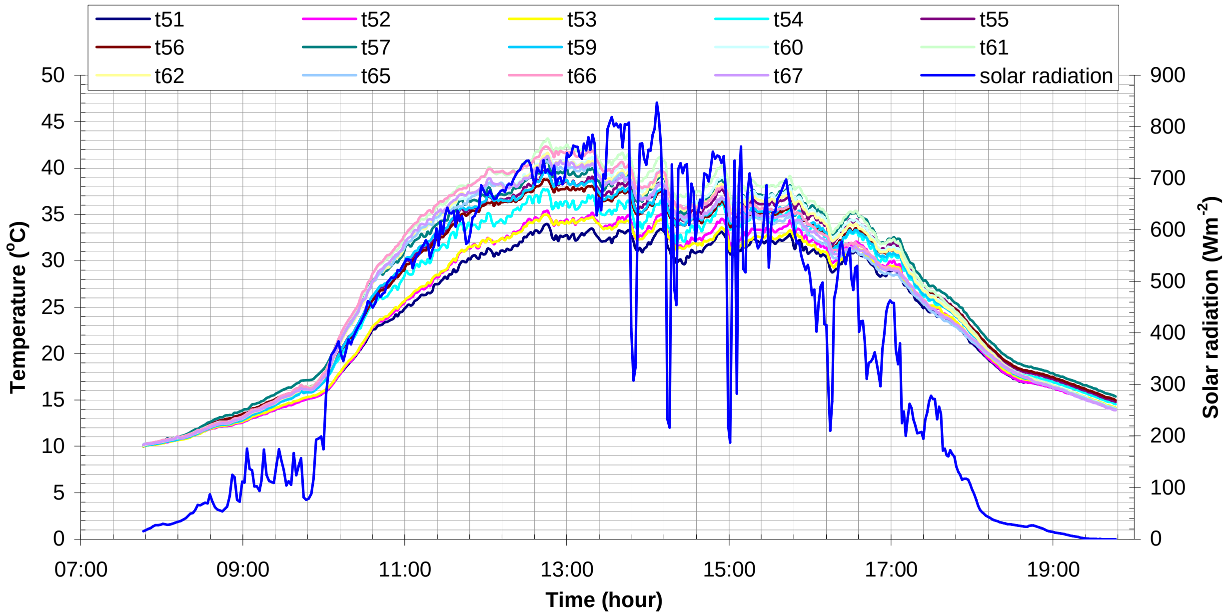

Figure 6.4.6.10 Diurnal variation of solar radiation and aluminium back plate temperature for the ACPPVC-50 system. The thermocouples were located as shown in figure 6.3.5.

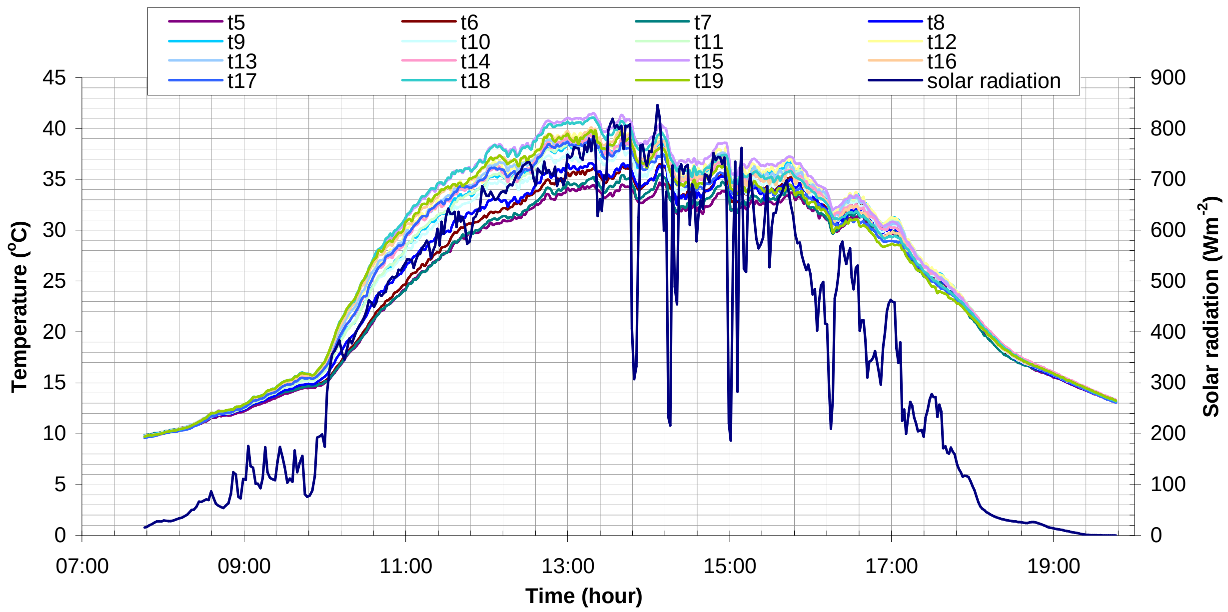

Figure 6.4.6.11 Diurnal variation of solar radiation and aluminium back plate temperature for the flat non-concentrating PV panel. The thermocouples were located as shown in figure 6.3.4.

6.4.7 **Electrical and Thermal Performance Analysis of a Flat Non-Concentrating PV Panel and an ACPPVC-50 Concentrating Panel Mounted at 18° to the Vertical for Four PV Strings Connected in Series**

Experimental investigations were undertaken for 18° inclined system to reduce shading on the top row of solar cells. This avoids power losses which otherwise occur due to the shaded top row of solar cells. Four PV strings were connected in series for this experiment. The test was conducted on the 23rd of September

2002 and the measurements were taken over an eleven and a half hour period. The I-V curves for the flat non-concentrating and the ACPPVC-50 systems for different incident solar radiation intensities are shown in figures 6.4.7.1 and 6.4.7.2 respectively. Since only four rows of PV strings were connected for both systems, there were no shaded solar cells from the supporting frame in the east-west direction. The flattening of the I-V curve near to the maximum power point can be explained by the extra power drop across the relay card and the resistive losses in each component because the current to voltage ratio.

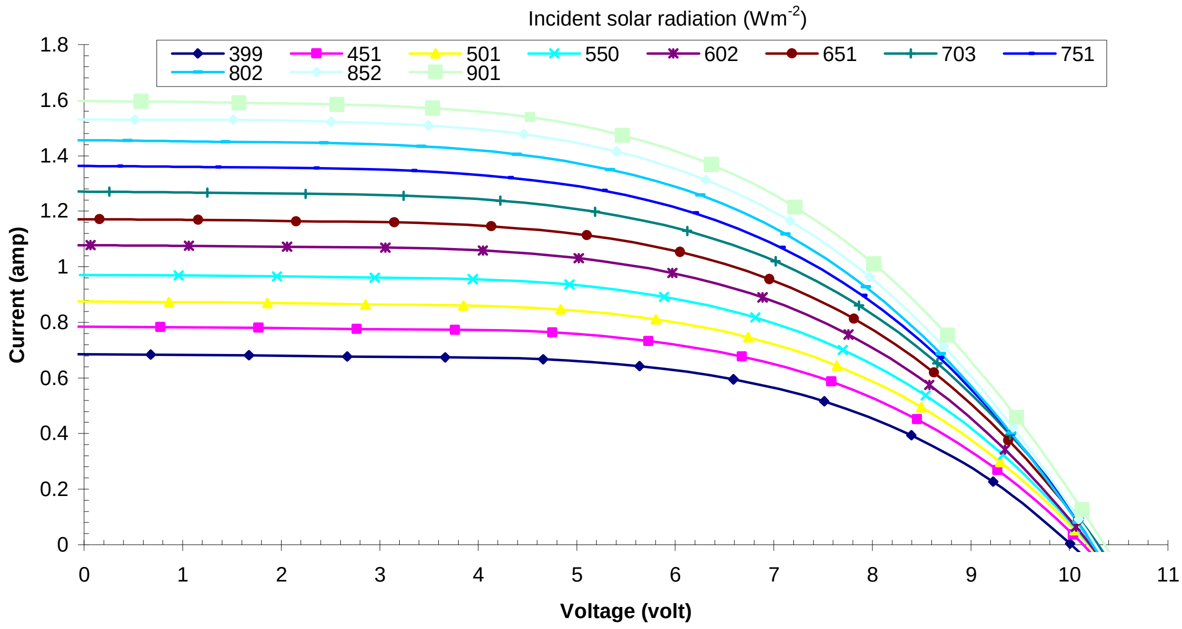

Figure 6.4.7.1 I-V curves for different intensities of solar radiation for the flat non-concentrating system with four PV strings connected in series.

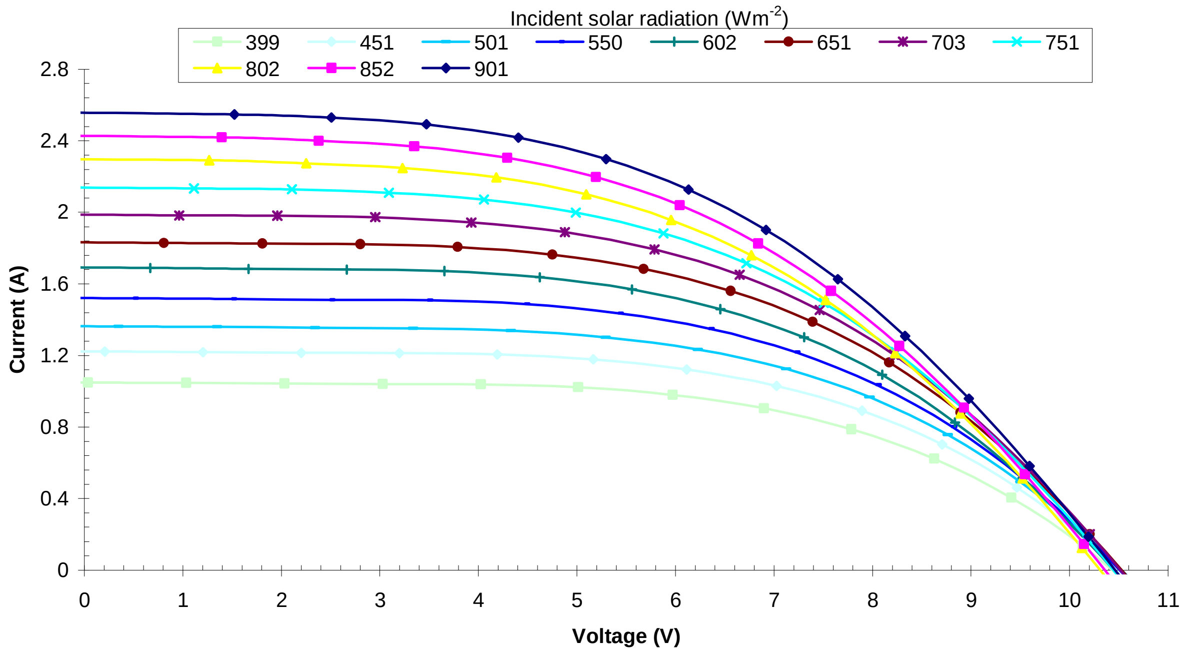

Figure 6.4.7.2 I-V curves for different intensities of solar radiation for the ACPPVC-50 system with four PV strings connected in series.

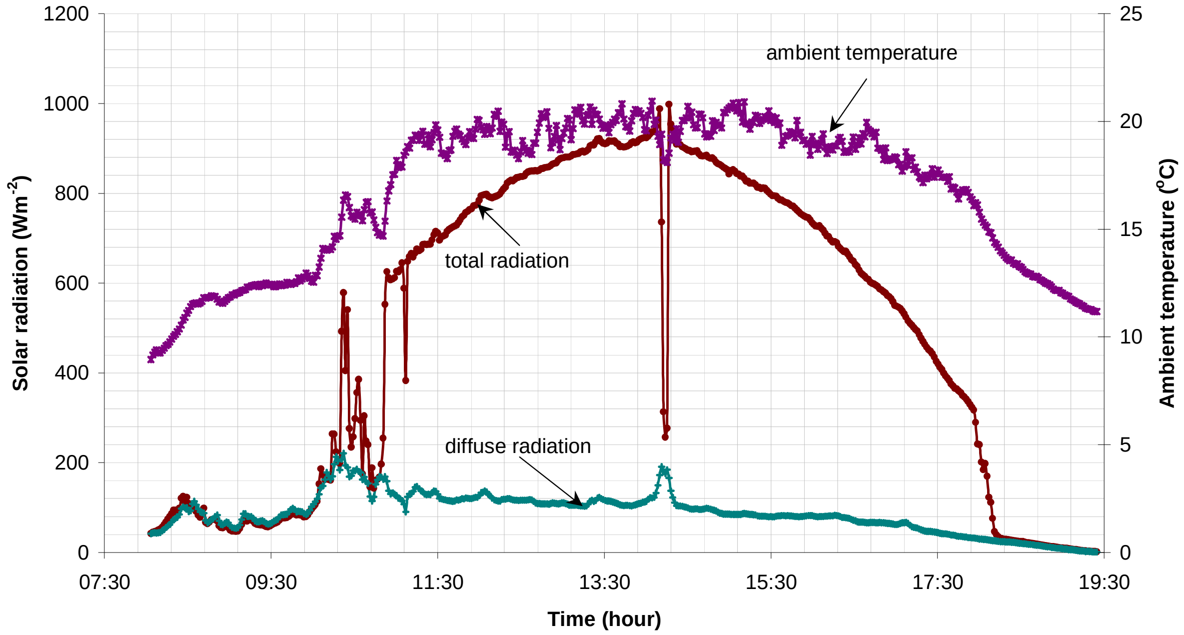

Figure 6.4.7.3 Variation of total radiation, diffuse radiation and ambient temperature with time on the 23rd of September 2002.

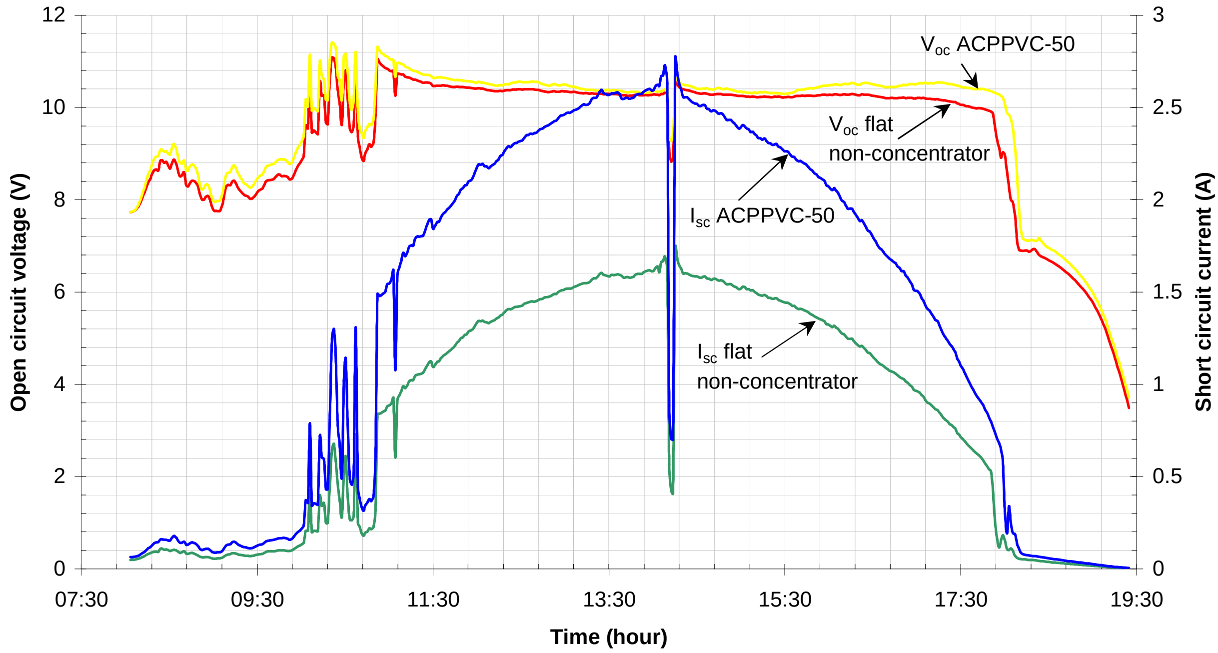

Figure 6.4.7.4 Variation of short circuit current and open circuit voltage for the flat non-concentrating PV panel and the concentrating ACPPVC-50 system with time. Four PV strings were connected in series for both systems.

Figure 6.4.7.3 shows that the variation of total solar radiation, diffuse radiation and ambient temperature with time on the 23rd of September 2002. The maximum total radiation recorded was 960 Wm^{-2} on the plane of the test system and the maximum diffuse radiation was 200 Wm^{-2}. The maximum ambient temperature was 21°C. The variation of short circuit current and open circuit voltage for both the flat non-concentrating and the concentrating ACPPVC-50 systems are shown in figure 6.4.7.4. The open circuit voltage is nearly constant for both PV panels whereas the short circuit current increases linearly with incident solar radiation intensity.

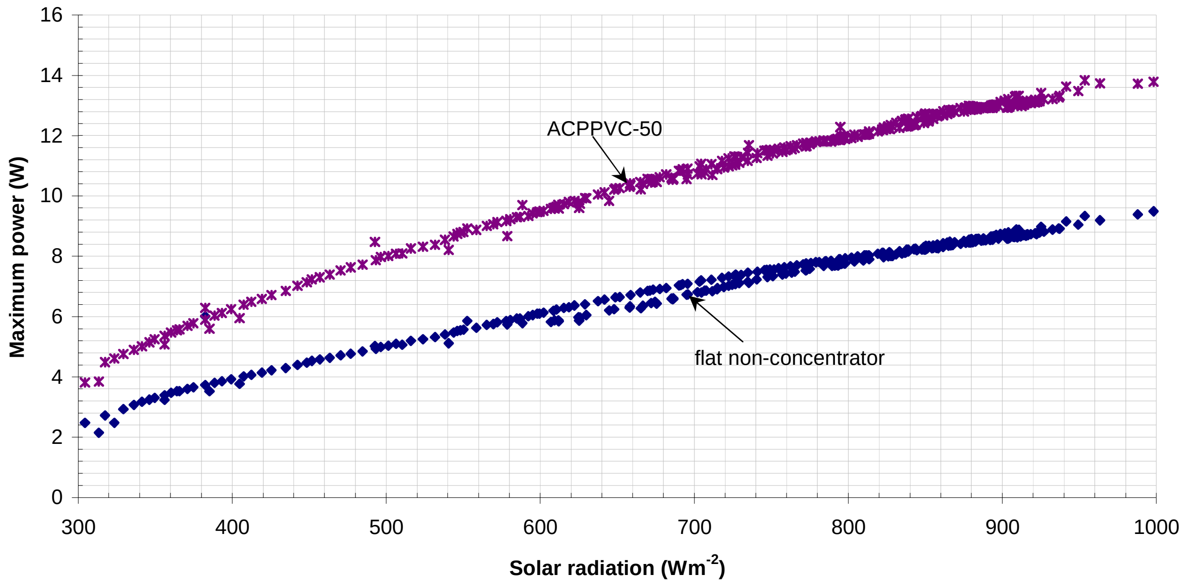

Figure 6.4.7.5 Maximum power point for the flat non-concentrating and the concentrating ACPPVC-50 systems with incident solar radiation intensity.

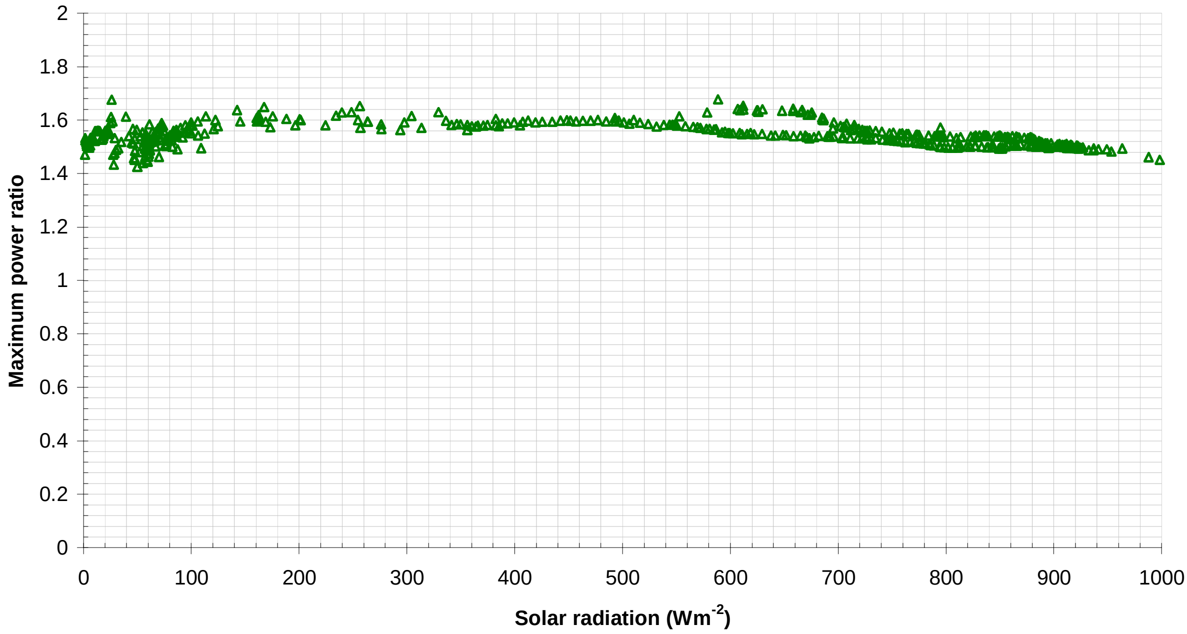

Figure 6.4.7.6 Maximum power point ratio for the flat non-concentrating and the concentrating ACPPVC-50 systems with incident solar radiation intensity.

Figure 6.4.7.5 shows the maximum power point for the flat non-concentrating system and the ACPPVC-50 system with incident solar radiation intensity. For a concentration ratio of 2.0, the effective solar radiation intensity at the absorber will increase by a factor of 2 if the optics are perfect i.e. perfect geometry and no reflection losses. This implies that at a given incident solar radiation intensity the maximum power point can be doubled for the ACPPVC-50 system compared to the flat non-concentrating system if the ACPPVC-50 optics are perfect. For both systems the maximum power point varies linearly with incident solar radiation intensity. The change of power ratio with incident solar radiation intensity is shown in figure 6.4.7.6. The average maximum power ratio between the flat non-concentrating and the ACPPVC-50 systems is approximately 1.6. This implies significant additional losses for the ACPPVC-50 system when compared to the flat non-concentrating system. Possible sources of losses and their reduction are discussed in chapter 7. The maximum efficiency achieved for the flat non-concentrating system is almost 8% compared to 6.2% for the ACPPVC-50 system as shown in figure 6.4.7.7

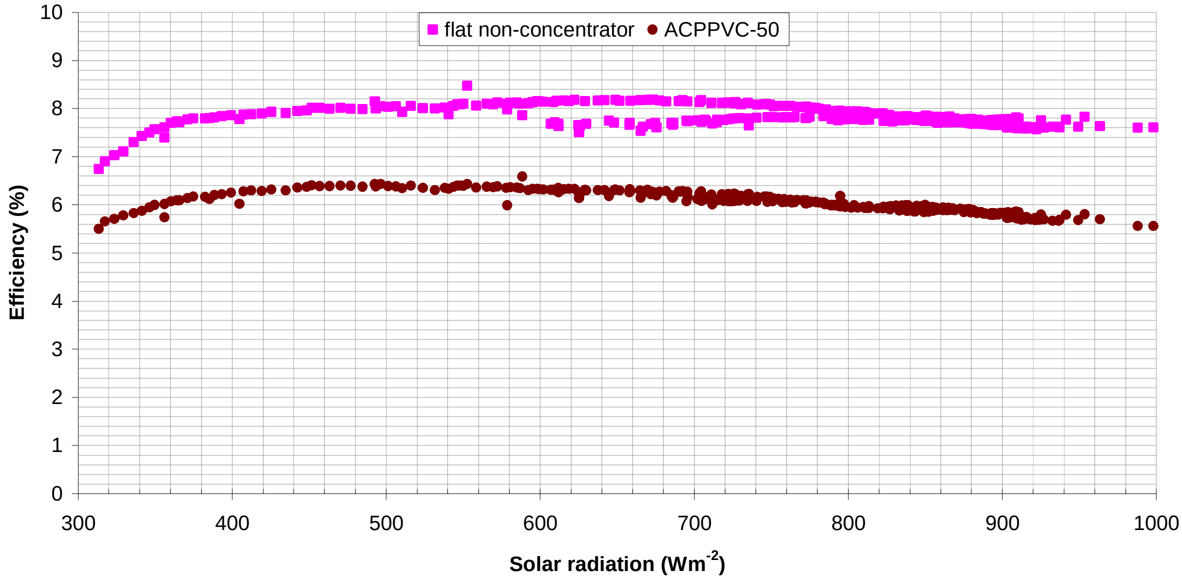

Figure 6.4.7.7 Comparison of efficiency for the flat non-concentrating and the ACPPVC-50 with incident solar radiation.

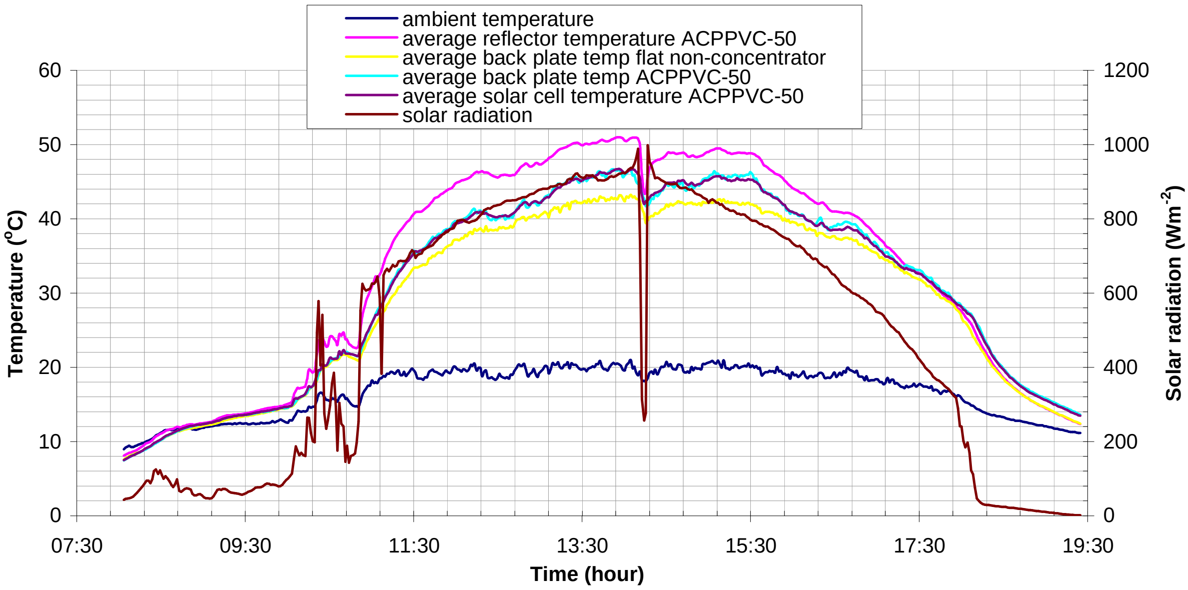

Figure 6.4.7.8 Diurnal variation of solar radiation, ambient temperature, average back plate temperature of the flat non-concentrating system, average reflector temperature of the ACPPVC-50, average solar cell temperature of the ACPPVC-50 and average back plate temperature of the ACPPVC-50.

Figure 6.4.7.8 shows the variation of ambient temperature, average back plate temperature of the flat non-concentrating PV system, average solar cell temperature of the ACPPVC-50, average reflector temperature of the ACPPVC-50 and average back plate temperature of the ACPPVC-50 with time. A maximum temperature of 52° can be seen at the reflector surface for the ACPPVC-50. A temperature difference of 6ºC can be seen between the back plate and the reflector troughs of the ACPPVC-50. All temperatures were measured at the thermocouple locations detailed in figures 6.3.3 and 6.3.4. The solar cell temperatures were measured at the edge of either side of the ACPPVC-50 system to prevent shading on the actual cells. The temperature at the edge of the solar cell was similar to that of the aluminium back plate.

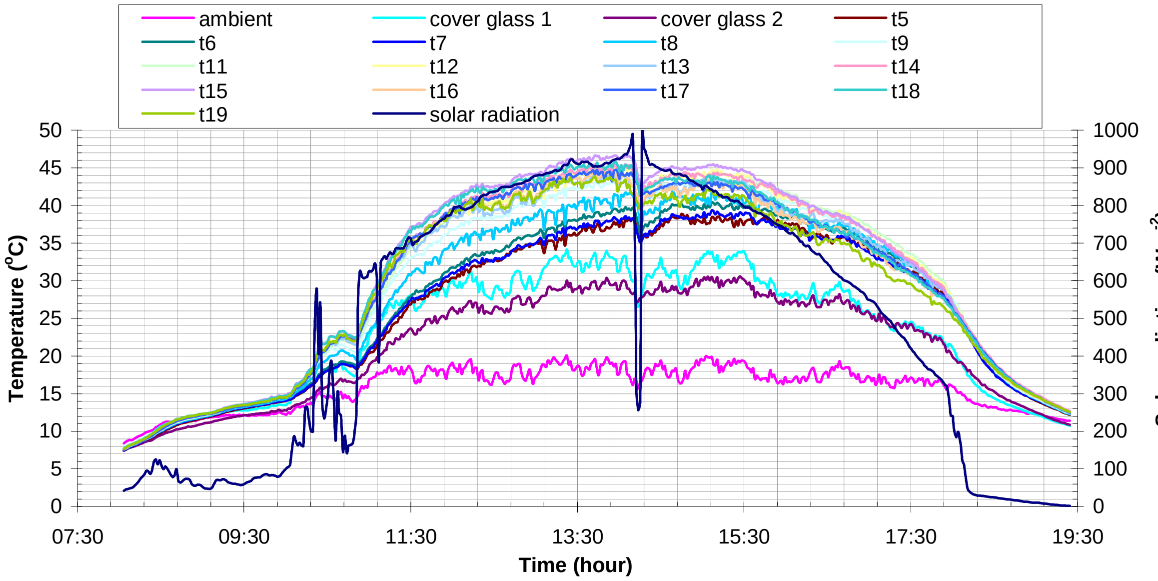

Figure 6.4.7.9 Diurnal variation of solar radiation and back plate temperatures for the flat non-concentrating system. The thermocouples were located as shown in figure 6.3.4.

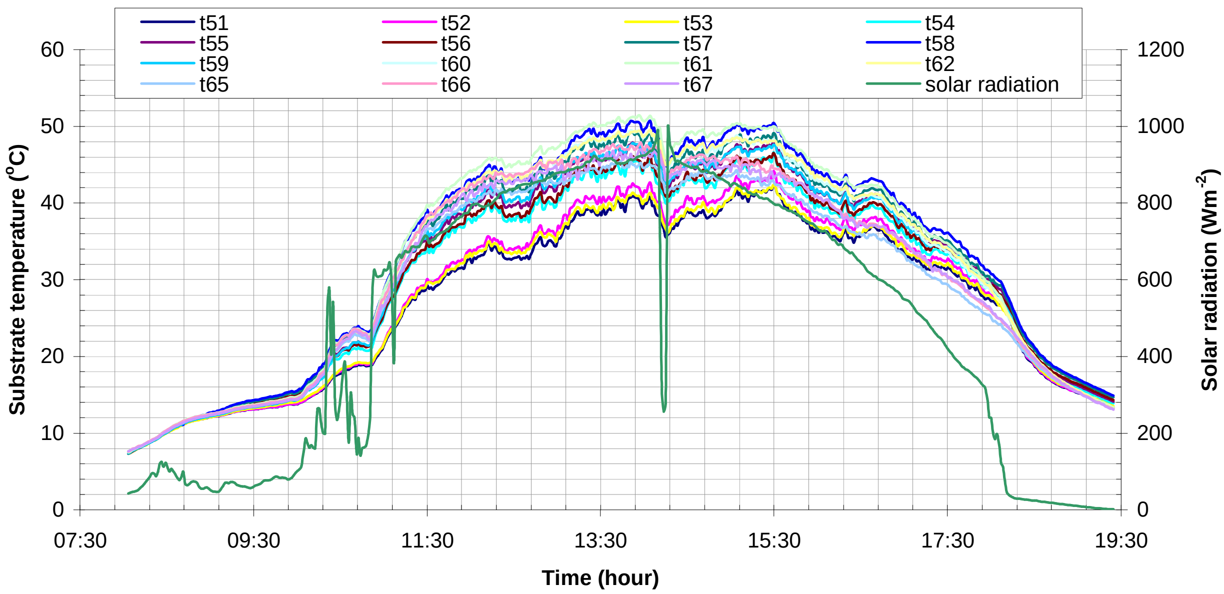

Figure 6.4.7.10 Diurnal variation of solar radiation and back plate temperatures for the ACPPVC-50. The thermocouples were located as shown in figure 6.3.5.

The measured temperatures at different locations on the aluminium back plate and the cover glass for the flat non-concentrating PV panel are shown in figure 6.4.7.9. Figure 6.4.7.10 shows the temperature of the rear aluminium back plate of the ACPPVC-50. The temperature contours of the aluminium back plate for both the flat non-concentrating system and the ACPPVC at the times of 11:30, 13:30, 15:30 and 17:30 are shown in figures 6.4.7.11 to 6.4.7.14. Figure 6.4.7.15 illustrates the temperatures at different thermocouple locations for the reflector trough with time for the ACPPVC-50 system. For both systems, the central region of the aluminium back plate had the highest temperature when compared to other thermocouple locations. The thermocouples were located at identical positions on the aluminium back plate for both systems. Due to shading there is a significant temperature difference between the two sets of solar cells at either end of the ACPPVC-50 before and after solar-noon as shown in figure 6.4.7.16.

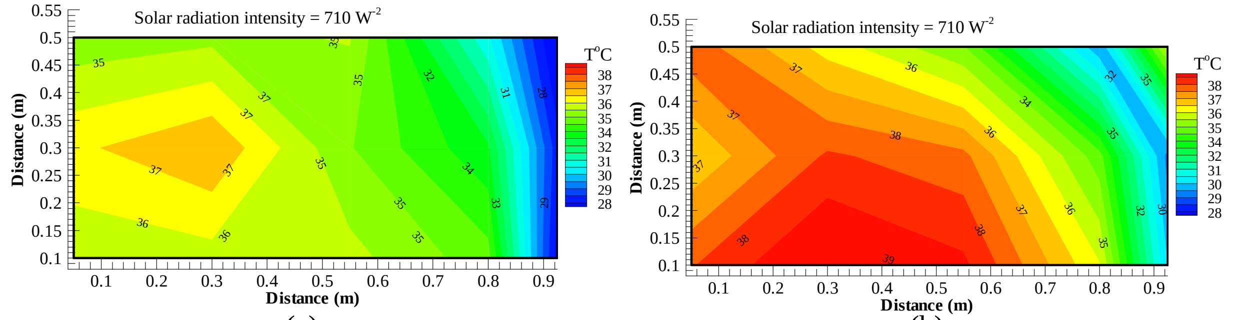

(a) (b)

Figure 6.4.7.11 Measured temperature contours of the aluminium back plate at 11:30 on the 23rd of September 2002 for (a) flat non-concentrator (b) ACPPVC-50.

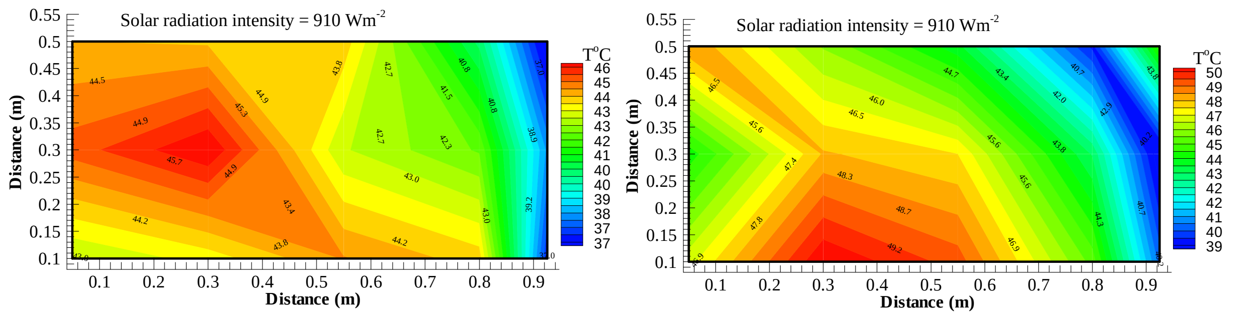

(a) (b)

Figure 6.4.7.12 Measured temperature contours of the aluminium back plate at 13:30 on the 23rd of September 2002 for (a) flat non-concentrator (b) ACPPVC-50.

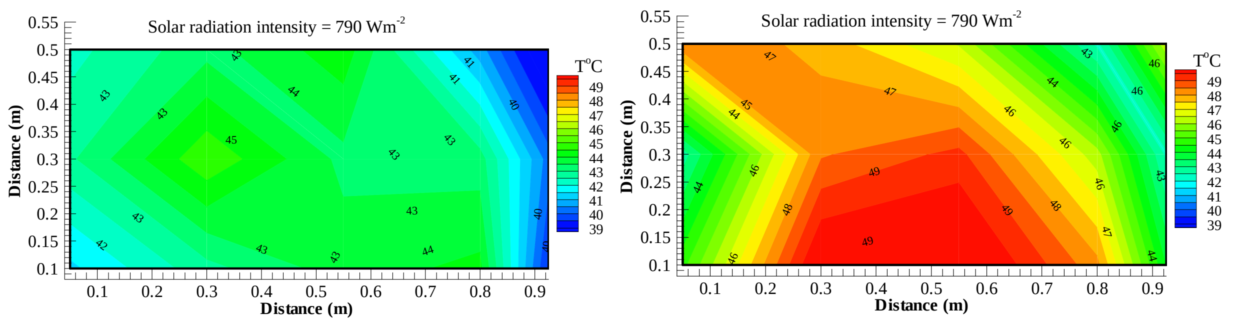

(a) (b)

Figure 6.4.7.13 Measured temperature contours of the aluminium back plate at 15:30 on the 23rd of September 2002 for (a) flat non-concentrator (b) ACPPVC-50.

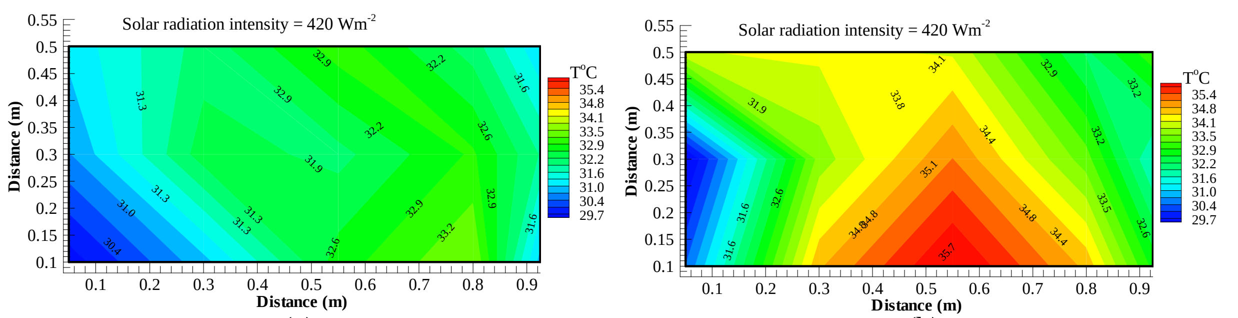

(a) (b)

Figure 6.4.7.14 Measured temperature contours of the aluminium back plate at 17:30 on the 23rd of September 2002 for (a) flat non-concentrator (b) ACPPVC-50.

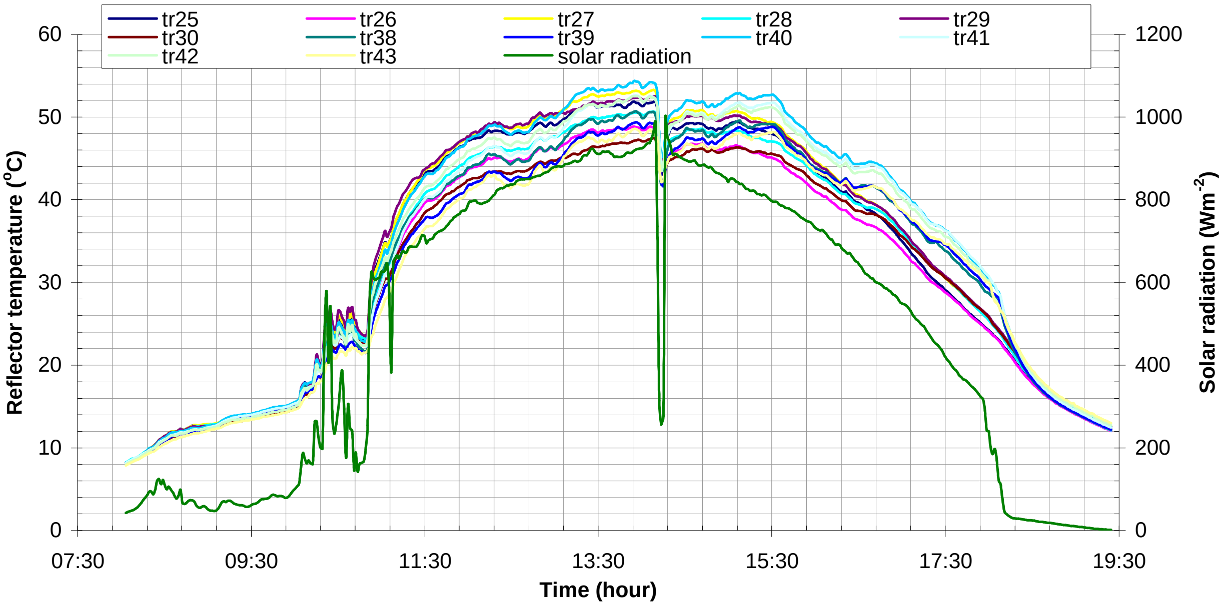

Figure 6.4.7.15 Diurnal variation of solar radiation and reflector substrate temperatures of the ACPPVC-50. The thermocouples were located as shown in figure 6.3.3.

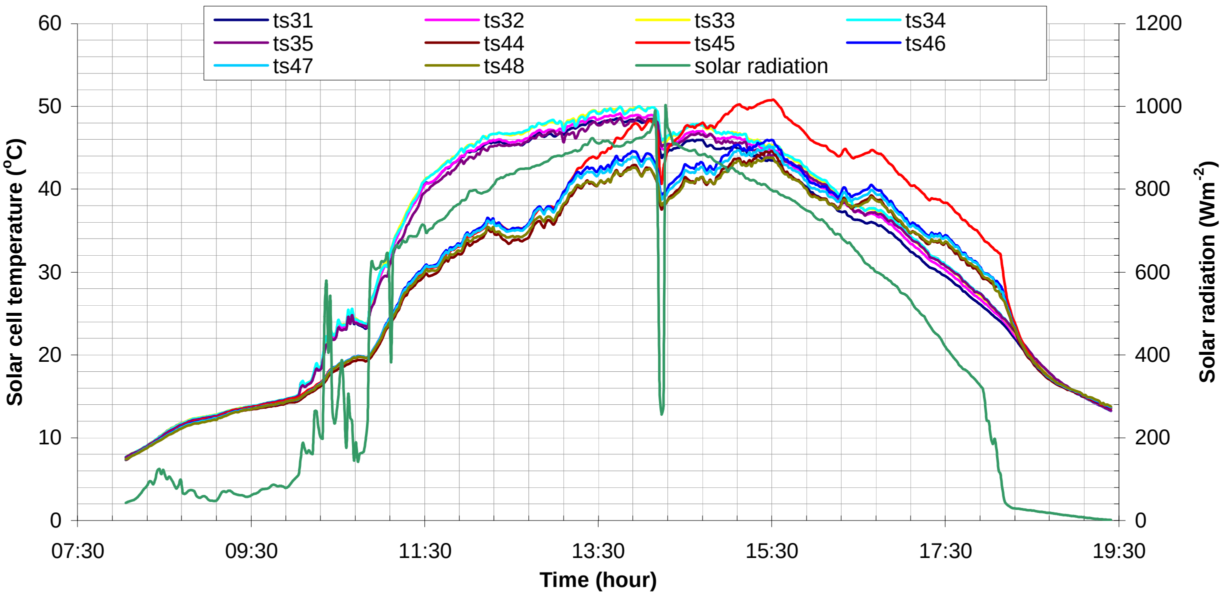

Figure 6.4.7.16 Diurnal variation of solar radiation and solar cell temperatures for the ACPPVC-50. The thermocouples were located as shown in figure 6.3.3.

6.4.8 Electrical and Thermal Performance Analysis of a Flat Non-Concentrating PV Panel and a Concentrating ACPPVC-50 Panel Mounted 18° to the Vertical for Five PV Strings Connected in Series

The electrical and thermal performance of both systems was tested with five PV strings connected in series. Increasing the number of stings connected in series increases the output voltage while the current remains constant for a given solar incident radiation intensity. The variation of incident total radiation, diffuse radiation and ambient temperature with time are shown in figure 6.4.8.1. Figure 6.4.8.2 shows the measured short circuit current and open circuit voltage for the flat non-concentrating and the ACPPVC-50 panel with time. The maximum short circuit current of the ACPPVC-50 was 2.49 A and that of the flat non-concentrating PV panel was 1.5 A, implying a short circuit current ratio of 1.66, while the open circuit voltage was similar for both systems at a given solar radiation intensity.

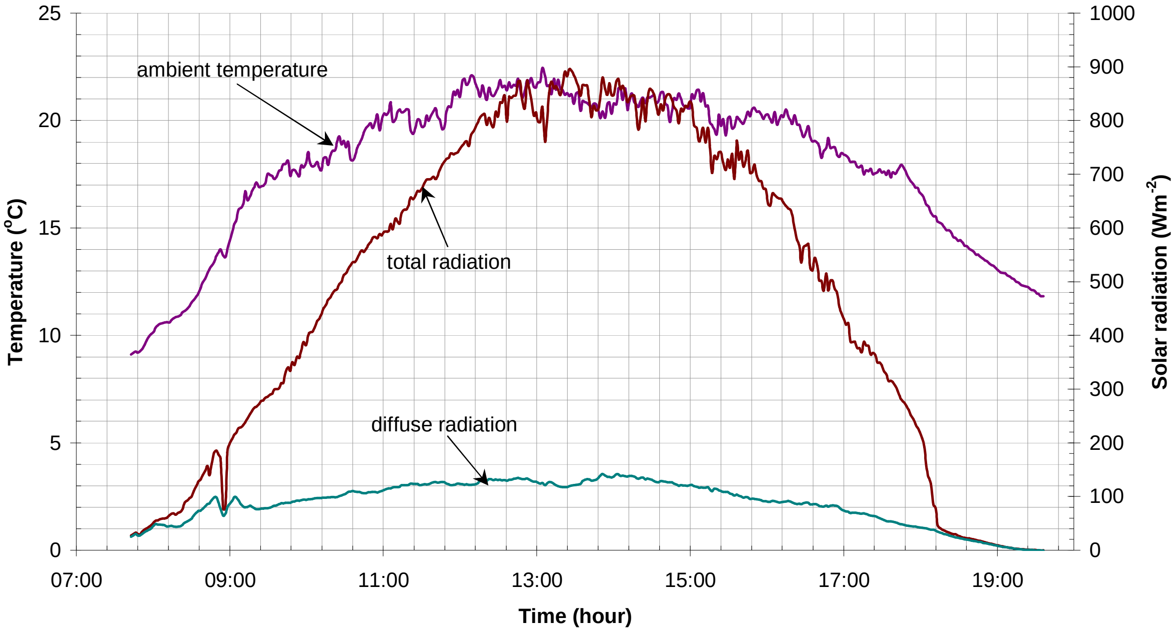

Figure 6.4.8.1 Total radiation, diffuse radiation and ambient temperature with time on the 21st of September 2002.

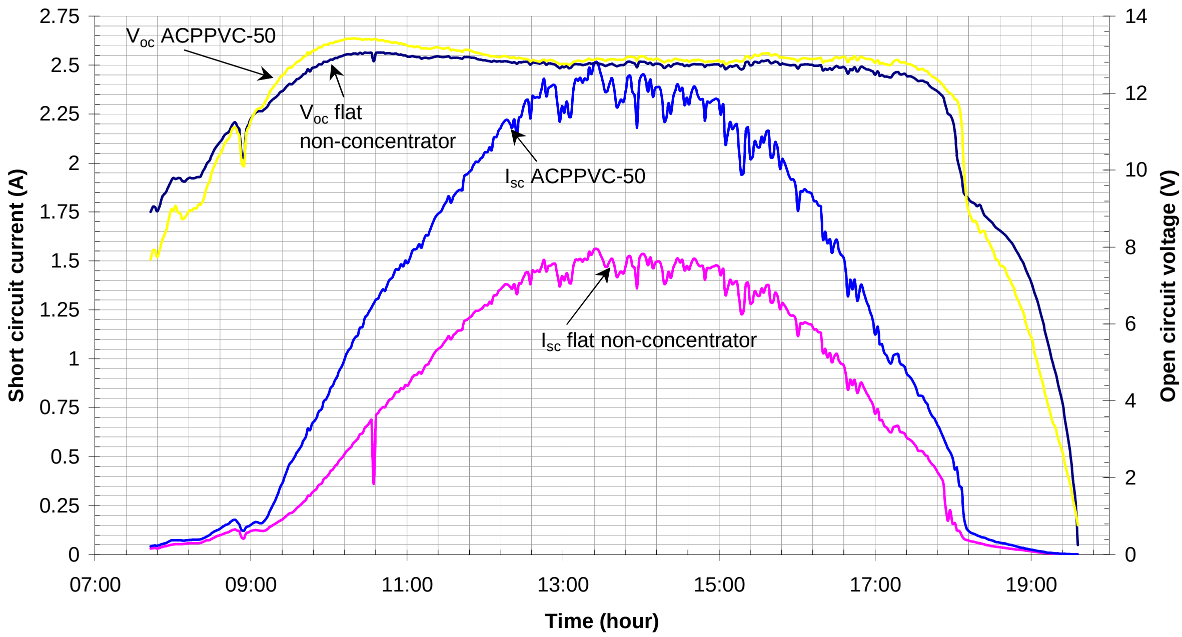

Figure 6.4.8.2 Short circuit current and open circuit voltage for the flat non-concentrating and the ACPPVC-50 system with five PV strings connected in series on the 21st of September 2002.

The maximum power point for both systems varies linearly with incident solar radiation intensity as shown in figure 6.4.8.3. The variation of efficiency with incident solar radiation intensity is shown in figure 6.4.8.4. The maximum power available from the flat non-concentrating panel was 10.8 W compared to 17.2 W for the ACPPVC-50 which indicates a power ratio of 1.59. The values of efficiency for both systems are reduced because of the shadow cast by the wooden frame at the lower solar incidence angles. The efficiency increased exponentially above a solar radiation intensity of 200 Wm^{-2} until it attains a nearly constant maximum value of 8.2% for the non-concentrating system and 6.2% for the ACPPVC-50 system. Low values of efficiencies can be explained by ohmic losses between the interconnected solar cells and the cell spacing, this was verified experimentally by using 52-mm and 2-mm inter cell tab spacing for the individual solar cells and is detailed in chapter 7.

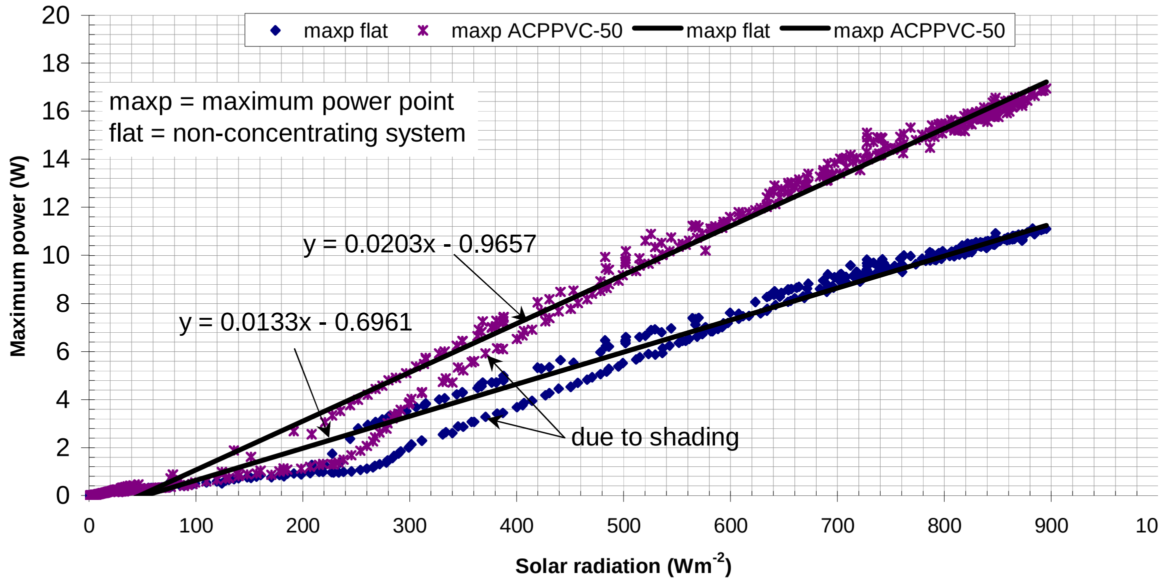

Figure 6.4.8.3 Maximum power point with incident solar radiation intensity for the flat non-concentrating and the ACPPVC-50 systems.

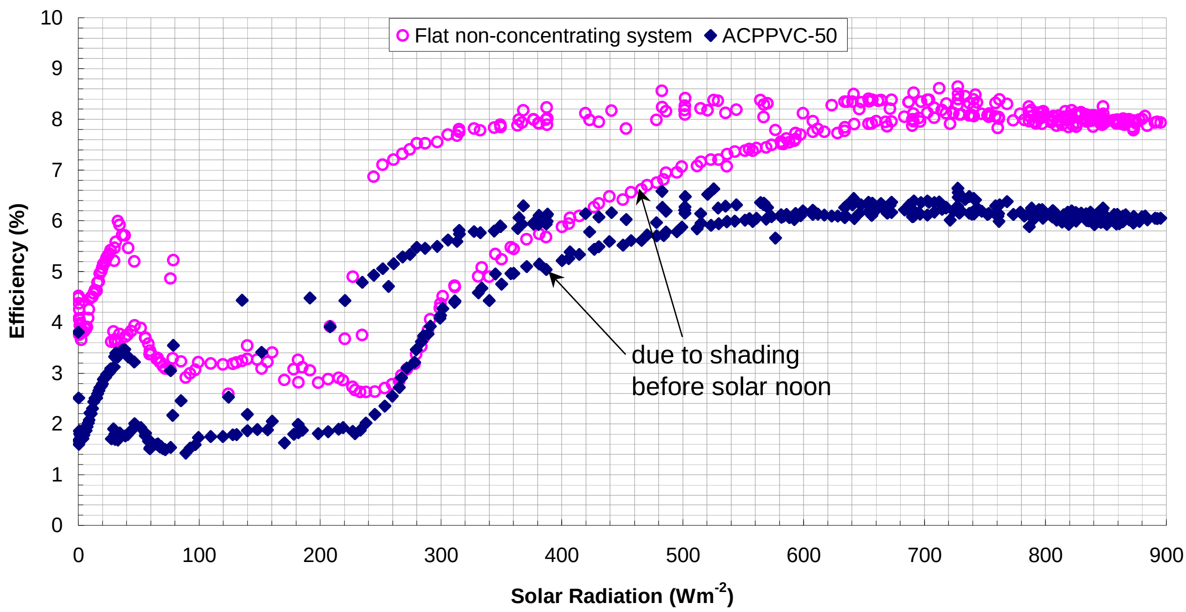

Figure 6.4.8.4 Electrical conversion efficiency with incident solar radiation intensity for the flat non-concentrating and the ACPPVC-50 systems.

Figure 6.4.8.5 shows the diurnal variation of maximum power point ratio with incident solar radiation intensity for the flat non-concentrating and the ACPPVC-50 systems. The maximum power point was calculated from each individual I-V curve generated at every set of measurements. A wide range of incident solar radiation intensities gave a maximum power point ratio of 1.60.

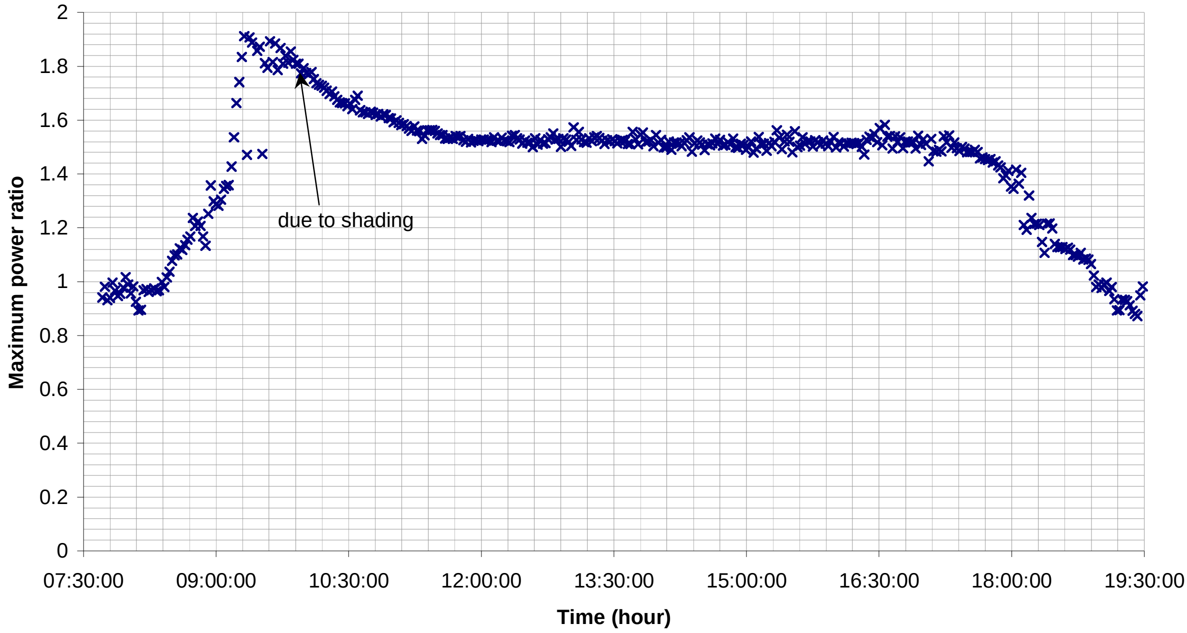

Figure 6.4.8.5 Diurnal variation of maximum power point ratio with incident solar radiation intensity for the flat non-concentrating and the ACPPVC-50 systems.

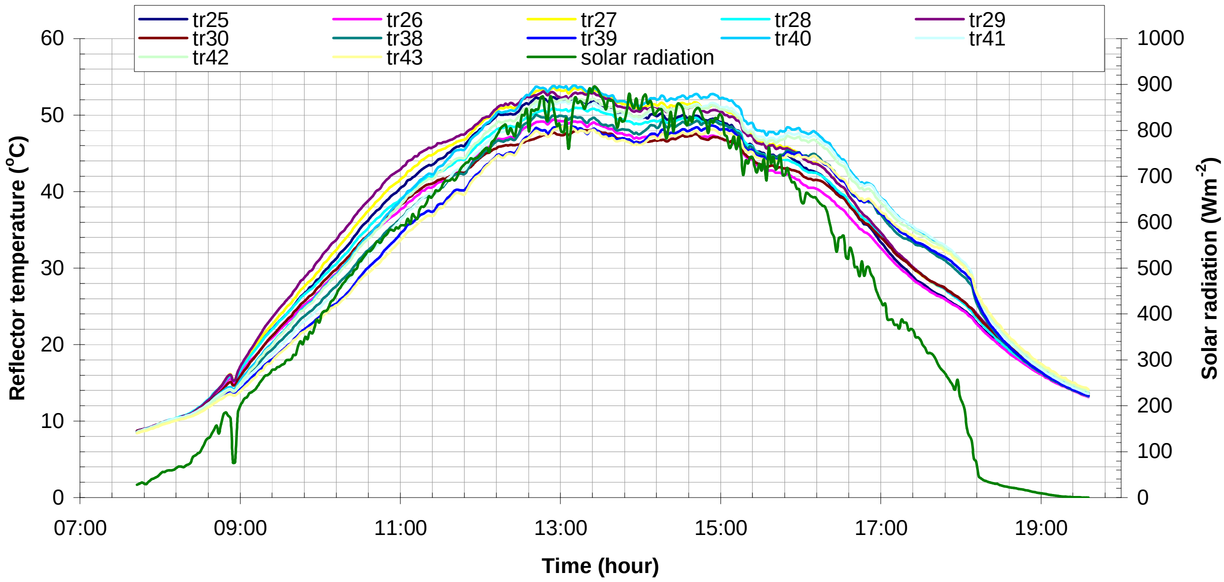

Figure 6.4.8.6 Diurnal variation of solar radiation and reflector temperature of the ACPPVC-50 on the 21st of September 2002. The thermocouples were located as shown in figure 6.3.3.

Figure 6.4.8.6 shows the measured reflector temperature of the ACPPVC-50 system with time on the 21st of September 2002. The thermocouples were located inside the individual reflector troughs as shown in figure 6.3.3. The temperature response is similar to the incident solar radiation intensity. The temperature of the top reflector trough was higher than that of the lower reflector trough because of convective heat transfer. Figure 6.4.8.7 shows the measured solar cell temperature with time for the ACPPVC-50 and figure 6.4.8.8 shows the aluminium back plate temperature and glass temperature with time. A temperature difference of 10°C occurred between thermocouple locations ‘ts31’ and ‘ts44’. From figure

6.4.8.8 it can be seen that the average back plate temperature is 28°C higher than the ambient temperature. This could be 10°C less than in the actual solar cell surface temperature.

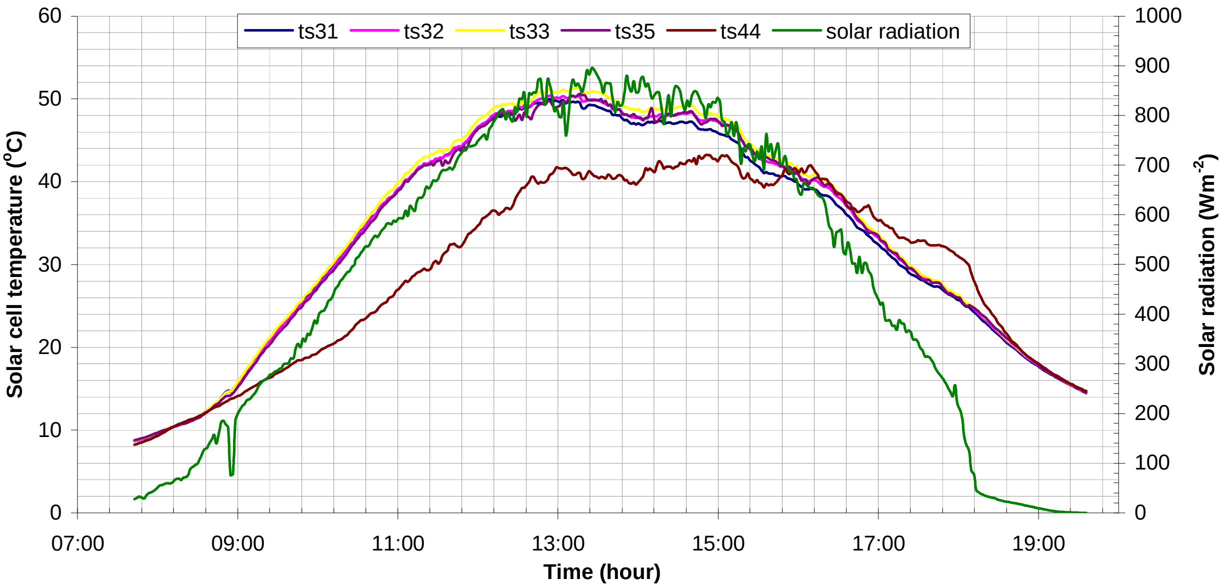

Figure 6.4.8.7 Diurnal variation of solar radiation and solar cell temperatures for the ACPPVC-50 on the 21st of September 2002. The thermocouples were located as shown in figure 6.3.3.

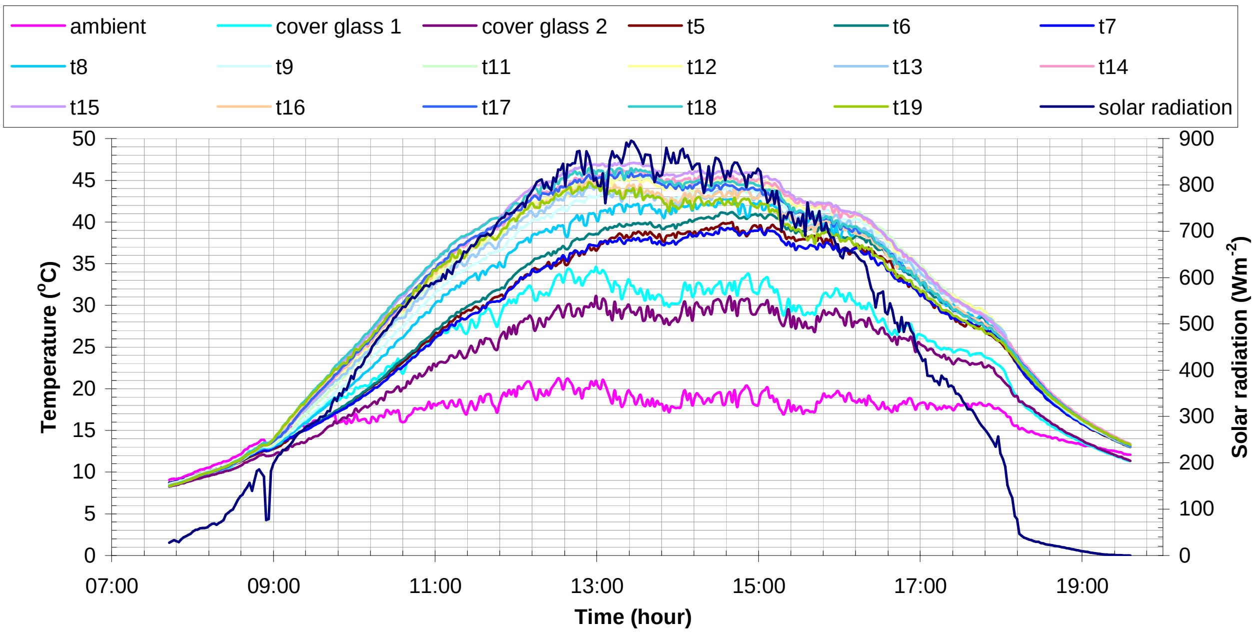

Figure 6.4.8.8 Diurnal variation of solar radiation, aluminium back plate and cover glass temperature of the flat non-concentrating system on the 21st of September 2002.

6.4.9 Electrical and Thermal Performance Analysis of a Flat Non-Concentrating PV Panel and a Concentrating ACPPVC-50 Panel Mounted 18° to the Vertical With Six PV Strings Connected in Series

An experimental investigation was undertaken on the 3rd of October 2002 for both systems with six PV strings connected in series. The highest intensity of incident solar radiation was 950 Wm^{-2} and the ambient temperature was 18ºC as shown in figure 6.4.9.1. Measurements were carried out at 30 seconds intervals throughout the 10 hours of day light. The variation of short circuit current and open circuit voltage with time for the flat non-concentrating and the ACPPVC-50 systems are shown in figure 6.4.9.2. The sudden reduction in short circuit current seen in figure 6.4.3.2 occurred due to a reduction in incident solar radiation resulting from intermittent cloud cover.

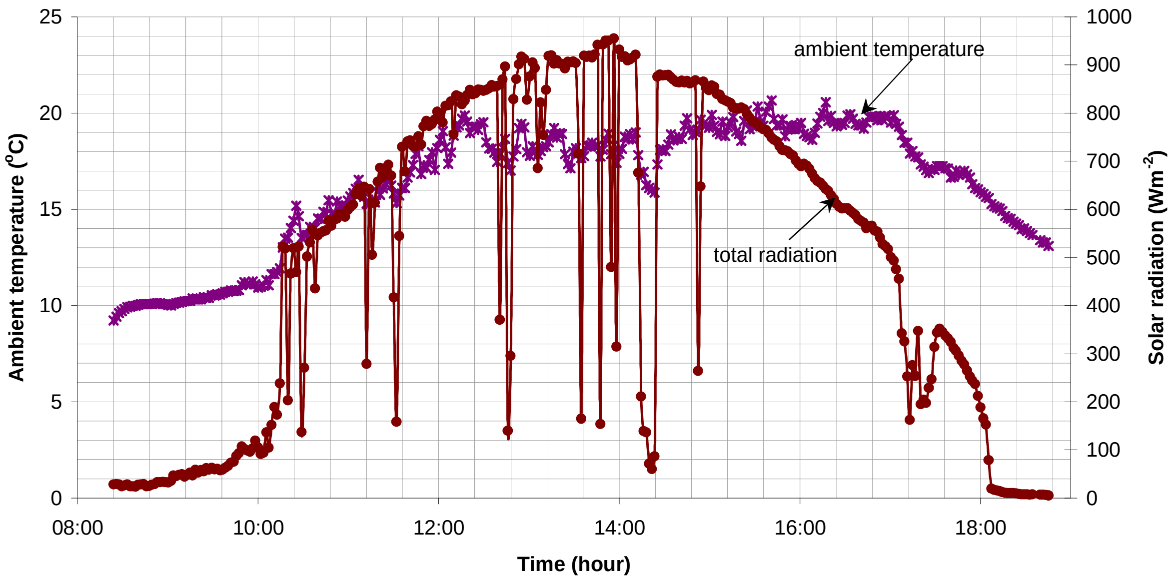

Figure 6.4.9.1 Total radiation and ambient temperature with time on the 2nd of October 2002.

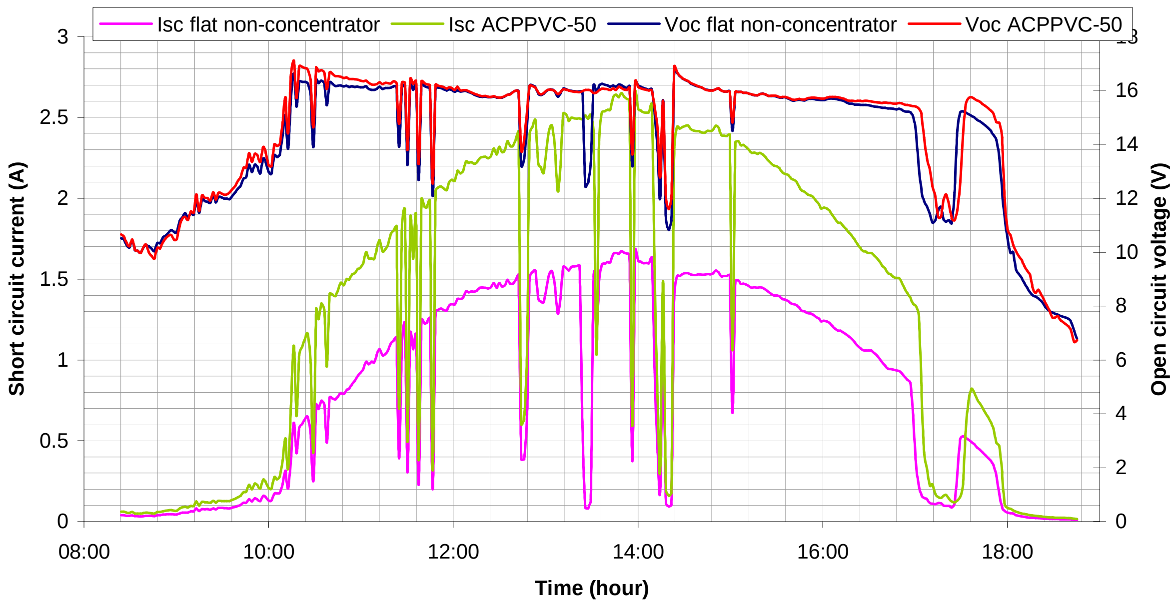

Figure 6.4.9.2 Short circuit current and open circuit voltage with time for the flat non-concentrating and the ACPPVC-50 system with six PV strings connected in series.

Figure 6.4.9.3 shows the effect of maximum power with incident solar radiation intensity for both systems. The change in electrical efficiency with incident solar radiation intensity is shown in figure 6.4.9.4. The maximum efficiency achieved by the flat non-concentrating system was 8.2% whereas the maximum efficiency for the ACPPVC-50 is 6.5 %. This is due to i^2r losses in the interconnections between solar cells. The maximum power from the flat non-concentrating system is 15 Watts and the maximum power for the ACPPVC-50 system is 23 Watts when the intensity of incident solar radiation was 950 Wm^{-2}. Figure 6.4.9.5 illustrates the change of the maximum power point ratio of the ACPPVC-50 to the flat non-concentrating system with incident solar radiation intensity. At lower incident radiation intensities, the minimum values of the maximum power point ratio are due to shading and the solar incidence angles. At lower solar incidence angles the optical losses are higher as detailed in chapter 3.

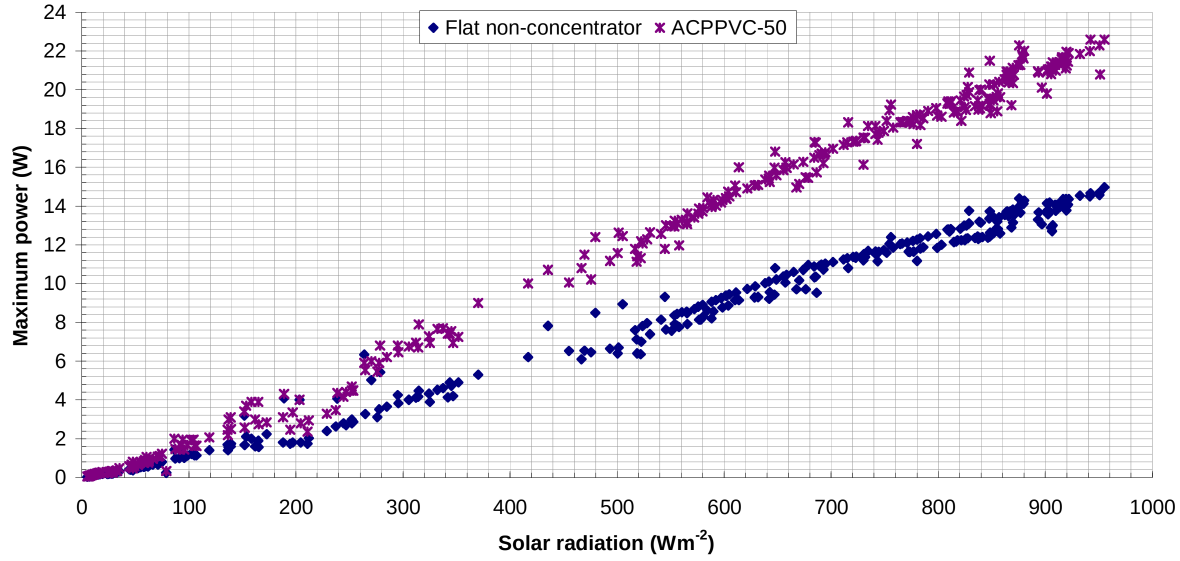

Figure 6.4.9.3 Maximum power against incident solar radiation intensity for the flat non-concentrating and the ACPPVC-50 systems.

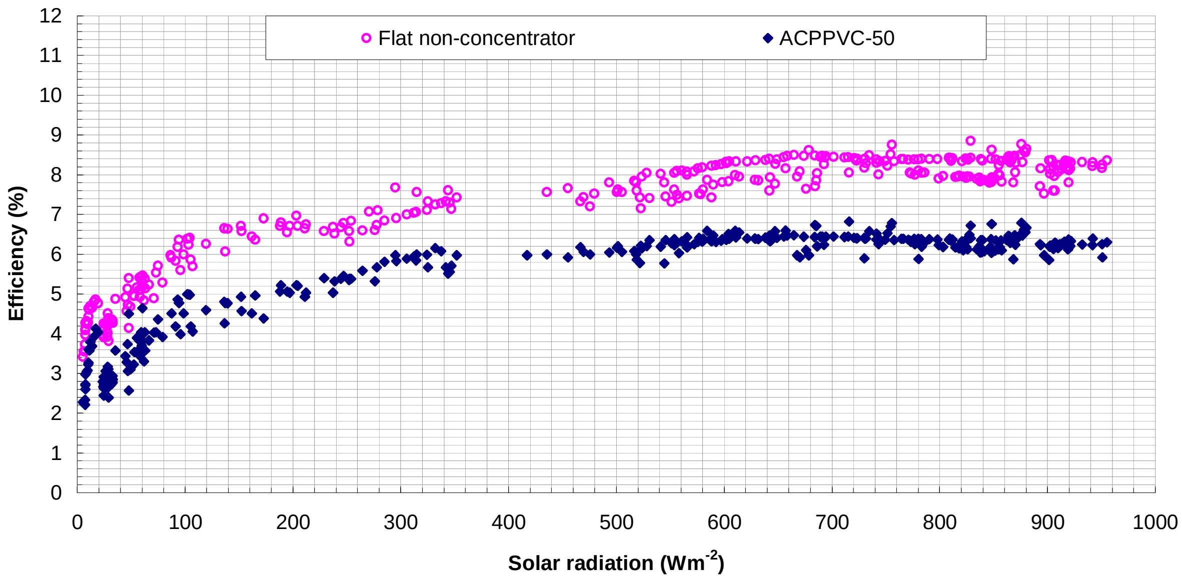

Figure 6.4.9.4 Electrical conversion efficiency against incident solar radiation intensity for the flat non-concentrating and the ACPPVC-50 system.

Variation of the ambient temperature, the average back plate temperature, the average reflector temperature and the average solar cell temperature with time on the 2nd of October 2002 are shown in figure 6.4.9.6. A 30ºC maximum temperature rise was measured inside the reflector trough. A 10ºC temperature difference was measured between the aluminium back plate and the reflector trough. The wind speed at the back of the aluminium back plate caused a convective flow. For a wind speed of 4 ms^{-1} or higher the flow becomes turbulent and a higher heat transfer coefficient of 20 Wm^{-2} can be expected, thereby lowering the PV cell operating temperature.

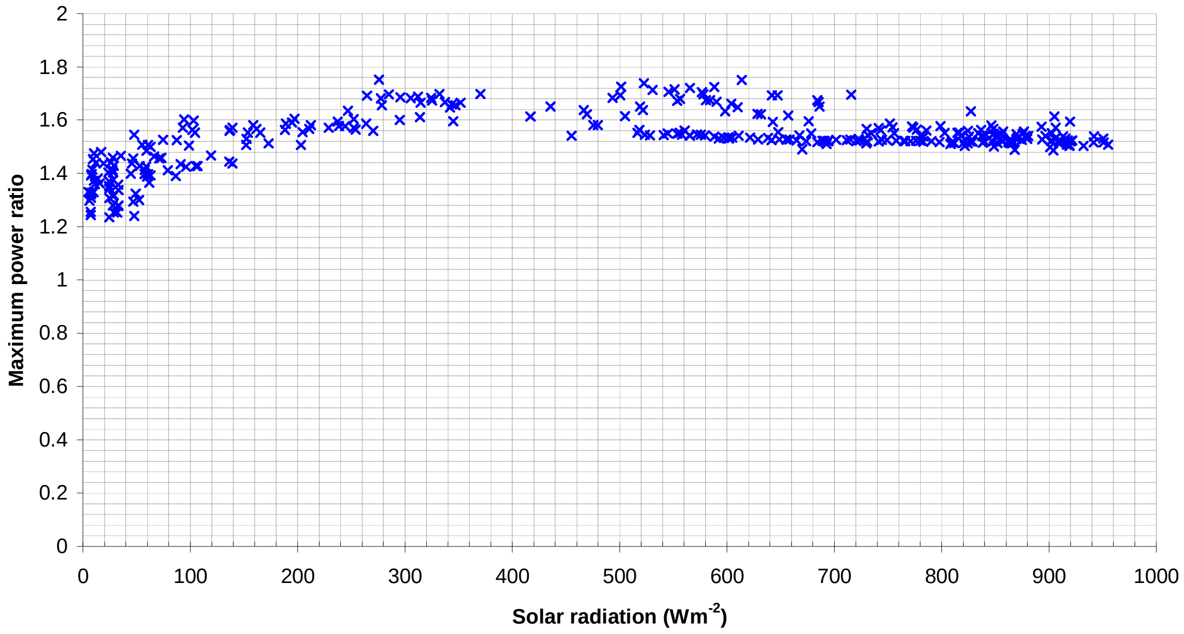

Figure 6.4.9.5 The variation of the maximum power point ratio for the flat non-concentrating and the ACPPVC-50 system with incident solar radiation intensity.

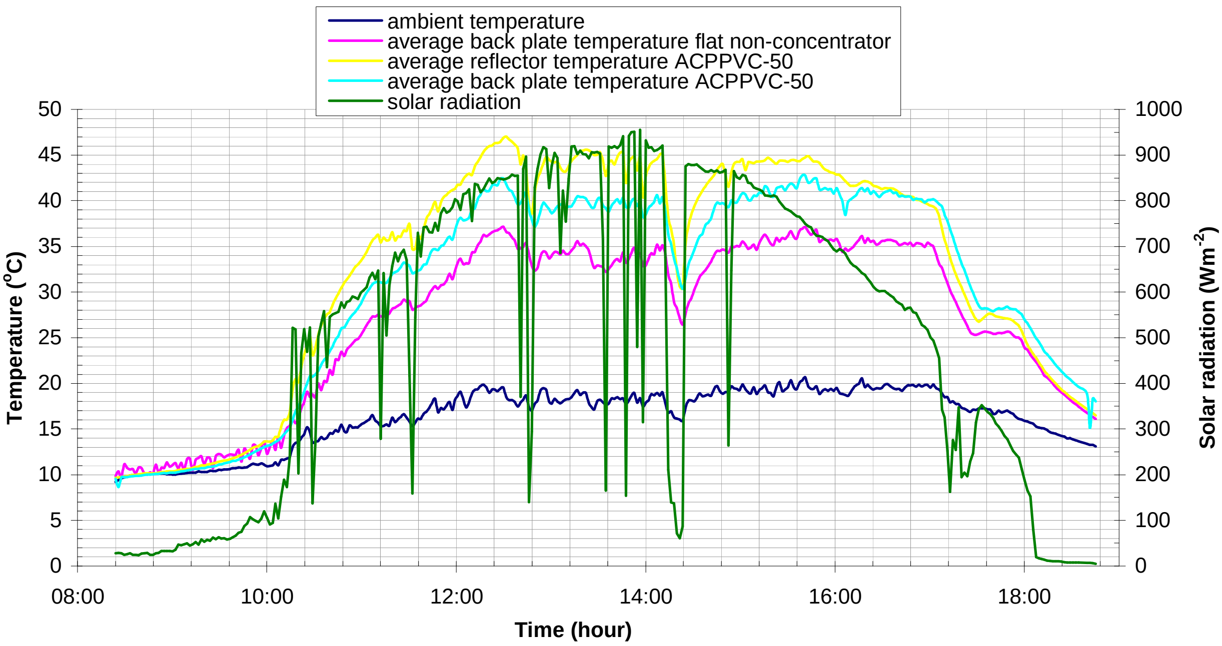

Figure 6.4.9.6 Diurnal variation of solar radiation, ambient temperature, average back plate temperature, average reflector temperature and the average solar cell temperature for the ACPPVC-50 system.

6.5 Conclusions

A detailed experimental investigation into the performance of an asymmetric compound parabolic photovoltaic concentrator has been detailed in this chapter. System 1, comprised of eight PV strings each of five cells connected in series, was investigated for electrical performance and system temperatures for an average of 10 hours for twenty days with and without the concentrators presents. Different numbers of PV strings were connected in series to investigate the effects of edge shading on electrical and thermal performance. The reflector troughs were removed from System 1 to give a flat non-concentrating PV panel for comparison to the ACPPVC-50. In both cases the active solar cell area was the same i.e. the electrical output was generated from the same PV cells. With less than a 1% fluctuation in incident solar radiation intensity for the experimental investigation the power increased by more than 1.62 when using the concentrator compared to the flat non-concentrating system. The aluminium back plate temperature of the ACPPVC-50 system was only 12°C higher than that of the flat non-concentrating system. This indicates significant convective flow at the back of aluminium back plate decreasing the operating solar cell temperature. The flat non-concentrating system achieved nearly 8.5% electrical efficiency when the reflector troughs were removed compared to an electrical conversion efficiency of 6.8% for the ACPPVC-50 with a fill factor of 65%.

A second asymmetric compound parabolic photovoltaic concentrator was constructed to compare concurrently electrical and thermal performance. Experiments were undertaken for twenty five days with an average of 10 to 12 hours sunshine. System 1 was a flat non-concentrating system with identical dimensions to System 2 i.e. the concentrating system. Both systems were investigated for 0° and 18° inclination angles to the vertical. Different numbers of PV strings were connected in series for both systems and their electrical and thermal performance monitored. In addition to the east-west shadow cast by the wooden frame for both systems, a third partial shadow was observed when the systems were mounted vertically. Short circuit current increased by 1.66 times for the ACPPVC-50 compared to the flat non-concentrating system whereas the open circuit voltage was similar for both systems. The maximum power increased by approximately 1.65 for the ACPPVC-50 compared to the flat non-concentrating system however the maximum back plate temperature increased by only 6.5°C for the ACPPVC-50 compared to the flat non-concentrating system. This indicated significant heat loss from the back aluminium plate. The highest efficiency achieved by the flat non-concentrating panel was 12% when a single PV string was considered and that of the ACPPVC-50 was 10.5%. However an average of 8% electrical conversion efficiency was achieved by the flat system compared to the electrical conversion efficiency of 6.8% for the concentrator. The tin/lead coated copper tab between individual solar cells has a resistance of 1.5Ω which implies a power loss of $1.5i^2$ Watt (where i is the instantaneous current produced by the PV panel) which is more significant when two or more PV string connected in series. This indicates that significant power losses occur in the tab between consecutive solar cells in addition to the optical losses at the reflector as detailed in chapter 3. From the CFD analysis a 6°C temperature gradient inside the solar cells along the vertical direction was predicted. This will cause electrical mismatch loss between individual solar cells and may explain the lower electrical conversion efficiency of the ACPPVC-50 compared to the flat non-concentrating system.